GRAPHIC
Groundwater Resources Assessment under the Pressures of Humanity and Climate Change

Global assessment of the impacts of climate variability on total water storage:

Implications for groundwater resources management.

Michael William Allen

MSc Thesis WSE-GW.19-04-Michael William Allen
26/08/2019

Updated Version; 30/11/2019

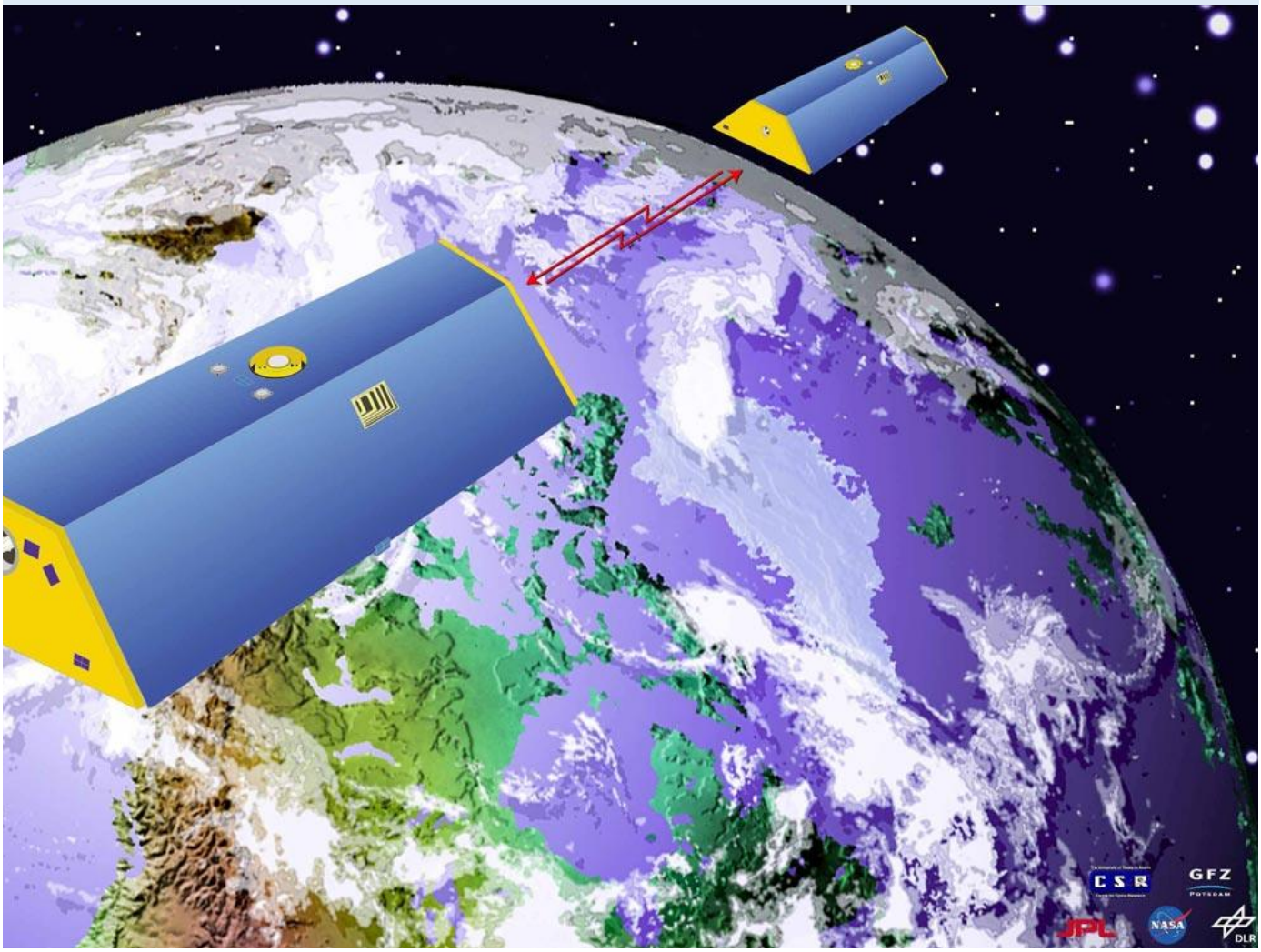

Image: GRACE satellites graphic https://www.jpl.nasa.gov

Global assessment of the impacts of climate variability on total water storage: implications for groundwater resources management

Master of Science Thesis
by
Michael William Allen

Supervisors
Tales Carvalho-Resende
Tibor Stigter

Examination committee
Tibor Stigter, Neno Kukuric,
Tales Carvalho-Resende,
Graham Jewitt

This thesis is submitted in partial fulfilment of the requirements for the academic degree of

Master of Science in Water Science and Engineering
IHE Delft Institute for Water Education, Delft, the Netherlands

Master of Science in Environmental Engineering
Instituto Superior Técnico, Universidade de Lisboa, Portugal

Master of Science in Hydro Science and Engineering
Technische Universität Dresden, Germany

MSc research host institution
IHE Delft

August 2019

Abstract

Due to global trends in climate and human activity, groundwater is becoming increasingly more important as a water source. Alongside the effects of climate change and anthropogenic factors, natural climate cycles, like El Niño–Southern Oscillation (ENSO), the Pacific Decadal Oscillation (PDO) and the Atlantic Multi-decadal Oscillation (AMO), have considerable impacts on the groundwater recharge. However, to date, only a small number of studies have sought to gauge these impacts on a global scale and to consider their implications in terms of management and policy decisions. This body of work looks at one approach to assesses the effect of global climatic oscillations cycles on total water storage and groundwater storage in large aquifers (area over 100 000 km²).

To evaluate this methodology, a study has been done on 26 large aquifers located in varying climatic regions of the world. The impact of interannual and multidecadal climate variability on groundwater resources were assessed by running wavelet analyses on the monthly time series of several oceanic indices and modelled Total Water Storage (TWS). Two approaches were taken in calculating TWS. The first one is made through the analysis of data from the Gravity Recovery and Climate Experiment (GRACE), which provides information from 2002 to 2016. This short time frame meant it is unable yet to capture the multidecadal climate oscillations, so a second approach was employed. The second approach uses a Simple Water Balance (SWB) Model which comprises of two-variables, precipitation, and evapotranspiration. This model was used to reconstruct past water storage changes from 1980 to 2017. it is important to note that the SWB Model results only look at groundwater storage flux.

The results showed the SWB-Model approach is a good multi-regional tool for the examination of the effects of climate variations on (GWS) groundwater storage change around the world. In the majority of the studied aquifer systems, the SWB-Model showed to be a powerful tool in the extension of GRACE TWS change data. There are several strong indicators of where the Model results best represent the groundwater storage change. These include aquifer size and how well the area boundary match. The study also highlighted the strong multi-decadal links between AMO and GWS change that occurs in many global aquifer systems. Its positive phases see increases in storage in Australia, India, Southern Africa, and parts of central Asia and decrease in south East Asia the amazon and the Sahel Zone. PDO was seen to have its biggest impacts when its positive or negative phases matched that of ENSO. When the positive phases were aligned, aquifer systems in India, Syr-Daray, and Australia saw decreases in storage and increases in America.

These results can be used to address the threat of water scarcity and manage groundwater to mitigate the threats of climate variability and change. They indicate where more detailed local studies are necessary to collect data to further support the development of long-term groundwater management strategies of large (in some cases transboundary) aquifers.

Acknowledgements

I would like to begin by expressing my gratitude to my supervisors. Thanks to Tales Carvalho Resende – without your guidance, knowledge and immense enthusiasm for the project this would not have been possible. Special thanks also to Tibor Stigter who provided constructive comments, positivity and guidance every time I needed it.

There are many individuals and institutions that have in one way or another contributed to the successful completion of this theses. Thanks to Luis, Teresa and Christian for the contributions to this amazing course and to our experience on it. I also want to acknowledge a very special thanks to my colleagues and friends, especially to the GroundwatCH family, there could not have been a better bunch to have along for this adventure.

Lastly, a special thanks to my family – Will, Nicky, Brigitte and Casey for their encouragement and support throughout the course, and particularly through this last six months of thesis research and writing.

Table of Contents

List of Figures

List of Tables

Abbreviations

TWS = Total Water Storage

SWB = Simple Water Balance

ENSO = El Nino Southern Oscillation

AMO = Atlantic Multi-decadal Oscillation

PDO = Pacific decadal Oscillation

NAO = North Atlantic Oscillation

IOD = Indian Dipole Oscillation

GWL = Groundwater Level

GWS= Groundwater Storage

EWH = Equivalent Water Height

CSR = Texas Centre for Space Research

JPL = NASA's Jet Propulsion Laboratory

GRZ = Deutsches GeoForschungsZentrum

WTC = Wavelet Coherence

CWT =continues wavelet transform

XWT = cross wavelet transform

MPI-ESM = Max Planck Institute for Meteorology – Earth System Model

Chapter 1 INTRODUCTION

1.1 THE PROBLEM

Ground water contains the world's largest stock of accessible freshwater ((Siebert et al., 2010) (Gorelick & Zheng, 2015). It accounts for about one-third of the world's freshwater withdrawals (Siebert et al. 2010), but by its very nature remains a "*hidden resource*". Because of this hidden nature, groundwater resources are often characterized by poor to no management. Moreover, due to its use in local settings, development often occurs in an unrestrained way, and planning for this development is not incorporated into river basin management and policy. This means that much resource-use falls outside of established and emerging groundwater governance frameworks (FAO, 2015) (Brekke et al., 2009)

Such unconstrained development has allowed abstraction to increase globally by around 300 percent over the past 50 years (Carvalho Resende et al., 2018). Unrestricted pumping for agriculture and other uses now threaten the sustainability of some aquifers. Beyond this, we can see that the allocation and use of groundwater is often poorly aligned with society's broader goals around equity, sustainability and efficiency (Coarvalho Resende, 2015)

Growing water scarcity is one of the leading challenges that the globe will be facing in the coming decades ("Global Risks 2015 10th Edition," 2015). Water requirements are projected to be pushed beyond sustainable water supplies by 40 percent by 2030 ("Global Risks 2015 10th Edition," 2015). Water use is growing at twice the pace of population growth, and by 2025, it is estimated that two-thirds of the world population will be experiencing water "stress conditions" (Global Risks, 2015) . This challenge will only grow in importance as the world's population continues to grow, their living standards increase, and the effects of climate change intensify.

1.2 KNOWLEDGE GAPS

An increased focus on groundwater over the past decade means a lot of work has been done on over-extraction and the effects of climate change. A lot of this focus has come thanks to the NASA Gravity Recovery and Climate Experiment (GRACE) which has allowed unprecedented large-scale monitoring of global aquifers (of a few hundreds of kilometers) (Velpuri et al., 2019). Continuous observations since 2002 of short-term temporal variations in the Earth's gravity field, which are attributed to changes in terrestrial water storage (TWS), has providing valuable information on recent groundwater storage changes at basin scales (Liesch et al, 2016). The GRACE results have been effective at moving the conversation to groundwater and sustainability (Alley et al. 2015).

In the last few years increasing attention has been paid to looking at the role that natural climate variability plays in influencing the global groundwater storage changes. This is now seen as an increasingly urgent water management issue (Nezlin et al, 2004). There have been a number of studies addressing the topic of how precipitation and infiltration are related (Wang et al., 2015) and how

climate variability will effect precipitation around the world (Xie et al, 2015). But there are very few studies on how climate variability is affecting groundwater storage in the world's largest aquifers.

There is also a need to improve understanding and modelling of climate variation in relation to the hydrological cycle (Gurdak et al., 2007). In many regions the effects of inter-annual to multi-decadal climate variability on recharge rates along with mechanisms and other subsurface hydrologic processes are largely unknown (Jean Kuss & Gurdak, 2014).

Addressing this knowledge gap is very important for several reasons:

1. With the predicted changes in the global climate, groundwater has the potential to be an important resource that can be used to aid society's adaptation to climate change. This is particularly relevant because large aquifer systems are seeing some of the greatest increases in populations and their accompanying economic growth. Therefore, it is essential to understand this inter-annual to multi-decadal climate variability connection to groundwater because of the real and near-term implications for water-resource management.
2. Most of the world's groundwater is found in only a few very large aquifer systems, on the order of 100 000 km² and over (Margat & Jac van der, 2013). Due to their size most of them are transboundary, and often encompass a number of countries. Transboundary complications add a unique challenge to the management of these aquifers, and almost always increases the barriers to achieving sustainable goals. Out of the more than 550 Transboundary Aquifers IGRAC & UNESCO-IHP identified, only six are in a legal agreement in regards to their sustainable management (Eckstein & Sindico, 2014).
3. There is a lack of groundwater monitoring and in some places these observation networks are even seen to be shrinking (WMO-UNEP, 2008). A lot of these large aquifers have dynamics that are not yet fully understood because of data scarcity and accessibility (Carvalho Resende et al., 2018). With a lack of understanding and information around how these water bodies are being affected by changing environmental and anthropogenic factors, the potential for good management outcomes are strongly reduced. Within the last decade the potential effects of natural climate variability on groundwater storage has become an increasingly urgent water management issue (Nezlin et al, 2004). Moreover, a lot of the current tools to facilitate integrated appraisals of adaptation and mitigation options across multiple water-dependent sectors are inadequate. (WMO-UNEP, 2008)

1.3 PREVIOUS WORK

Studies have indicated that the ocean-atmosphere oscillation patterns of ENSO, PDO, and AMO and associated hydroclimatic variability may affect aquifers recharge rates and groundwater level variability (Gurdak *et al.*, 2007). A lot of work has been done on the effects of high frequency (short term seasonal variation) and low frequency (inter- annual to multi-decadal variation) climate variation on surface water. However less is known about the complex interactions of inter-annual to multi-decadal climate variability (low frequency) that more strongly influence groundwater levels and recharge (Jean, Kuss, & Gurdak, 2014). Studies that have been addressing this relationship mainly focus on the western United States, Canada, and the Pacific (Fleming et al, 2006 and van der Velde et al, 2006).

As far as changes in groundwater storage are concerned, until recently there has been a lack of remote sensing techniques that could be applied to determine them directly. In recent years, NASA's Gravity

Recovery and Climate Experiment (GRACE) has revolutionized the approach to how temporal changes in Total Water Storage (TWS) balances can be undertaken. There are now an increasing number of studies using this technique to contribute to efforts to address groundwater storage change (Gemitzi & Lakshmi, 2018). However, GRACE only supplies data from 2002, and given that the dynamics of groundwater are not solely a function of temporal patterns in pumping, but are also affected by inter-annual to multi-decadal climate variability (Jean Kuss and Gurdak, 2014), observations over longer time-periods than that which GRACE analyses currently permit are required to separate the respective impacts of anthropogenic activities (land use changes, abstraction) and climate on water resources.

Carvalho Resende *et al,* (2018), addressed this need to extend storage information provided by GRACE to the "past" by developing a Simple Water Balance Model (SWB Model) to "reconstruct" past groundwater storage changes fluctuations. This allowed the potential effects of anthropogenic activities and climatic oscillations cycles such as the El Niño Southern Oscillation (ENSO) (2–7 year cycle), Pacific Decadal 20 Oscillation (PDO) (10–25 year cycle), and Atlantic Multi-decadal Oscillation (AMO) (50–70 year cycle) on large aquifers (area > 100 000 km²) in Africa.

1.4 THIS STUDY

This study builds directly on Carvalho Resende *et al,* (2018), which aimed to address these gaps in the knowledge in aid of better water resource management. This research is comprised of a global study to consider how varying climate indices have affected groundwater storage change over the past thirty years. There have been a number of studies which address these issues on a small local to regional scale, however there is a lack of quantitative evaluation of the potential effects of climatic oscillations cycles on large aquifers (Carvalho Resende et al., 2018). On top of this there has been a very limited number of studies assessing these impacts at global scale and what their implications in terms of management and policy decisions are (Carvalho Resende et al., 2018).

This study will use this SWB Model to recreate monthly Total Water Storage (TWS) change over differing aquifer systems for the last 37 years. As this model was made as an extension of GRACE, a comparison will be conducted to see how well they fit together. This body of work will then look to validate the SWB Model and their connection between groundwater and oceanic and atmospheric indices against groundwater observations.

1.4.1 Objective

The main objective is to build on the methodology laid out by Carvalho Resende *et al,* (2018) and assess if improving its accuracy and automating the climatic data processing through MATLAB will progress it as an approach and increase its usability.

In addition, the aim is to evaluate the SWB Model as a tool for groundwater resource management and planning. With many of these large aquifer systems covering areas varying in economic and socio-economic circumstance, where associated transboundary disputes reduce the potential for productive sustainable resource management, the approach needs to be easily usable and accessible. This evaluation of the SWB Model will be done through a global study using the approach to assess the impact of climate variations on groundwater storage change on different parts of the world.

1.4.2 Research Questions

With the general lack of monitoring and groundwater data available, there is a real need for managers and policy makers to have more information at their disposal to make informed and effective decisions, especially with groundwater growing in importance as a resource with climate change and population growth. The following research questions were designed to help address and fulfil this study's main objectives;

1. How useful is the SWB-Model as a tool for global scale groundwater evaluations against climate variability, and dose it fit within the framework of the UNESCO Groundwater and Climate Change (GRAPHIC) program?
2. Can the data processing be refined and automated through MATLAB to increase accuracies and usability of the methodology?
3. What are the circumstances and characteristic that make the SWB-Model most appropriate for the representation of GRACE and groundwater storage change?
4. How do global climatic oscillations cycles (like ENSO, PDO, and AMO) affect groundwater storage in large aquifers (area > 100 000 km²) around the world?
5. Is variability in groundwater storage changes on inter-annual to multi-decadal timescales better correlated to climatic factors or to temporal trends in groundwater pumping?

1.4.3 Study Outline

Firstly Chapter 2 indicates where the study areas are, and then introduces the main global-scale climate oscillations that are thought to influence water resources at a local level. Chapter 3 outlines the methodology used. Chapter 4 provides the results and analysis of the study. Chapter 5 provides a more extensive discussion of the results and their implications. Finally, the conclusion in Chapter 6 addresses the research questions, looks at the usability of the model and results in terms of ground water managers and policy makers, and reflects on the research involved.

Chapter 2 STUDY AREA & CLIMATE OSCILLATIONS

This chapter introduces the geographic and climatic settings that are key to this study. The first section presents general information about the selection of the study areas, and their geographic locations. The second section introduces the main global-scale climate oscillations that are thought to influence water resources at a local level.

2.1 STUDY LOCATIONS

To get a better understanding of how the SWB-Model works and where it can be applied, a global study was conducted. The study areas were selected to meet four main criteria:

- There needed to be many different types of environments – so a good spread across the globe was selected.
- On top of this Africa, as one of UNESCO priority areas, was looked at more closely.
- The size of the areas was restricted to being around 100,00km^2. This contributes to accuracy as this area is about the size of the GRACE footprint.
- It was important to not only select important regional aquifers (like High Plans, MDB and Ganges) but to include areas that see little monitoring as these are the places that this kind of approach will have the most utility .

An initial selection of 26 sites was made. It was thought that this number would allow for a number of sites to be selected in similar environments providing room for redundancy if some sites had to be later removed because of problems with data availability. In the end all 26 sites were used in the SWB Model and GRACE, but due to missing groundwater observations three locations couldn't be verified (Congo, Amu Darya and the Ganges). Figure 1 is a map of these study areas where green zones are aquifers and blue zones are river basins.

2.2 CLIMATE VARIABILITY AND INDICES

Climate variability, the natural climate fluctuations of various periodicities, has been well studied, much data has been gathered on a regular basis from around the world over the last 150 years. Past climates have also been reconstructed from the paleo-climate archives (ice caps, tree rings, paleo sands etc.), which have allowed climate scientists to observe global-scale climate oscillations on inter-annual to multi-decadal timescales. This record along with modern climate modelling has become a powerful tool for understanding these natural climatic cycles. These cycles are caused by the exchanges between the Earth's atmosphere, oceans, cryosphere, and continental hydrology (Carvalho Resende et al., 2018). The main global-scale climate oscillations that are thought to influence water resources on a local scale are the El Niño Southern Oscillation (ENSO), North Atlantic Oscillation (NAO), Pacific Decadal Oscillation (PDO), Indian Ocean Dipole (IDO) and Atlantic Multi-decadal Oscillation

(AMO) (Carvalho Resende et al., 2018; Gurdak et al., 2007). To help monitor these oscillations, scalar-valued indices are used, with there strength characterized as being positive, negative, and neutral (Carvalho Resende et al., 2018).

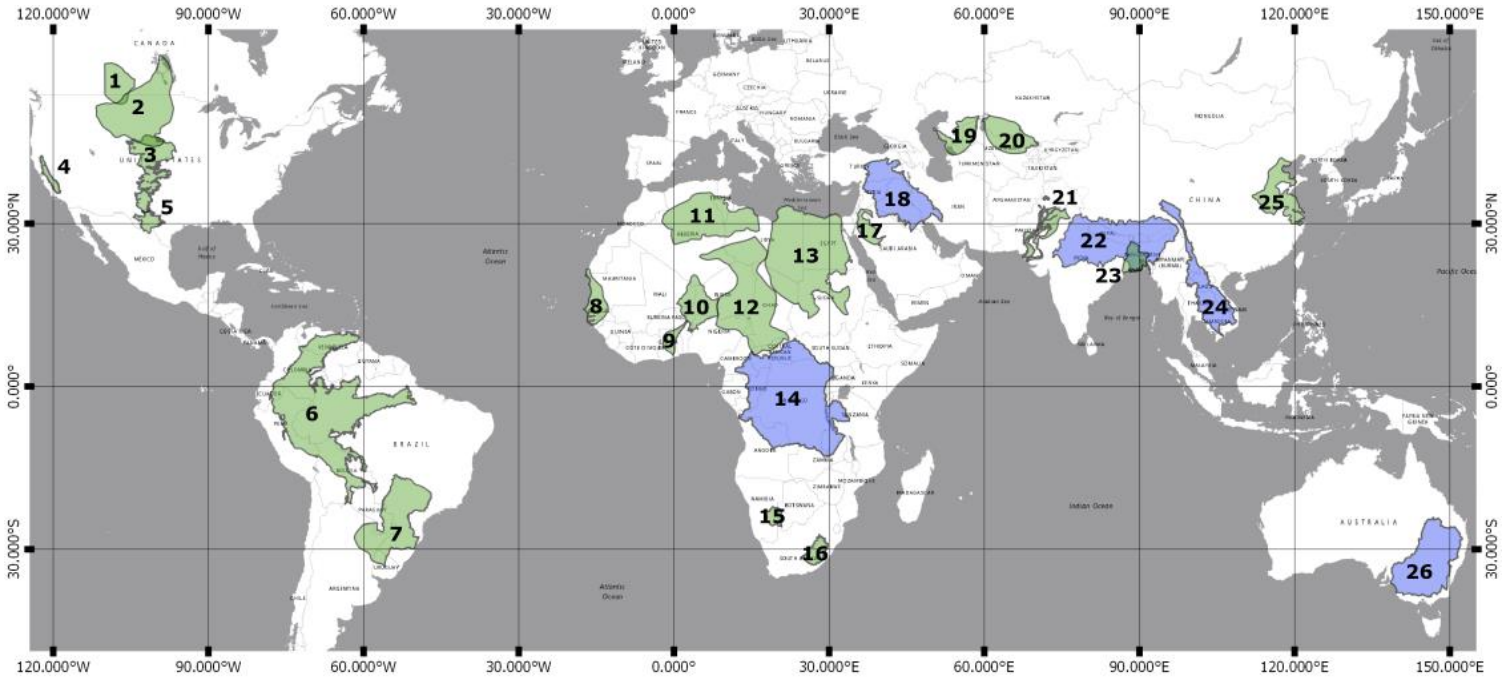

Figure 1: World Map of Study Areas: Blue indicates the river basins while green shows aquifers: 1) Northern Great Plains, 2) Judith, 3) High Plains, 4) Central Valley, 4) Edward Trunity, 6) Amazonas, 7) Guarani, 8) Senegalo-Mauritanean, 9) Volta, 10) Iullemeden, 11) North West Sahara, 12) Lake Chad, 13) Nubian, 14) Congo, 15) Stampriet, 16) Karoo Sedimentary, 17) Saq Ram, 18) Tigris Euphrates, 19) Amu-Darya, 20) Syr-Darya, 21) Indus, 22) Ganges, 23) East Ganges, 24) Mekong, 25) North Chain Plains, 26) Murry Darling Basin.

El Nino Southern Oscillation (ENSO)

ENSO is considered to be the strongest and most influential global signal of the inter-annual climate variability's and as such has been the focus of most studies (Neeling, 1994). Bjerknes 1969 hypothesises that ENSOs dominant physical processes arises through the coupled ocean - atmosphere interaction in the tropical Pacific (Neeling, 1994). Its two to seven year cycle has been occurring for at least 700 years, alternating between a positive phase (La Niña) and a negative phase (El Niño) (Carvalho Resende et al., 2018).

In the neutral phases – or neutral conditions – the Hadley circulation contributes an easterly component to tropical surface winds (Figure 2). This is strongly reinforced over the tropical Pacific by the Walker circulation driven by the strong sea surface temperature (SST) gradient, where warm wet air rises in the west (creating precipitation) and cool dry air sinking in the east (Neeling, 1994). In El Niño years this circulation is weakened, meaning less warmed surface water is being pushed west. This increases the temperature of the central and eastern equatorial Pacific Ocean and decreases the temperature gradient. The West Pacific convective center is displaced eastward, moving the region of intense tropical rainfall.

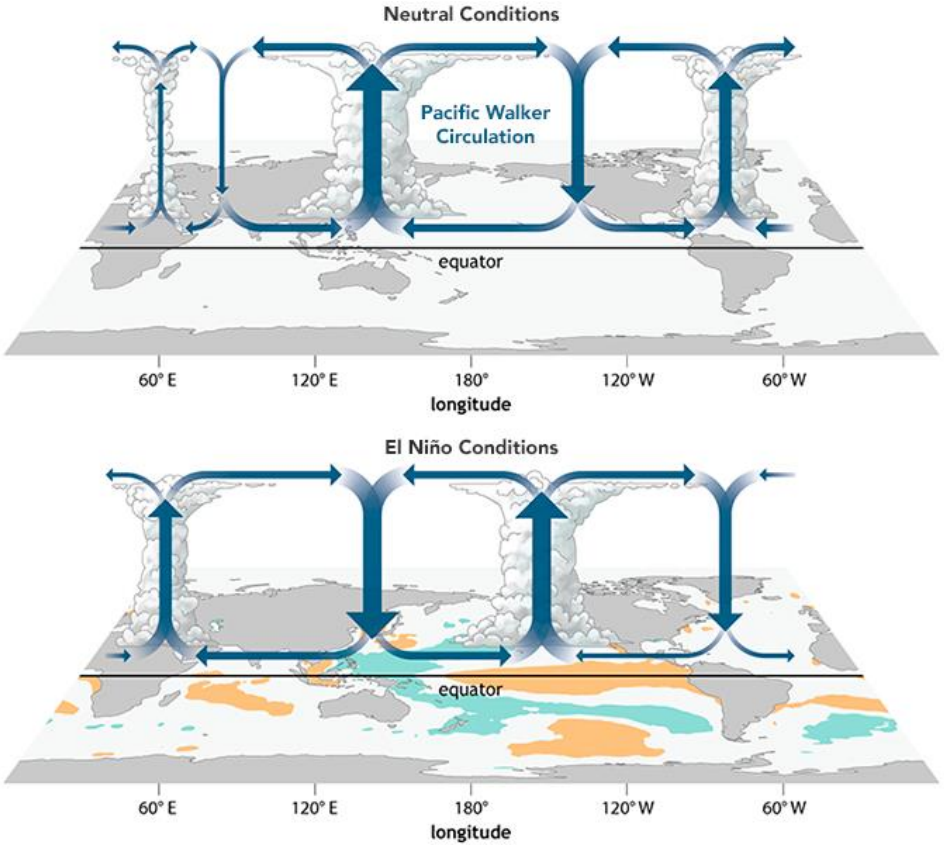

Figure 2: Neutral and El Nino Conditions (Illustration by NOAA/Climate.gov)

In Figure 3 below, La Niña is characterized by the opposite or a magnification of the neutral condition, with stronger than normal easterly trade winds and a westward shift of the region of intense tropical rainfall (Carvalho Resende et al., 2018).

Since the 1980s, the years 1982–1983, 1997–1998 have seen stronger than normal El Niño, and more recently 2015–2016. Although ENSO is centered in the tropics, the changes associated with El Niño and La Niña events affect climate around the world.

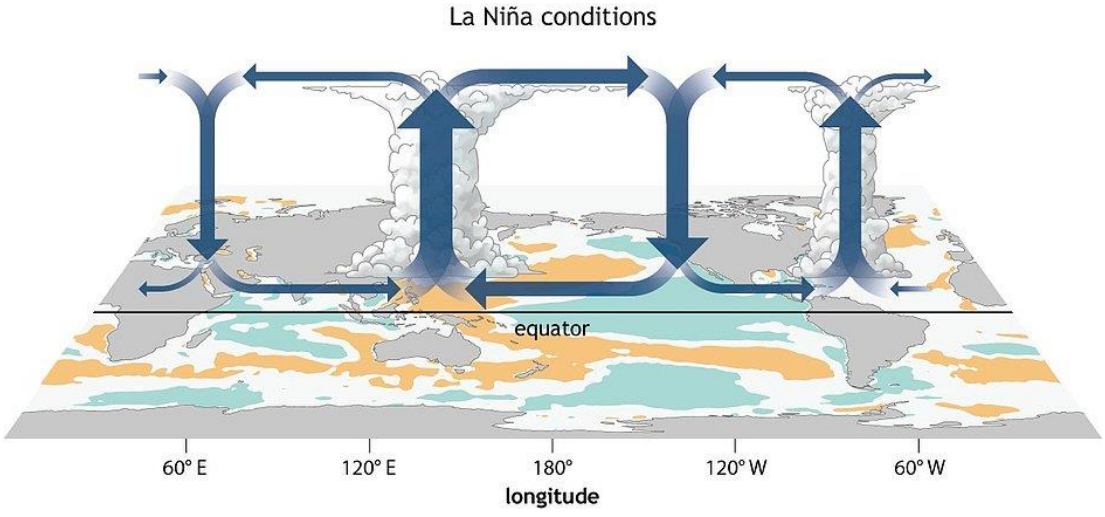

Figure 3: La Niña Conditions (Illustration by NOAA/Climate.gov)

Atlantic Multi-decadal Oscillation (AMO)

The AMO is a decadal variation influencing the Atlantic Ocean's climate. It is a pattern of oscillatory changes on the North Atlantic sea surface temperature (SST), which exhibits a negative and positive phase cycle of 20-40 years (Knudsen, Seidenkrantz, Jacobsen, & Kuijpers, 2011). Its full cycle of around 50-70 years however makes it difficult to observe whether the ocean circulation actually drives the phase changes, as the instrumental SST records only span around 150 years (Knudsen et al., 2011). Whether it is truly an oscillatory phenomenon or merely reflects a transient feature on a 'red noise' background is still debated. However, Paleo climatologic studies have confirmed that these changes have been occurring over the past 8000 years (Knudsen et al., 2011). Recently (within this study's observational time frame of 1980 to 2016) there has been a negative phase from 1970 to 1990, which subsequently flipped to a positive phase in the mid-1990s (Carvalho Resende et al., 2018).

Pacific Decadal Oscillation (PDO)

The PDO is a climate index based on patterns of variation in the sea surface temperature of the North Pacific Ocean. It is another dominant Pacific Ocean climate index and is thought of as a more enduring El Niño-like pattern with warm and cool periods lasting 20 to 30 years (Zhang et al. 1997). However the PDO is not a single physical mode of ocean variability like ENSO, but rather it is the sum of several processes with different dynamic origins (Carvalho Resende et al., 2018).

Indian Ocean Dipole (IOD)

The IOD is the dominant climate variation occurring in the Indian Ocean. It refers to the year-to-year SST change from the East to the West Indian Ocean. The IOD has three phases, positive, neutral and negative, and a phase switch of around three to five years. The neutral phase sees warm waters moving through Indonesia from the pacific to the west, this encourages warm air to rise here and then sink off the coast of Africa leading to westerly winds along the equator. Negative phases see these winds intensifying which leads to less warm water escaping into the Indian Ocean from Indonesia, further intensifying the winds. The positive phase has the opposite effect, and results in the winds weakening.

North Atlantic Oscillation (NAO)

Another important inter-annual climate variability influencing the global circulation is the NAO. This North Atlantic phenomenon is related to the north-south variation of atmospheric mass between the Icelandic low-pressure system and the Azores high-pressure system. The index for this climate variation looks at sea level pressure (SLP), it is positive when there is a below normal SLP over Iceland and above-normal surface pressure over the subtropical Atlantic, making the pressure gradient stronger (Carvalho Resende et al., 2018). A negative value accrues with the opposite, when the pressure difference between Iceland and the Azores is low. It sees irregular one to twenty-four year inter-seasonal, inter-annual, and multi-decadal variability, while also showing a dominant quasi-periodic oscillation of three to six years and a less significant eight to ten-year mode (Carvalho Resende et al., 2018).

Chapter 3 METHODOLOGY

This chapter will now outline the approach that has been taken in order to realise the research objectives laid out in the first chapter. Figure 4 shows a flow diagram of this approach and the steps needed, including where data processing took place. The numbering shows the order of the steps taken and, in the bottom left corner the action taken on the data is indicated in the Figure key through the type of box shape.

To get insights on the correlation between natural climate variability and groundwater levels (GWL) change in each study site, wavelet analyses between different climate indices (e.g. ENSO, PDO, AMO) and the modelled GWL change – derived from a SWB model were carried out for each studied aquifer system. This model required the acquisition and processing of global precipitation and evapotranspiration data. Two approaches were taken to validate the SWB model. Firstly, GRACE Total Water Storage (TWS) data was obtained and processed to compare against the SWB Model for the period between 2003 and 2015. Secondly, groundwater storage change was also compared against the SWB Model to add the validation with some ground truthing.

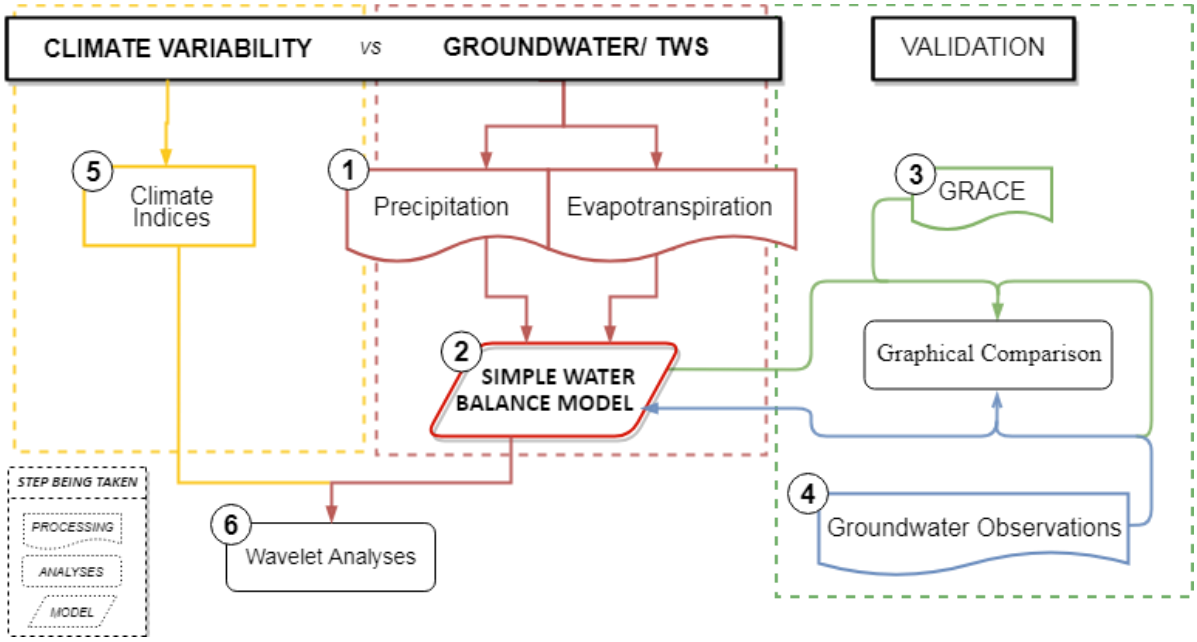

Figure 4: Flow diagram showing key research steps.

3.1 WATER BALANCE MODEL

The SWB model (MATLAB script can be found in Appendix 1: Simple Water Balance Model) used in this study builds upon that developed by Carvalho Resende et al. (2018) to assess the impacts of climate variability on total water storage across Africa and their implications for groundwater resources

management on a monthly basis from 1982 to 2012. Their original model was developed to provide an easy and simple approach to assess the impacts of climate variability on TWS change across Africa. This TWS change can be considered as the change in groundwater storage when a few assumptions are made, this will however be discussed later in this section. The SWB Model was developed to use global datasets that are freely available requiring relatively low labor intensity and financing. The model is based on a simplified variation of the general water balance.

$$\frac{dTWS}{dt} = P - ET - R \qquad \textbf{EQUATION 1}$$

In this equation, TWS is the total water storage and includes the changes in water stored in vegetation, ice, surface water and, the vadose zone and groundwater. P is precipitation, ET is evapotranspiration and R is runoff. This equation can represent monthly water budgets of a catchment – however, it does not show monthly accumulated fluxes. When used on the time series (of a monthly time step) each point is independent from the last month making it hard to conceptualize the TWS change through time (Figure 5).

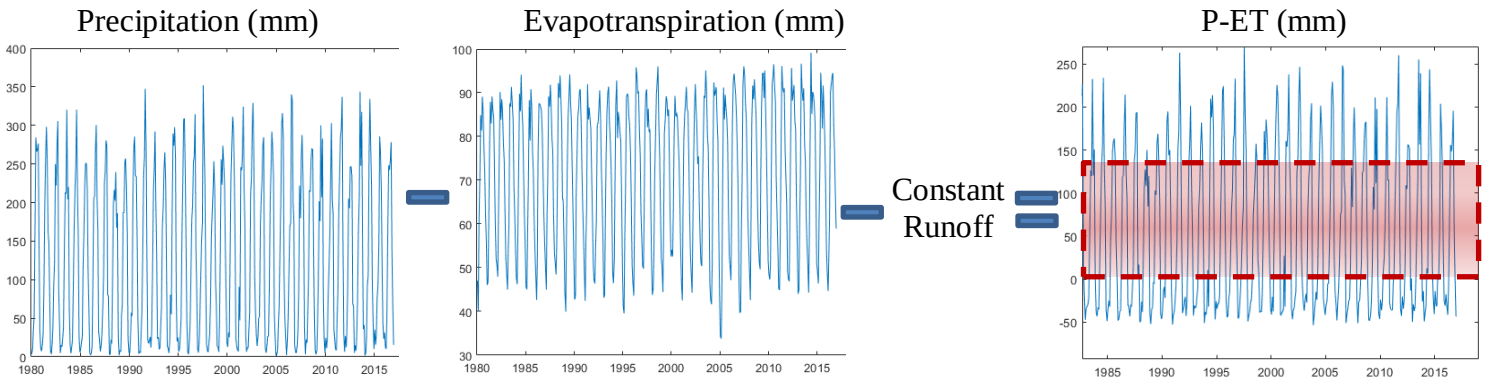

Figure 5: A Visualization (Mekong) for the subtraction of P from ET

Figure 5 shows the area of interest is the variations of the residuals (area roughly outside the red box). To inspect this monthly accumulated flux in order to see the periods and at what intensities water is being stored or depleted, a cumulative integral of the data was performed before the subtraction of ET from P (Figure 6). This shows how much water is being removed or stored over time, showing the trend along with the monthly and periodic fluctuations.

$$\boldsymbol{TWS_{MODEL}} = \int \boldsymbol{P_{dt}} - \int \boldsymbol{ET_{dt}} - \int R_{dt} \qquad \textbf{EQUATION 2}$$

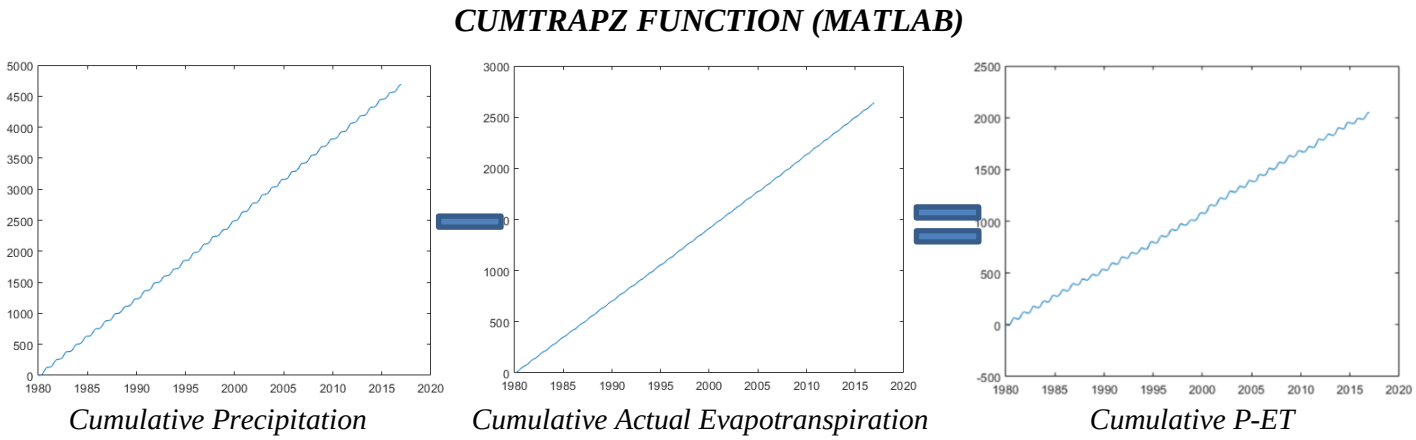

Figure 6: Visualization (Mekong) of the cumulative integral P - ET

Next the cumulative integral is de-trended (Equation 3). This is the subtraction of the mean (or a best-fit line), in the least-squares sense, from the data. It is also seen visually below in Figure 7.

With the removal of the R the equation becomes:

$$TWS_{MODEL} \approx detrend\left(\int P_{dt} - \int E_{dt}\right) \qquad \text{EQUATION 3}$$

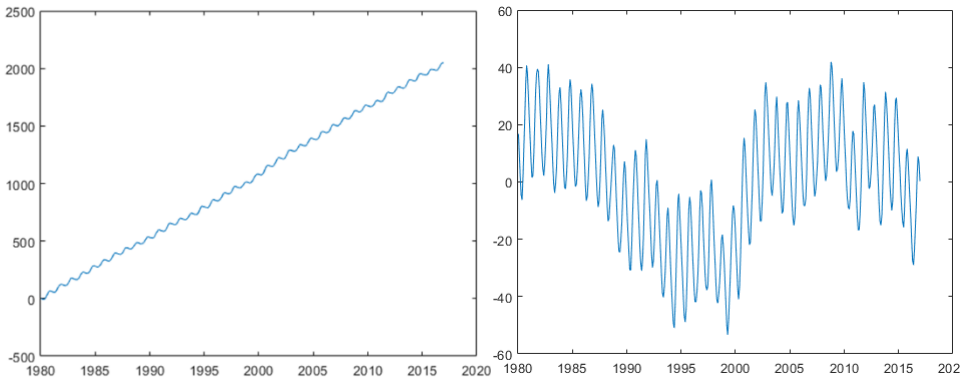

Figure 7: Visualization (Mekong) cumulative integral detrending, right graph is non de-trended, and left is de-trended

This detrending has four related purposes. Some of these rely on broad assumptions that need to be correct or close to the truth for conclusions about the GWS change to be drawn with any confidence. These four purposes are that:

1. The trend is often of little interest as we want to uncover the periodicities in the series (the mean is a cycle of frequency zero per unit time; it is a constant) (Hill, 2007). It can have strong effects that may mask the more interesting periodicities in the data, and thus it is removed prior to the analysis (Hill, 2007). The overall trends in water storage are not the focus of this work; rather the sub-trends of water flux in storage are examined.
2. Removing the trend obtains the flux integrated TWS anomalies and when this is done over the same time span as the GRACE mission results from the SWB Model and GRACE should match (Springer et al. 2014, and Thomas et al, 2019).

3. The systematic errors from the global climatic databases used for P and E will lead to predictable and consistent departures from the true value because of defects and inbuilt faults of the model apparatus. Systematic error occurs only in 1 direction, it always gives a similar error. By removing the linear trend these systematic errors are removed.
4. Runoff data was not collected so an assumption is made for the equation that runoff would either be considered to be constant or negligible compared to the groundwater body. Runoff can also be considered as removed (through detrending) if the fraction of precipitation that results in surface runoff is also considered constant. This can be the case for certain circumstances and areas, however, must be considered carefully as this is not always the case. If runoff is constant its trend will be linear, when the equation is de-trended runoff is removed.

In essence this detrending leaves the atmospheric deficit fluxes (an excess precipitation flux). In cases where surface water bodies are small – where there is no influence from snow and ice and soil moisture can be ignored – then TWS can equal GWS.

$$\boldsymbol{GWS \approx TWS_{MODEL} \approx detrend\left(\int P_{dt} - \int E_{dt}\right)} \qquad \textbf{EQUATION 4}$$

3.1.1 Evapotranspiration

Evapotranspiration data was downloaded from The Global Land-surface Evaporation Amsterdam Methodology (GLEAM). GLEAM uses a wide range of multi-satellite observations combined to estimate daily actual evaporation through a process-based methodology. This satellite-based observation approach was selected as it provides high-resolution, large-scale ET estimates covering the time frame needed for this research (1980 – 2016). The GLEAM results were also found by Miralles et al. (2016) to provide a robust data solution when compared with other global terrestrial evaporation data sets (such as the Penman–Monteith approach from the official MODIS Evapotranspiration Product and the Priestley–Taylor JPL model). However, it was still found that scrutiny is required to correct for systematic errors in these estimates, especially in a study like this spanning much of the globe. This study only addresses this issue where the systematic errors are considered linear. The data used was from version 3.2 – where the global datasets are available on a 0.25° (around 11 km) latitude-longitude regular grid and at daily temporal resolution and available in a Network Common Data Form (NetCDF). MATLAB was then used to extract the data for specific areas and times of interest and averaged to produce the monthly total value.

Grid Coordinates:

With the data in a global grid of 0.25° by 0.25° (720:1440 cells), accurately finding the cells representing each of the 26 study areas was essential. The coordinates for a specific study area were found in QGIS by converting its shape file into a raster and then translating this format into an ASCII file, this allowed the data to be exported and used. This primarily supplied a binary matrix of the study area (discussed in the next paragraph) and secondly supplied precise longitude and latitudes values for the bottom left hand corner of the matrix. This information along with the number of cells in its width and lengths meant the square area around the study area could be isolated and cut from the global data set by MATLAB giving a series (at a daily time step) of study area data matrices.

Mask:

This binary grid exported from QGIS (where values inside the study areas boundary were 1 and values outside the boundary were 0) was then used to create a mask to be used to further isolate the data down to only the values inside the study areas boundaries. This was done by multiplying this mask with the study areas' data matrices cut from the global data set. To make certain that the cells within the boundary that had the value 0 counted in the total average, the values outside of the boundaries in the mask were converted to "NaN". It was also important to add 1 to the starting cell grid coordinates in the MATLAB script as data in the PANOPLY format start at 0 where MATLAB starts at 1.

Days to months:

As the data came in yearly files (one file for each 37 years), the daily data matrixes were imported to MATLAB by months. Then this array of daily matrixes needed to be summed to give one matrix representing a monthly total at each cell. This could then be averaged giving that month's average evapotranspiration, this was done for each month of the year. Then a loop was done to include all thirty-seven years resulting in a list of monthly averages from 1980 - 2016.

3.1.2 Precipitation

Precipitation data was downloaded from Global Precipitation Climatology Centre (GPCC), where the Full Data Monthly V.2018 was used for the period from 1980 – 2016. The monthly Land-Surface Precipitation is from Rain-Gauges built on GTS-based and Historical Data. This data source was selected as it is optimized for best spatial coverage and for use in water budget studies. Gridded data was selected at a resolution of 0.25° degrees lat/long.

Due to the GPCC data being available in monthly averages, processing was found to be much easier. The full global data set came in one NetCDF file with data from 1891 - 2016, the monthly (time step) matrix was cut and exported from the global data set in the same way as evapotranspiration. However, the data obtained was organized in a flipped orientation – meaning when using the mask, it had to first be non-conjugatedly transposed. Just as with evapotranspiration, 1 was added to any coordinates as Panoply and MATLAB start their coordinates at O and 1 respectively. When cutting the data from the global data set it was specified to start at time-step 1069, corresponding to January of 1980.

This multidimensional array of gridded precipitation values for study areas was then multiplied by the transposed mask and any negative values where changed 0 (some cells showed tiny negative deviations from 0 and have been attributed to calibration errors). Lastly each matrix was averaged to produce a list of value of monthly totals.

How It Was Run

This model was run in MATLAB where the script seen in Appendix 1was used. It started by importing the precipitation and evapotranspiration data for the given study areas. This was done by first separating the data from the time stamps. Then using the "cumtrapz" command, both the evapotranspiration and precipitation data were computed into approximate cumulative integrals. This was done via the trapezoidal method with unit spacing. According to MATLAB the size of the input data

determined the dimension that it was integrated along. After this was completed evapotranspiration was subtracted from precipitation, and this was then subsequently detrended. The MATLAB function "detrend" subtracts the mean or a best-fit line from your data, the trend was identified in the least-squares sense. Removing a trend from the data enables you to focus your analysis on the fluctuations in the data about the trend.

These monthly averages need to be for the area within the boundaries of the study areas being looked at and for a time period – in this case 37 years (1980 – 2016). This next section will go through how this was done for both model inputs, evapotranspiration and precipitation.

3.2 GRACE

3.2.1 GRACE Introduction

The GRACE project is a joint scientific satellite mission between the National Aeronautics and Space Administration (NASA) and Deutsches Zentrum für Luft- und Raumfahrt (DLR)) that has allowed for the accurate measurements of the Earth's time-varying gravitational field (Wahr et al, 2006).

The irregularities of the earth's gravitational field (gravity anomalies) are analysed with satellite to satellite tracking (SST) of the mission's twin satellites. The satellites travel at an approximate distance of 220km from one another and follow an identical orbital plain. This is measured continuously using a microwave ranging system. When a satellite moves over areas with stronger gravity (where there is greater mass concentration) the leading satellite will experience an initial acceleration increasing the distance from the tailing satellite. The tailing satellite will then follow over the area with the gravity anomaly and experience the same acceleration thus closing the gap between them again. This continued chasing of the two satellites gives them the nickname "Tom and Jerry" (Sahoo, 2017).

Even slight changes of distances between the two satellites enables time-variable changes in surface mass to be calculated. These calculations allow the changes in water stores over terrestrial bodies from ice, lakes, groundwater, atmosphere and ocean to be derived (Sahoo, 2017). GRACE's spatial resolution is on the hundreds of kilometres scale, and these estimates are made over arbitrary regions as a monthly average (Swenson & Wahr, 2002). However, this method can be very accurate measuring down to 1cm of equivalent water thickness (Swenson & Wahr, 2002).

The processing software developed for the GRACE data has been independently made by three main processing centers: University of Texas Centre for Space Research (CSR), Deutsches GeoForschungsZentrum (GFZ), and NASA's Jet Propulsion Laboratory (JPL). These groups take the gravity data and through different processing strategies and tuning parameters, produce results with regionally specific variations and error patterns (Sakumura, Bettadpur, & Bruinsma, 2014). They can be considered as different observations (using the same data but different geophysical models, processing methods, and software) which describe the same signal and noise (Kusche, Schmidt, Petrovic, & Rietbroek, 2009).

3.2.2 Processing

The GRACE solutions used in this thesis were obtained off "the-GRACE-plotter" website (http://thegraceplotter.com/). Their user-friendly data grids of Equivalent Water Heights (EWH) as global time series are currently available from this website, and these data grids have had most geophysical corrections applied to them. The main sets of results produced by the differing gravity field models can be easily obtained. As mentioned above CSR, JPL and GFZ (all supported by the NASA MEaSUREs Program), were used and the EWH from the three solutions were downloaded for each of the 25 study areas.

Pre-data processing:

These three solutions are based off of the latest version of level 2 data (RL05), where their gravity solutions were decorrelated and smoothed (the time-variable part was post-processed through the DDK filters) to reduce nose and increase accuracy (Kusche et al., 2009). They are also processed by removing the non-hydrological gravitational contributions based on corrective numerical models (Mccullough, 2013). Models of glacial isostatic adjustment, mass of the atmosphere and high frequency wind and pressure driven ocean motions, so that the remaining variability can be attributed primarily to the redistribution of terrestrial water storage (Hossain, 2014).

The site, in order to plot the time series of the equivalent water heights, removes **the mean** or 'Static Field'. After the mean field is subtracted, the remaining signals vary around zero, showing there are mass gains (positive change), and mass losses (negative change). The surface mass change is mass/area, and since most of the temporal changes are related to water, they divide mass/area with water density (1000 kg/m^3), which yields the commonly used unit of 'equivalent-water-height' (centimeters). Thus, GRACE does not measure total/absolute water storage. Rather, it is more helpful to think of it as an accurate scale that can detect and quantify when mass changes (but we typically don't know where 'the zero' is). Their coefficients are converted into 1o x 1o equivalent water height grids. This conversion to grids also considers spherical harmonic coefficients from degree 2 to degree 90.

Downloaded

The data for each study site was obtained by positioning rectangular boxes over their locations on the presented global data map (see Figure 8). The average of the data within the box are then available for download in a monthly time step for the entirety of the GRACE mission from 2003 - 2014. The box was positioned over each study area by entering coordinates obtained from the four corners of the aquifer or basins shapefiles (used in QGIS). The EWH (for the selected study area) is then plotted for the full available time frame (CSR and JPL have data available from 2002 – 2016 and GRZ only has available 2003 – 2014) and this can then be download as a text file.

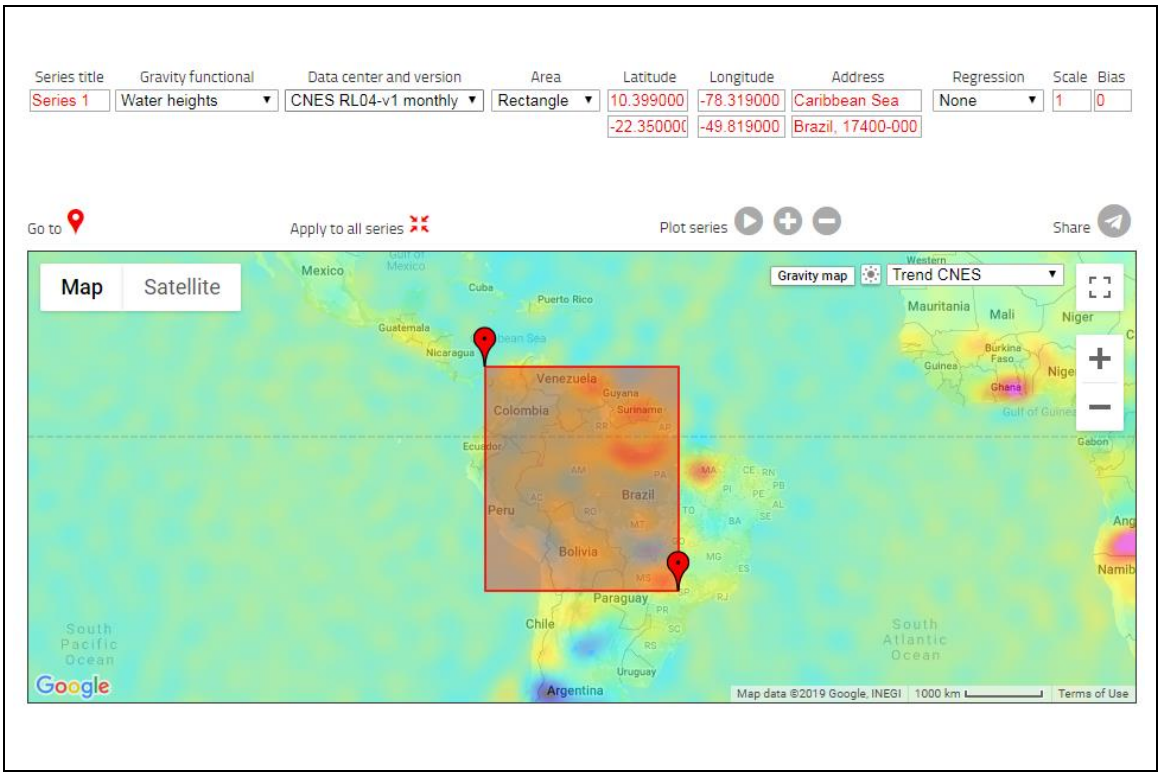

Figure 8: The-GRACE-plotter interface, downloading grace data for the Amazon

Post-data processing:

With the study areas covering all continents and environments (Figure 1) a versatile solution was needed to produce good results in all study areas. Sakumura et al. (2014) showed that an ensemble solution using the arithmetic mean of all three scaling approaches (CSR, GFZ or JPL) actually reduces the noise in equivalent water height by 5‑10 mm. Hence, in this body of work, the arithmetic mean of the CSR, GFZ and JPL solutions was implemented (Liesch & Ohmer, 2016).

Figure 9 shows the GRACE solutions vs their average and it can be noted that the average (seen in black) is always reducing the furthest distance from the model compared to the individual solutions.

Several gaps in GRACE data can be found in all solutions starting from 2002. However, the initial decade sees few of these gaps. Since 2011, data gaps in GRACE have been caused by battery management issues on the satellites. These gaps occur approximately every five‑six months, and last around four weeks. The gaps were filled by linear interpolation of the adjacent months.

The GFZ solution sees large gaps in its data both at the start and at the end of the mission. As the average of the three solutions is required, the time frame for GRACE data needed to match that of this shortest available data set covering a period 2003 to the end of 2014.

Once the gaps in the GRACE data had been managed and the three solutions were averaged the results were then standardized as to make ready their comparison with the modelled data and groundwater observations.

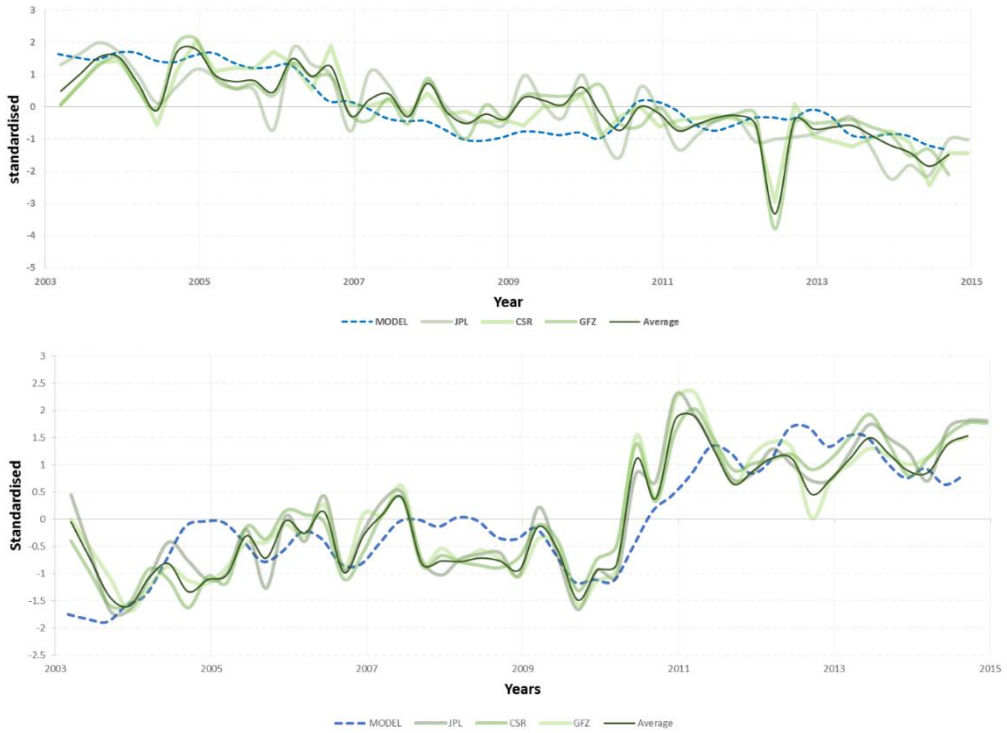

Figure 9: GRACE individual solutions vs average of all three: (a) Saq Ram, (b) Judith

3.2.3 Problems with GRACE

When using GRACE satellite data there are several challenges that come up. These are to do with the technical limitations and lack of real-world observations to check against. Here are the three most influential ones:

(1) No vertical resolution:

GRACE data has no vertical resolution (Wahr et al., 2006). The changes of mass at the surface, in the atmosphere, and underground are indistinguishable (Wahr et al., 2006). This is in some way the contrasting problem to land surface modelling where certain processes may not be accounted for. Grace data accounts for almost all water movement processes but can't distinguish between them. This relationship makes them complimentary to each other, where GRACE can be used to help validate TWS change models and the modelling can help identify contributions of the differing water storages to the TWS.

(2) Lack of groundwater data:

With other types of remote sensing missions, their estimates often need to be verified for them to be considered as "meaningful results" (Wahr et al., 2006). The physics around Newton's law of gravity and the second law of motion and how they relate to orbital motion and mass anomalies are so well understood it is often possible to estimate these errors from the GRACE fields themselves (Wahr et al., 2006). Though this need for real validation is reduced it is still essential to compare it against real data for any confidence in the results produced. Depending on the data solution you use in some cases like areas of arid environments or abstraction can have results that vary greatly (Wahr et al., 2006). However, the average of the three solutions see these variations minimized. This validation is normally

done through ground truthing and here observed water levels will be compared with the obtained GRACE data for validation.

(3) Type of aquifer:

GRACE GWS changes are likely to result from unconfined aquifers storage changes because storage coefficients in confined aquifers are typically a couple of orders of magnitude less than those in unconfined aquifers (Scanlon et al., 2010a; Scanlon et al., 2010b). Therefore, GRACE is mainly applicable to aquifers with renewable groundwater. Furthermore, leaking of errors and uncertainties from models used in GRACE observations processing leads to difficulties to address GRACE trends for aquifers located close to lakes (Victoria, Chad, Malawi, Tanganyika, Baikal, Aral Sea) and glaciers (Coarvalho Resende, 2015)

Additionally, it is worth mentioning that not all groundwater depletion arises from pumping. In some aquifers, long-term drainage and water table declines resulting from climate change—perhaps thousands of years ago—can cause depletion under predevelopment conditions (Alley & Konikow, 2015).

3.3 GROUNDWATER OBSERVATION

Due to the general lack of data, the selection of records for the validation of the model was done based on the longest continuous monthly long-term groundwater level records available in literature and their representativeness.

Table 1 indicates the different sets of data used in the study. Observations were generally located within 20 km from a surface water body and they are taken from shallow aquifers as this is what GRACE can detect. This is partly to do with how deeper confined aquifers having a lagged response to large scale climate change, and often these are not affected by these short term (interannual to multidecadal) climate variability (Jalota *et al*, 2018). The records provide groundwater levels at a monthly basis for different periods ranging from five to 20 years. Some gaps in the chronicles exist – though these were filled by interpolation of the adjacent months for this study. The WebPlotDigitizer (Version 4.2) software was used to reverse engineer images of data visualizations to extract the underlying numerical data. It is a semi-automated, free to use, open source tool that works with a wide variety of charts (XY, bar, polar, ternary, maps etc.).

A single long-term time series of groundwater level is given for each studied aquifer/basin by standardizing well data. When several records are available per aquifer system, groundwater level of each well is standardized and then averaged across all wells to form a single time series. This procedure eliminates the difference and locality of well levels (Wang *et al*, 2016)

Aquifer System		Groundwater-level time frame	Well/Borehole depth	Source
1	Central Valley Aquifer	1994-2015	Average of 4 shallow piezometers	USGS and California Department of Water Resources
2	High Plains Aquifer	1982-2010	Average of 23 shallow piezometers	USGS
3	Northern Great Plains Aquifer	1982-2011	Average of 22 shallow piezometers	USGS and Geological Survey of Canada
4	Judith Aquifer	1982-2015	Average of 20 shallow piezometers	Geological Survey of Canada
5	Edwards Trinity Aquifer	1982-2005	Average of 8 shallow piezometers	Texas Water Development Board
6	Amazonas Aquifer	2010-2015	Shallow piezometer (Manaus - vicinity of Amazonas River)	Neves Miranda, 2017
7	Guarani Aquifer System	2004-2009	Shallow piezometer <20 m	Cabrera et al., 2010
8	Guarani Aquifer System	2008-2014	Shallow piezometer <20 m	Nava and Manzione, 2015
9	Northwestern Sahara Aquifer System	1982-1997	Shallow piezometer (located near the aquifer boundaries)	Nazoumou, 2002
10	Nubian Sandstone Aquifer System	1998-2004	Shallow piezometer (vicinity of Lake Nasser)	Hussein, 2018
11	Senegalo-Mauritanian Basin	1997-2002	Shallow piezometer (vicinity of Senegal River)	Gning et al., 2015
12	Illuemeden Basin	1991-2007	<75 m (<75 km from the Niger River)	Updated from Favreau et al., 2009
13	Lake Chad Basin	2006-2011	85 m (Maiduguri – vicinity of Lake Chad)	Vasollo, 2017
14	Volta Basin	1980-1996	20m (Ouagadougou)	Mouhouyouddine et al., 2017
15	Congo River Basin	N/A	N/A	N/A
16	Stampriet Aquifer System	1985-2008	<50m	Updated from UNESCO, 2016
17	Karoo Sedimentary	1994-1999	<10m	IGRAC, 2017
18	Saq Ram Aquifer	2000-2010	Shallow piezometer (next to Zarka)	Al-Zyoud et al., 2015
19	Tigris Euphrates River Basin	2006-2011	<100m	Seeyan et al., 2014
20	Amu Darya Aquifer	1990-2000	Shallow piezometer in Khorezm region	Ibrakhimov et al., 2007
21	Indus Aquifer	1987-2004	<100m	MacDonald et al., 2016
22	East Ganges Aquifer	1985-2006	<100m	Shamsudduha, 2011
23	North China Plain Aquifer	1982-2008	Average of 3 shallow piezometers	Cao and Zheng, 2016
24	Mekong River Basin	1994-2006	Average of 3 shallow piezometers	Johnston et al., 2013 and CWRPI, Vietnam
25	Murray Darling River Basin	1980-2011	Average of 3 shallow piezometers	Australian Water Resources Assessment, 2012

Table 1: List of aquifer systems and their groundwater observations. From the row on the left moving right 1) Number, row 2) Name, 3) shows the timeframe of the collected observations, 4) Depth of observation and 5) the source of the data

3.4 CLIMATE INDEXES

A climate index is a common way to identify the status of a particular climate variation pattern. It is a number scale where identifying factors needed to describe the phenomenon are boiled down to track states of the pattern over time.

All the time series data for the climate variability indexes for this body of work were obtained from National Oceanic and Atmospheric Administrations (NOAA), Earth System Research Laboratory or ESRL. Here free monthly indices are available for download for the time period between 1980 - 2016. They were all downloaded as a text file and reduced to two columns (date and index). As there are different ways for calculating these indexes (enabling a look at different climate aspects – ocean temperature, pressure, radiation, wind or a combination of these) this next section will briefly discuss what each index of interest in this study is really measuring.

El Nino Southern Oscillation (ENSO)

As ENSO is a multifaceted climate variation, involving different aspects of the ocean and the atmosphere over the tropical Pacific, there are several indices that can be used. For this study a bi-monthly Multivariate index (MEI.v2) was chosen and obtained at the ESRL website. This time series made up by the leading combined Empirical Orthogonal Function (EOF) sees five different variables being taken into account: 1) sea level pressure (SLP); (**2**) sea surface temperature (SST); **3-4**) zonal and meridional components of the surface wind; and **5**) outgoing longwave radiation (OLR) over the tropical Pacific basin (30°S-30°N and 100°E-70°W). To take into account ENSOs seasonality and to reduce the effects of higher frequency intra-seasonal variability, the index is calculated for 12 overlapping bi-monthly "seasons" (Dec-Jan, Jan-Feb, etc.).

Atlantic Multi-decadal Oscillation (AMO)

This time series is calculated from the Kaplan SST dataset (Gridded global SST anomalies from 1856-present and is derived from UK Met Office SST data) which is updated monthly.

Pacific Decadal Oscillation (PDO)

The Pacific Decadal Oscillation index was also obtained using EOF analyses. It is based on the temporal covariance matrix and is calculated off the monthly SST, looking at the SST anomalies poleward of 20°N in the Pacific basin.

North Atlantic Oscillation (NAO)

The North Atlantic Oscillation is often defined as the normalized pressure difference between the Azores and Iceland. Here we used data from the SW of Iceland (Reykjavik), Gibraltar and Ponta Delgada (Azores).

Indian Ocean Dipole (IOD)

The Dipole Mode Index is derived by the SST gradient between the western equatorial Indian Ocean (50E-70E and 10S-10N) and the south eastern equatorial Indian Ocean (90E-110E and 10S-0N).

3.5 WAVELET ANALYSES

To analyse both amplitude and frequency of the correlations between climatic indices and the SWB Model time series, a wavelet transform was used.

Why wavelet transform:

This method of examining periodicities in the frequency domain is popular for its ability to examine non-stationary processes (Grinsted et al, 2004). Unlike traditional mathematical methods like the Fourier analysis, it can expand time series into time frequency space and can therefore find localized intermittent periodicities (Grinsted et al, 2004). Often geophysical time series are not found to be normally distributed and for such cases the methods of applying the continuous wavelet transform (CWT) can be useful (Grinsted et al, 2004).

To summarize, spectrum analysis will identify the correlation of sine and cosine functions of different frequency with the observed data. If a large correlation (sine or cosine coefficient) is identified, you can conclude that there is a strong periodicity of the respective frequency (or period) in the data.

Where this approach was obtained:

These wavelet analyses were done through a MATLAB toolbox available free for non-profit use. The script was developed by Grinsted et al. (2004). It allows for a CWT, cross-wavelet transform (XWT), and wavelet coherence (WTC) plots.

The three plots:

CWT expands the time series into time–frequency space, and is useful in analyzing localized intermittent oscillations in a time series (Grinsted et al., 2004). The other two plots are used for looking at links between two time series. It looks at whether areas of high common power in time frequency space show consistent phase relationships and therefore are suggestive of causality between the time series (Grinsted et al., 2004). The CWTs of the time series are used to construct the XWT and WTC. XWT indicates regions in time–frequency space where the time series show relative phases and high common power. WTC will locate regions in time–frequency space where there is significant coherence (even with low common power) (Grinsted et al., 2004).

How to read the plots:

The analyses conducted in this study focus on the WTC (an example can be seen in Figure 10: Example of wavelet plot (Guarani – WTC: Model vs ENSO)Figure 10). When looking at the WTC plot a high correlation between the two-time series is seen in yellow, this is outlined in black if the confidence intervals are 95%. Whether the time series have a positively or negative phase relationship is indicated through arrows → and ←, while the arrows ↓ and ↑ show that time series 1 lags time series 2 by 90°. The interpretation of lags in these zones can be challenging, however, and should be done carefully, as a lead of 90° can also be interpreted as a lag of 270° or a lag of 90° relative to the anti-phase (opposite sign). A good indication that there is a connection and link between time series is that the phase arrows generally point in only one direction for a given wavelength.

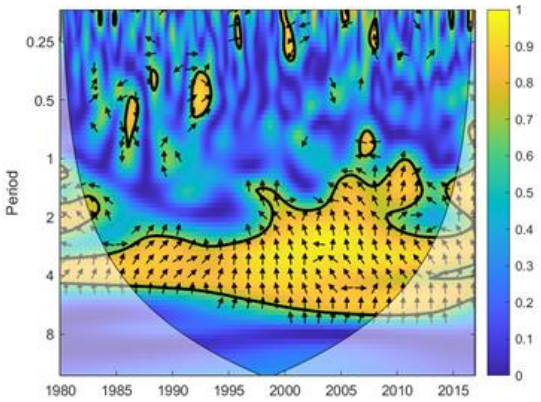

Figure 10: Example of wavelet plot (Guarani – WTC: Model vs ENSO)

Chapter 4 RESULTS AND ANALYSIS

This chapter will now present the results of the four main steps in the approach laid out in the last methodology chapter. As the main fundamental set of data in this body of work, the SWB Model results will be looked at first, to go over what they are showing and how they can be read. Next the comparison with the GRACE data will be presented, followed by the validation of the model through groundwater observations. Lastly the results of the wavelet analyses will be shown.

4.1 SWB MODEL RESULTS

The type of results produced by the SWB Model can be seen in Figure 11 (the full collection of results can be found in the Appendix 4 to 7). Overall the inter-annual fluctuations saw the largest range in wet and monsoon like environments. For example, changes of around 500mm over a year can be seen in Amazonas. In contrast, areas like Saq-Ram where precipitation is far less saw 5mm fluctuations. Generally arid areas saw smaller fluctuations compared to the larger overall undulations of the full 30 years. The fluctuations around the mean on the other hand ranged from 40 to 1200mm over all areas.

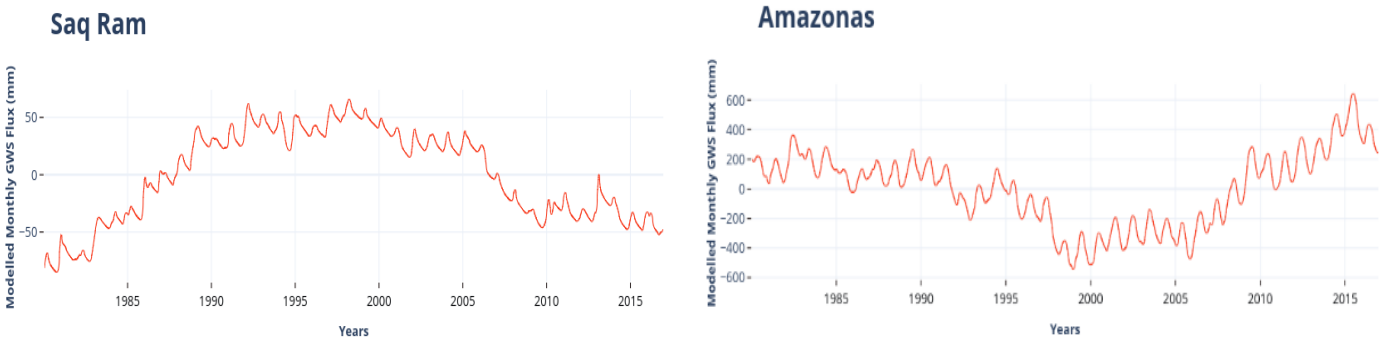

Figure 11: Example of SWB Model results, Saq Ram on the left and Amazonas

Before the analyses are carried out, care must be taken to clarify what the Simple Water Balance (SWB) modelled results are showing, and where it is easy to make wrong interpretations. The fluctuations are

sub-trends that show the precipitation flux from month to month compared to all months. What the SWB Model is not showing you is the overall trend in storage or water level – this is removed in the cumulative integration step. By removing this trend (if all assumptions hold true) you are looking at groundwater storage flux.

To help in better understanding what the model is illustrating, Figure 12 shows the SWB Model results for the Mekong. It has had its cumulative integral detrending leaving the fluctuations around the trend as shown in the methodology section.

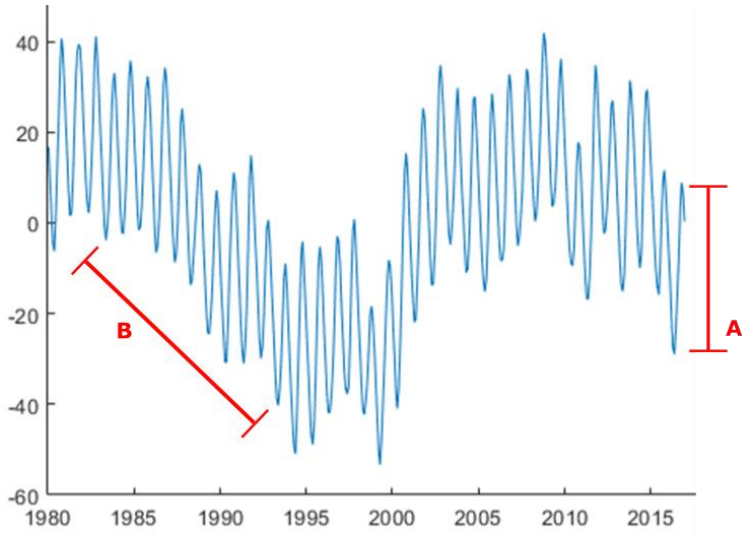

Figure 12: Illustrative example of model results: Mekong

The small fluctuations seen in Figure 12, indicated by line A, show the inter-annual changes in groundwater recharge. Where the peak indicates wetting periods and the troughs show dry spells. Line B shows the data's sub-trends, these indicate if the fluxes are reducing to below the mean (trend line or 0 on the y axes) or if they are increasing and moving above the mean.

Therefore, when trend is mentioned in this analysis it is not referring to the storage trends but specifically to the intermittent trends of the water storage flux. Issues can arise in this approach that can make it easy to make false conclusions. Like the fact the detrending is removing a linear trend where there are often significant non-linear trends in the overall data. This will be discussed later on in the discussion.

4.2 SWB MODEL COMPARISON AND VALIDATION

Due to the simplicity of the SWB Model and the complex and intricate nature of the system it is representing, checking the reliability the SWB Model is crucial for any reliable conclusions to be drawn. For this several approaches can be employed to better understand where, and in what circumstances, the SWB Model is appropriate to use and where its limitations prevent it from accurately representing an area. One of the approaches used is the comparison of GRACE with the SWB Model, Due to the way the SWB Model is calculated, both of their underlying equations are calculating TWS anomalies, so should match. The SWB Model will then be validated with real world groundwater level observations. Next, to discern the accuracy of these global data sets the results are examined from the continent of Africa, the results will be compared against other outputs from different global data sets of P and E.

Africa is used as it is the region with the least reliable data. Finally, the results of the model will be compared with the climate indices through wavelet analyses.

4.2.1 GRACE vs SWB Model

This section addresses the comparison of the SWB Modelled results against the TWS change data obtained from the GRACE satellite mission. The comparison period is 2002-2014 as this covers the entirety of the GRACE mission. The SWB Model was run for the same time period so the detrending and standardization would match that of GRACE. The results will be looked at by going through the four global geographical regions containing the studied aquifers and basins in this project; Africa, Asia, North America and South America.

AFRICA:

The GRACE and SWB Model comparison for the African continent illustrates in most of the aquifer systems a good relationship. The model seems to represent the results found from GRACE well, with both data sets closely mirroring each other. However, there are some that do not see this relationship. To break down the results, areas with the same climatic zones will be examined together – starting with the Sahel, then North Africa, central Africa and lastly southern Africa.

Sahel Zone: This is the climatic zone of transition between the Sahara and the Sudanian Savanna, and includes the Senegalo Mauritanean, Lake Chad, Irhazer-Iullemeden and Volta aquifer systems. The SWB Models oscillations seen in this zone have peaks and troughs that closely mirror the GRACE data. The SWB Models amplitudes also fit that of GRACE with little deviation (though GRACEs data tends to edge on the larger side).

North Africa: The Nubian and North Western Saharan systems show some of the poorest results from the entire continent. Both SWB Models show oscillations that are out of sync with the GRACE data. In particular, the North West Sahara's trend does not match with a sharp spike in 2009 and a following decline.

Central Africa: Surprisingly the Congo aquifer sees one of the best matching GRACE and SWB Model results even though it is one of the complex river networks in the world and sees the second largest river discharge in the world. Unfortunately, no observational data was able to be collected for this site but it will be discussed later in the discussion.

Southern Africa: Both the southern African systems show different results. Karoo Sedimentary sees a good result with close plots. However, Stampriet has a poorly fitting trend with a large spike in the data around 2007 (similar to North Western Sahara) and its fluctuations are very muted compared to the irregular GRACE data.

Another overall feature of the data sees the GRACE data showing larger (amplitudes) and more frequent fluctuations. There is less consistency to the GRACE data compared to the SWB Model. It appears jagged compared to the smother lines of the SWB Model.

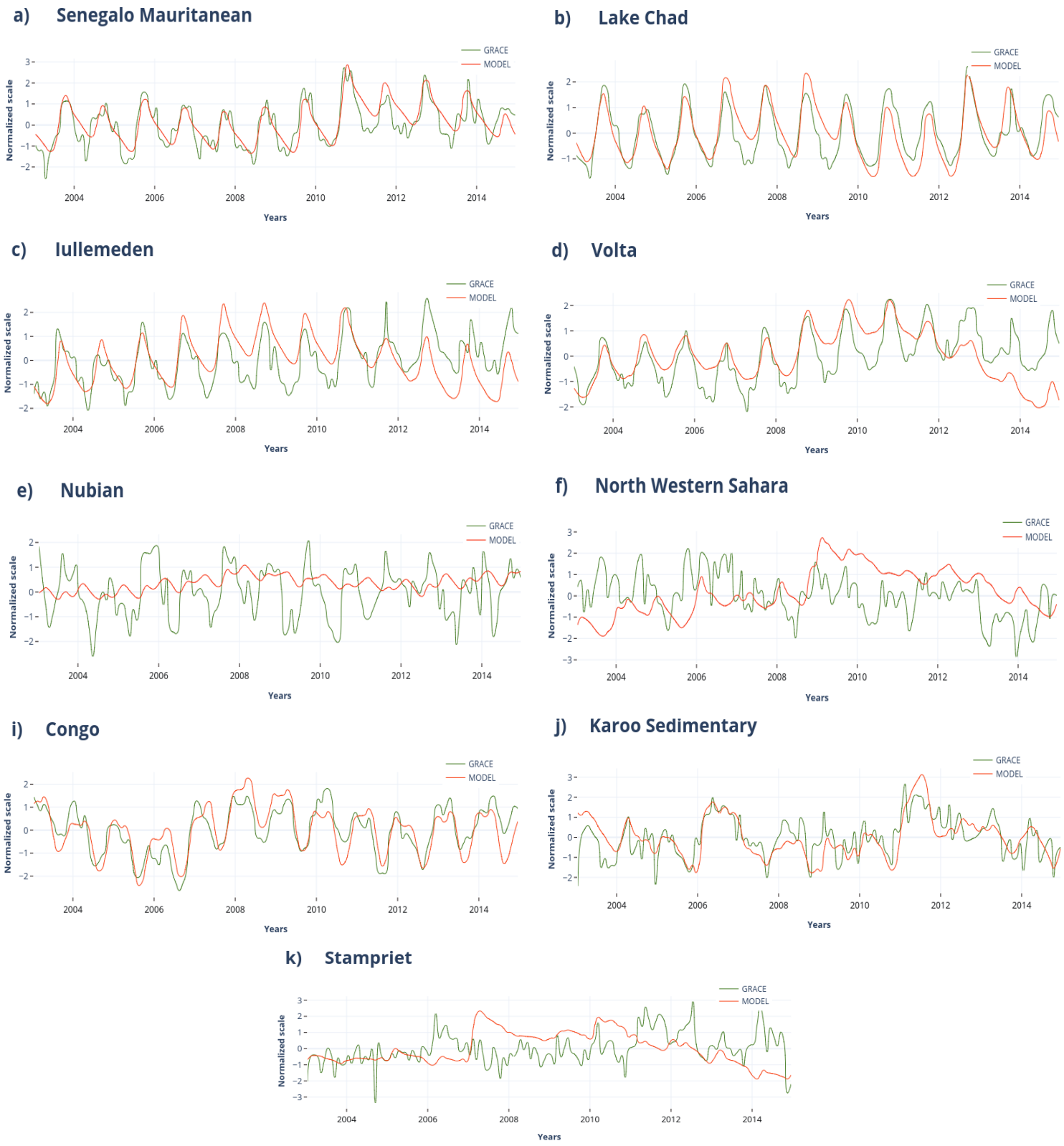

Figure 13: GRACE vs SWB Model for the African study areas (2003 – 2014). a) Senegalo Mauritanean, b) Lake Chad, c) Iullemeden, d) Volta, e) Nubian f) North West Sahara, g) Karoo Sedimentary, h) Congo.

ASIA*:*

Overall the again the SWB Model appears to provide a good representation of GRACE Results in Asia (Figure 15). There are strong similarities in the timing of the peaks and troughs of the oscillations. The exceptions for a good fit here are the aquifers Amu Darya and the East Ganges.

Arid Region: Amu-Darya and Syr-Darya are geographically close, they are both around the same size, and are characterised by dry cold desert environments. As such, they show similar GRACE results in terms of fluctuations, shape and timing. The shape and amplitude of the SWB Model results for Amu-Darya are also seen to be similar. However, where Syr-Darya sees a good fit between GRACE and the SWB Model, Amu-Darya sees the opposite trend seeing a gradual increase over time compared to the decreasing tendency of GRACE.

Saq Ram and Indus are also both considered to be from similar arid climates, laid out in the Köppen-Geiger Climate Classification Map (Figure 14). However, Saq Ram appears to have this jagged GRACE result with a poorly fitting SWB Model and the other sees a good fit with more rounded, less sporadic (compared to Saq Ram).

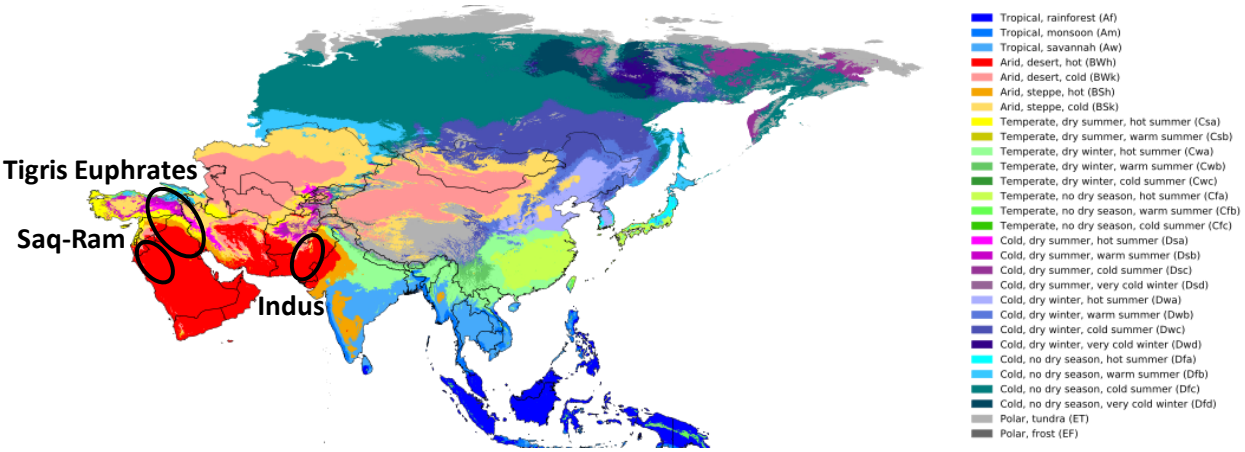

Figure 14: Köppen-Geiger Climate Classification map of Asia (Beck, et al., 2018)

The Tigris Euphrates provides interesting results. Around 50 percent of its area belongs to this arid region category. However, the shape of the GRACE data reflects that of the more water rich areas (discussed in next paragraph), with amplitudes being closer to smooth peaks and troughs compared to the other arid locations.

Monsoon Regions: In the two monsoon regions of Asia, the East Ganges and the Mekong, they show similar smooth, regular and large amplitudes in their graphs. Both see a good fit with the GRACE and SWB Model. However, the trend in the East Ganges diverges from the steady one seen in the GRACE data, to show an increase from 1980 to 2008.

The last two study areas, Australia's Murray Darling basin and China's North China Plain, have differing climates. However, both areas demonstrate a nicely corresponding fit even with the GRACE data showing complex, irregular fluctuations (irregularities are picked up by the model). This may be due to their dry environments interspersed with seasonal spots of precipitation.

Figure 15: GRACE vs Model for the Asian sites (2003 – 2014). a) Amu Darya, b) Syr Darya, c) Saq Ram, d), Indus, e) Tigris Euphrates, f) East Ganges, g) Mekong, h) Murry Darling, i) Northern china Plain.

NORTH AMERICA:

Figure 16 looks at the results from North America. These five study areas all show the best results of any continent, in both intermittent trends and oscillation – especially the Northern Great Plains (Figure 16d). Although there are some deviations, almost all of the big peaks and troughs are present in both GRACE and the SWB model results. The High Plains is seen to be the worst fitting model.

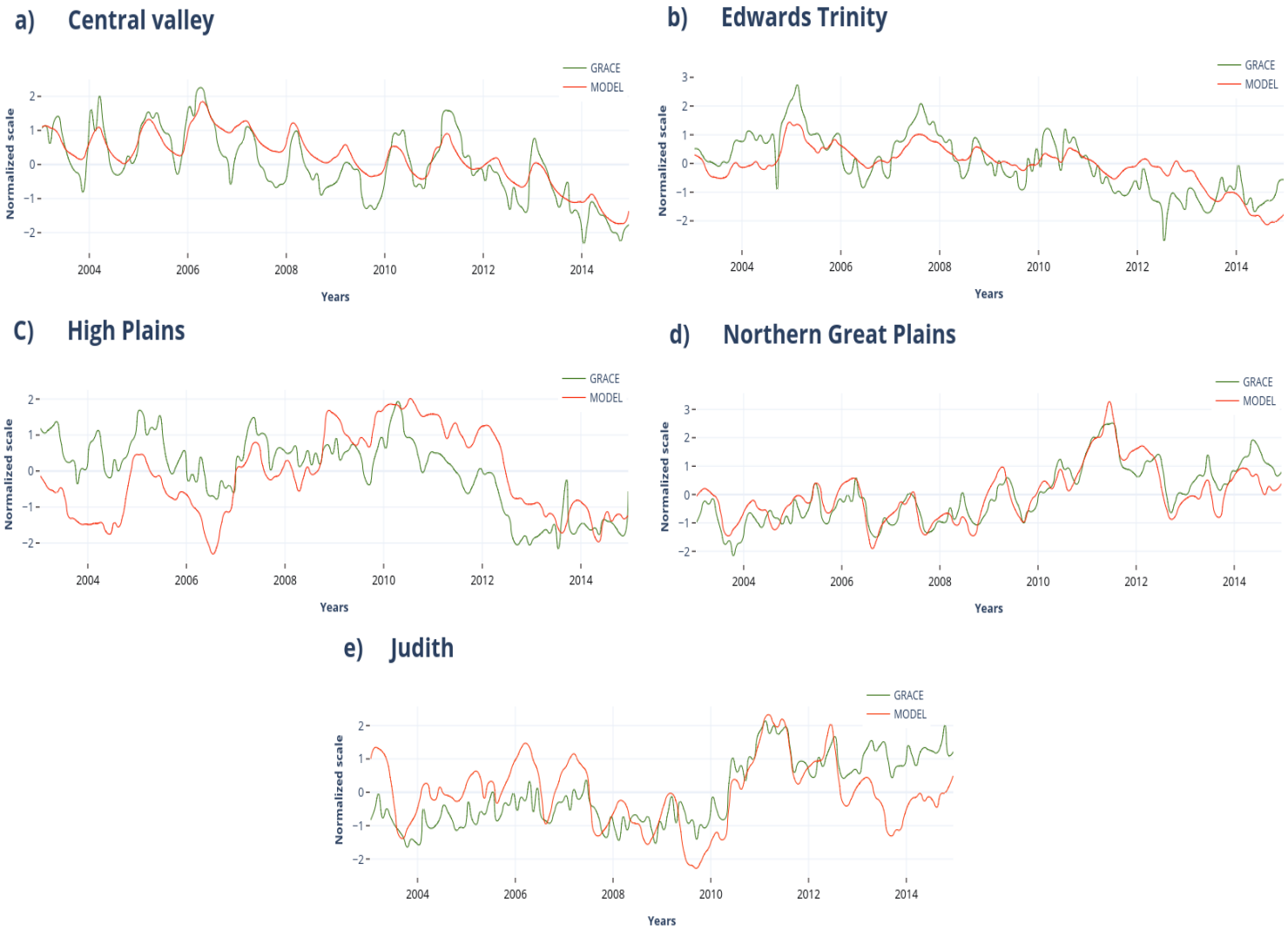

Figure 16: GRACE vs Model for the North America continent (2003 – 2014). a) Central Valley, b) Edwards Trinity, c) High Plains, d) Judith, e) Northern Great Plains

SOUTH AMERICA:

Figure 17 shows the results of the GRACE vs SWB Model for South America. Figure 17a shows the Amazonas with a good fitting model, similar sized oscillations are seen along with spacing and timing with GRACE. Figure 17b shows Guarani, where the fit with GRACE is also good.

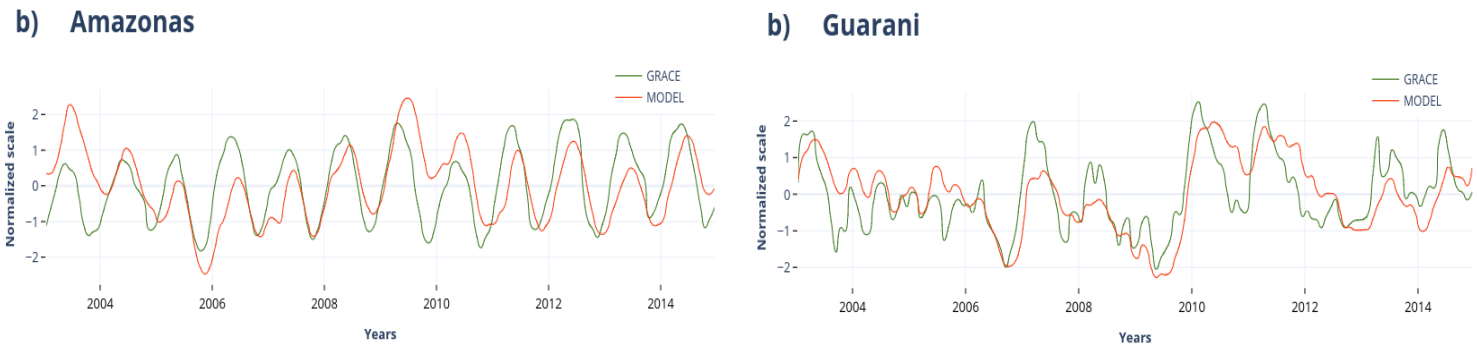

Figure 17: GRACE vs Model for South America (2003-2014). a) Amazonas, b) Guarani

4.3 GROUNDWATER vs SWB MODEL

In this section the model will be validated with the available groundwater observations (GWL) found for each study area. This will help identify how well the flux integrated TWS anomalies calculated by the model represent the groundwater storage flux. Because each aquifer system has different zones of time where observations where found and for different lengths of time the x axes is shown for the entirety of the study to make comparisons of the data more effective.

AFRICA:

Again, to start, the aquifer systems from the continent of Africa. will be looked at first and grouped by climatic zones. The overall results for Africa are mixed. In almost all examples the model sees larger amplitudes in its fluctuations than the GWL.

The SWB model is also seen in most cases to have its position and period of fluctuation out of sync with the GWL. However, because of the short timeframe that the data provides it is difficult to draw strong conclusions.

SAHEL: Senegalo Mauritanian and Volta both see a good fitting trend and harmonised oscillations with similar amplitudes. Senegalo Mauritanian appears to have one of the best fitting results. Lake Chad and Iuellemeden seem to have the worst fitting plots. The Iuellemeden sees strong fluctuational amplitudes and in places seem to be an inverse pattern compared to the GWL.

NORTH AFRICA: Nubian and the North West Sahara (NWSAS) both see poorly fitting models. NWSAS sees significantly reduced fluctuations compared to the GRACE data however, its close adherence to the large changes in the data is picked up.

SOUTHERN AFRICA: Karoo Sedimentary and Strampriet can both be seen to have good fitting models. Whereas in the GRACE data only Karoo Sedimentary saw a good fit.

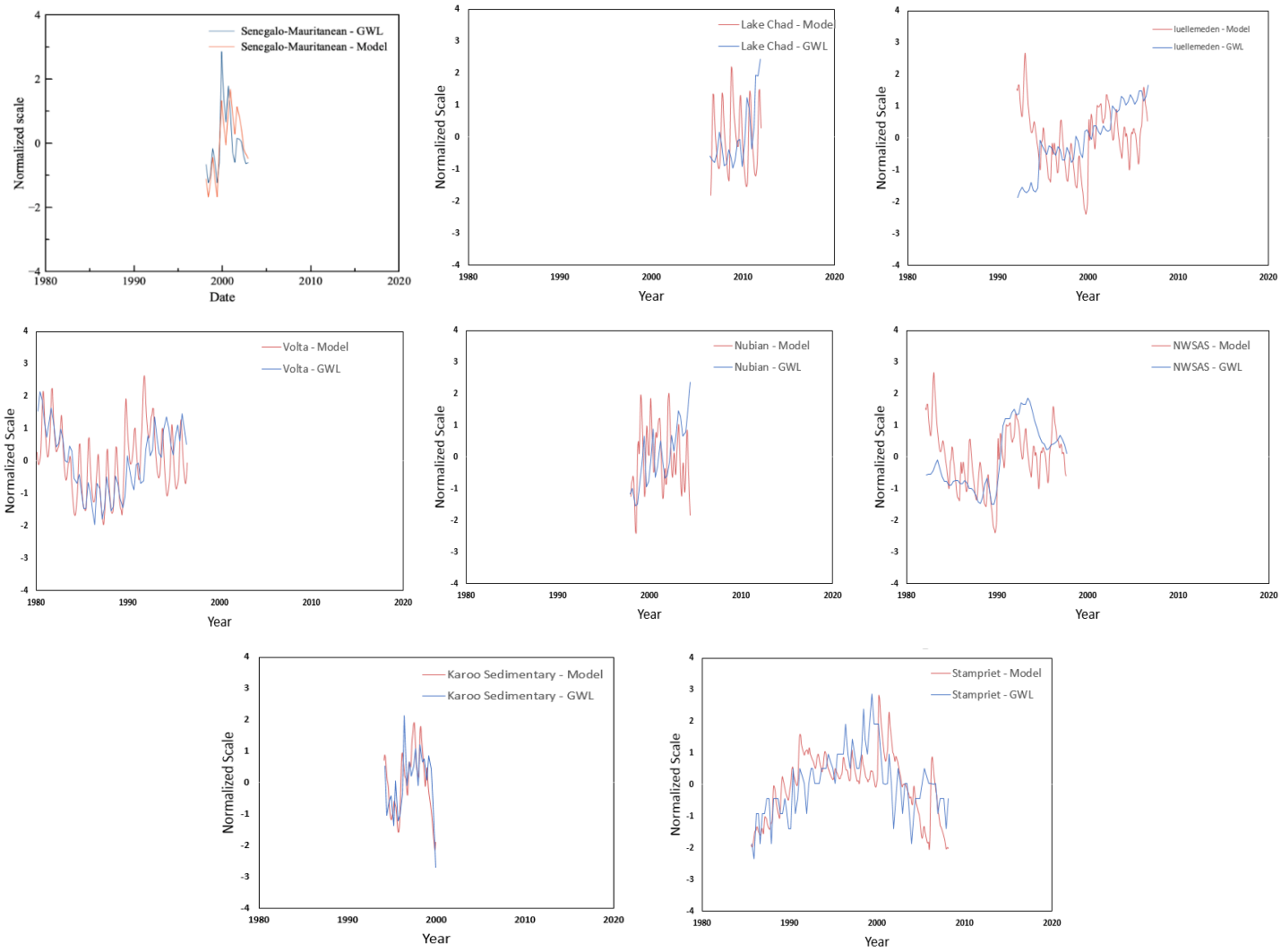

Figure 18: Africa aquifer systems. SWB Model vs groundwater observations

ASIA:

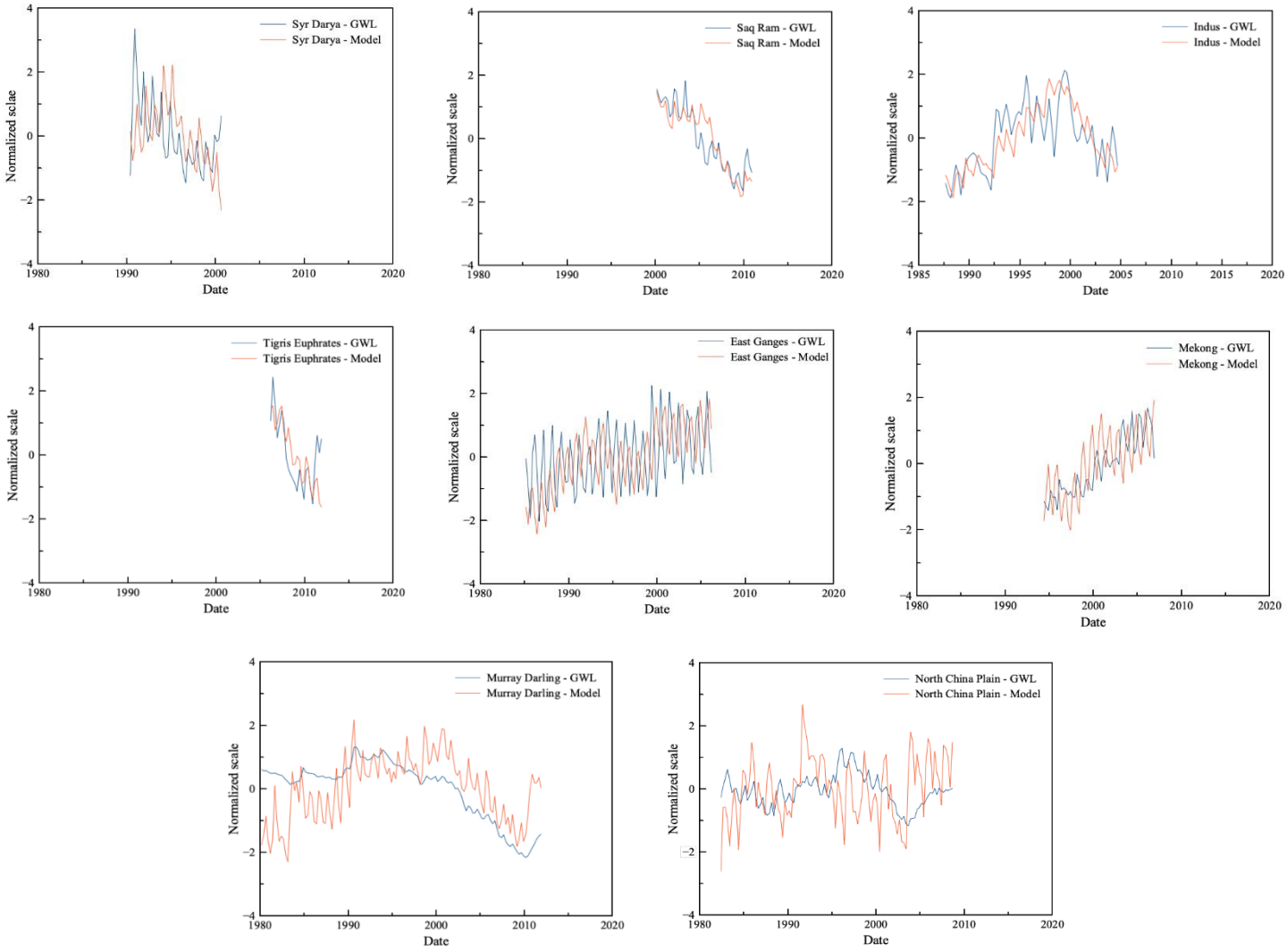

Figure 19 shows the SWB Model vs GWS change for the Asian study areas. All the modelled interment trends closely represent the observed groundwater level. The models' harmonic periods, where their peaks and troughs are positioned compared to the groundwater, also match well for most of the plots seen here.

ARID AREAS: In

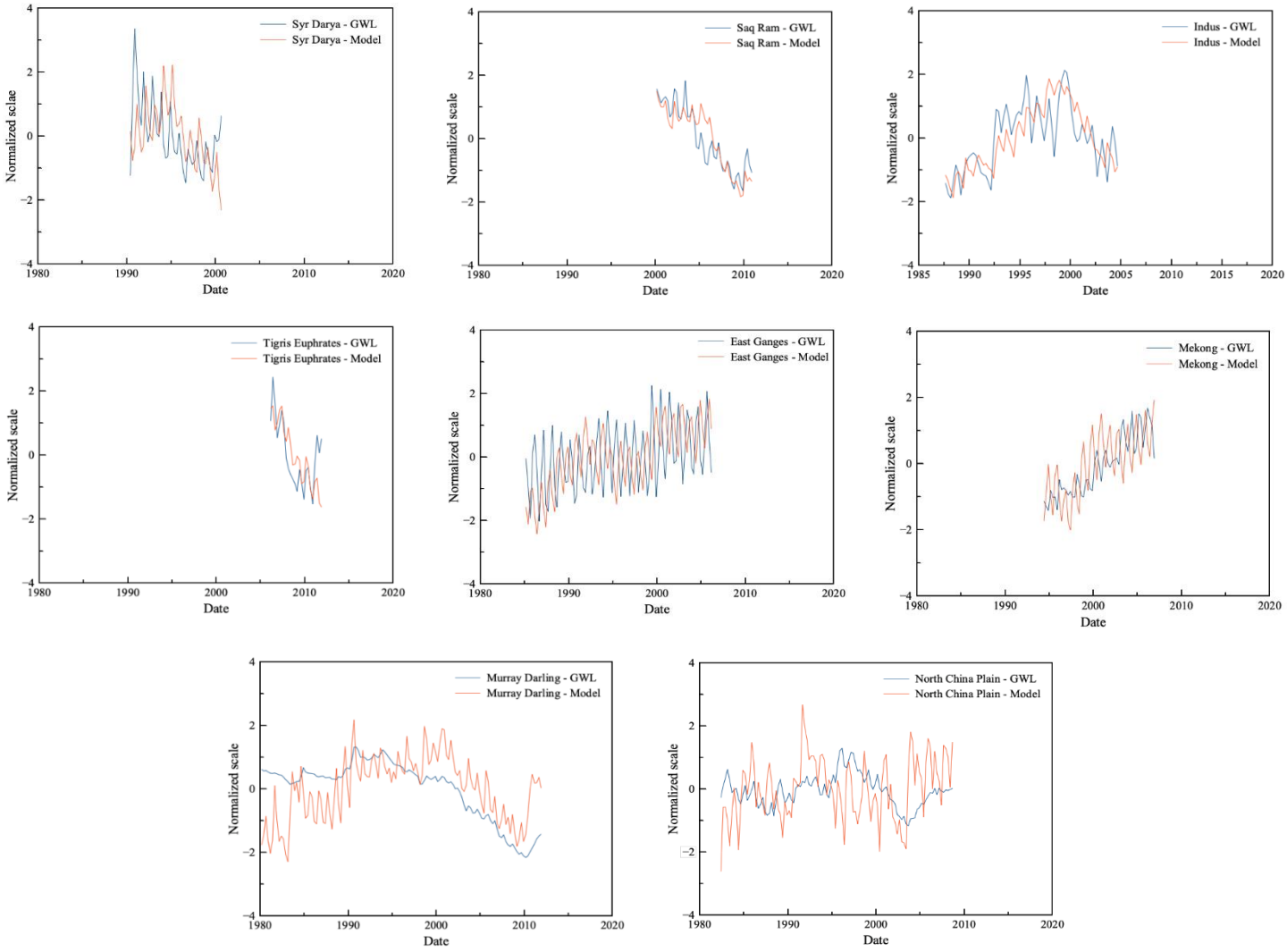

Figure 19a, b, c and d (the study areas in arid environments) there is a clear and good representation of the groundwater's overall trend by the model. There is also in most of them a strong link between the oscillations. However, in the Syr Darya plot there is a poor fit on the smaller frequency level. Where the harmonics are not "in sync", they appear to have the same timing though deviate from one in amplitude or positioning on the normalized scale. Indus also sees this.

MONSOON AREAS: The East Ganges and the Mekong see the same trend and the model fitting to it. However, the Mekong graph shows model amplitudes larger than that of the groundwater, where the East Ganges shows the ground water amplitudes larger than that of the model. The East Ganges also shows its oscillations are out of sync to the groundwater changes in many sections.

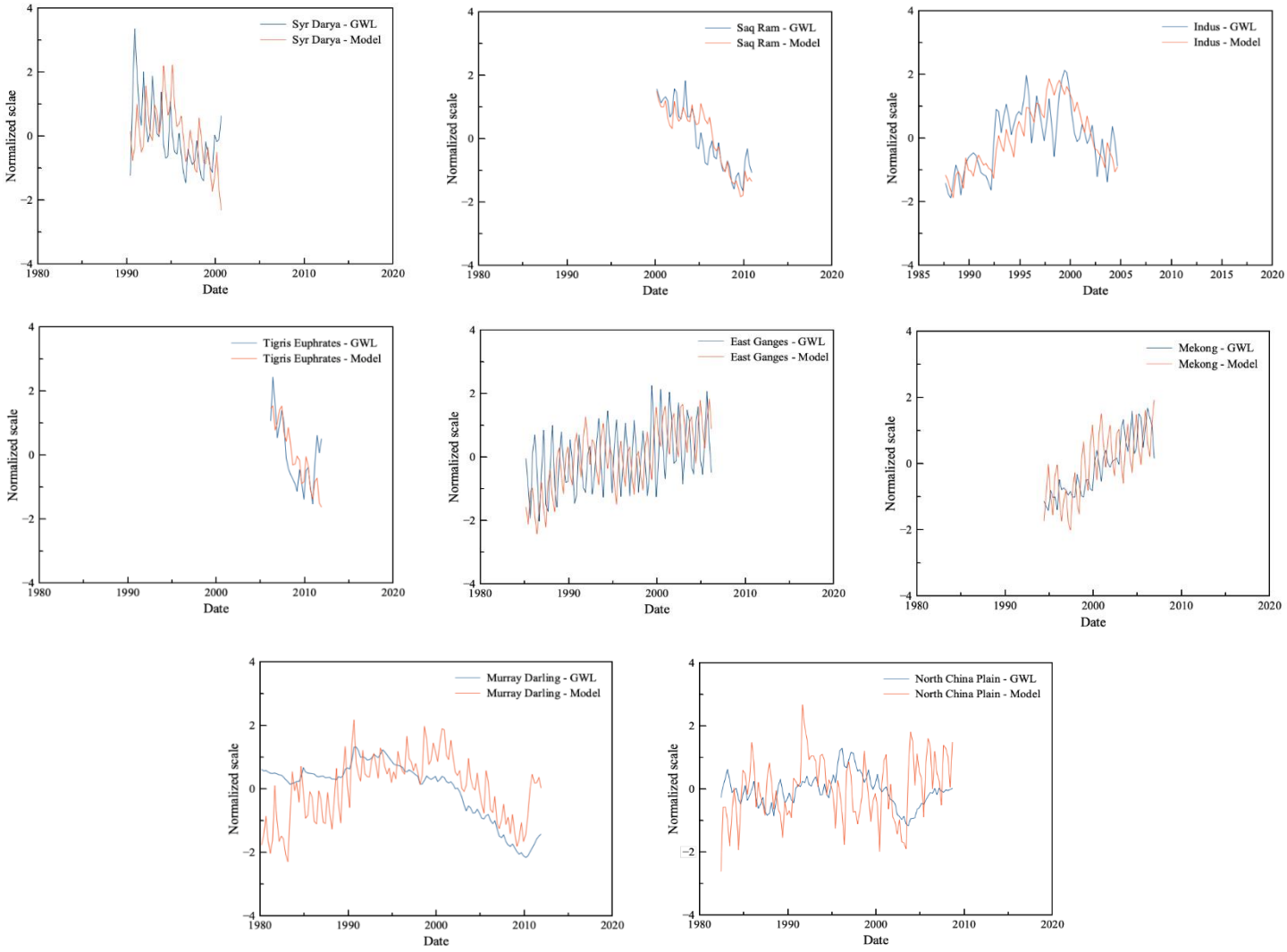

Figure 19: Asia aquifer systems. SWB Model vs groundwater observations

OTHER AREAS: In the study areas with the longest groundwater observations – Murray Darling Basin and the North China Plain – the plotted model amplitudes are much larger than the groundwater. Moreover, the placing of these fluctuations are not always in sync, and they can vary greatly.

NORTH AMERICA:

In this section we look at the groundwater observations against the modelled results for the North American continent (Figure 20).

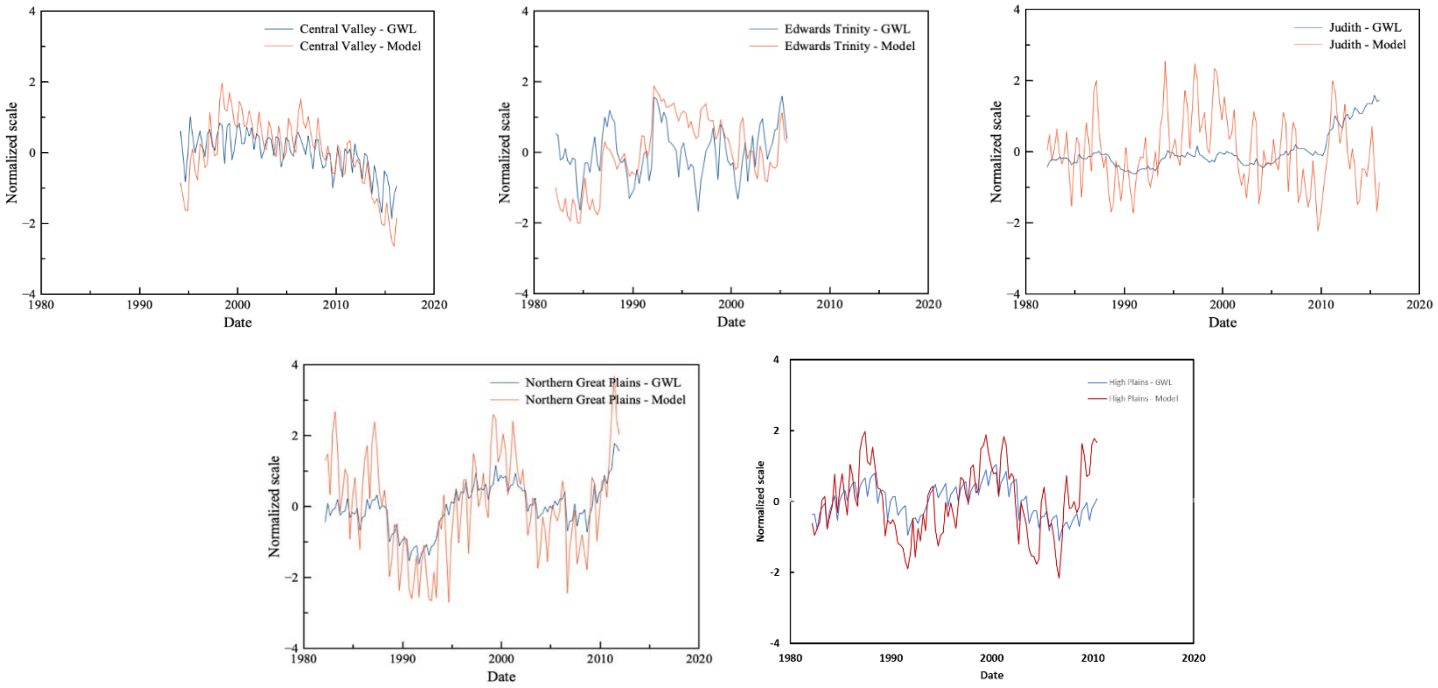

Figure 20: North-American aquifer systems. SWB Model vs groundwater observations

In all these study areas there is a good fit between the model and groundwater levels compared to the other continents. Edward Trinity sees the model following the GWL data however deviations occur where it seems to exaggerate large sections of the GWS change. Judith's, the Northern Great Plain and the High plains all see their large fluctuations center on the GWL data, however Judith sees this divergence at the end.

SOUTH AMERICA:

There is no trend in the GWL observations looking at the South American continent (Figure 20). Moreover, for Amazonas the fit is poor. However, the period of time being looked at is too short to really get a good idea about how well the SWB Model represents the groundwater observations.

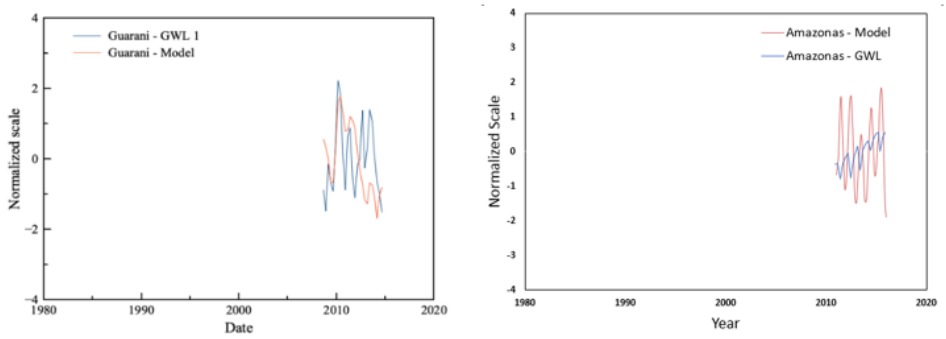

Figure 21: South America aquifer systems. SWB Model vs groundwater observations

4.4 SWB Model vs SWB Model (AFRICA)

As discussed in section 4.3.1 the plots comparing the SWB Model to GRACE in the African study areas (Figure 22) see the poorest similarities. It has been shown that data collected for GPCC, made up of real ground observations, is characterised by lower reliability in the African continent compared to other regions. Places with the most reliable data like USA and Australia saw the best results (Figure 15h and Figure 16). On top of this the reliability of GLEAM (or any remote evapotranspiration database) needs to be considered due to the inbuilt uncertainties. So, to better understand how the global climatic databases are affecting model results, several study areas in Africa were chosen for focused comparison. Africa was selected to do this analysis for several reasons. Firstly, the model has already been run using a different data set by Carvalho Resende et al, (2018). Secondly, Africa has the least reliable meteorological data so using it as a case study will highlight the biggest variations in the data sets, if there are any. Three model runs are compared with differing combinations of data sets for P and E (Figure 22). One data set is from the GWB model produced in this report, where GPCC is used for the precipitation and GLEAM is used for the evapotranspiration. Another will look at the model of GPCC and MPI-ESM (Max Planck Institute for Meteorology – Earth System Model) for evapotranspiration. And lastly CRU is used for precipitation and MPI is used for evapotranspiration.

The figure show all Sahel sites have models with similar results. In North Africa, Nubia shows deviations in one section of all three models and North Western Sahara shows all three models to have a close alignment. The Congo also sees a fit in all three models. Lastly the southern study areas show the worst fits – with the strongest deviation being seen in the Stampriet model run here (GPCC – GLEAM).

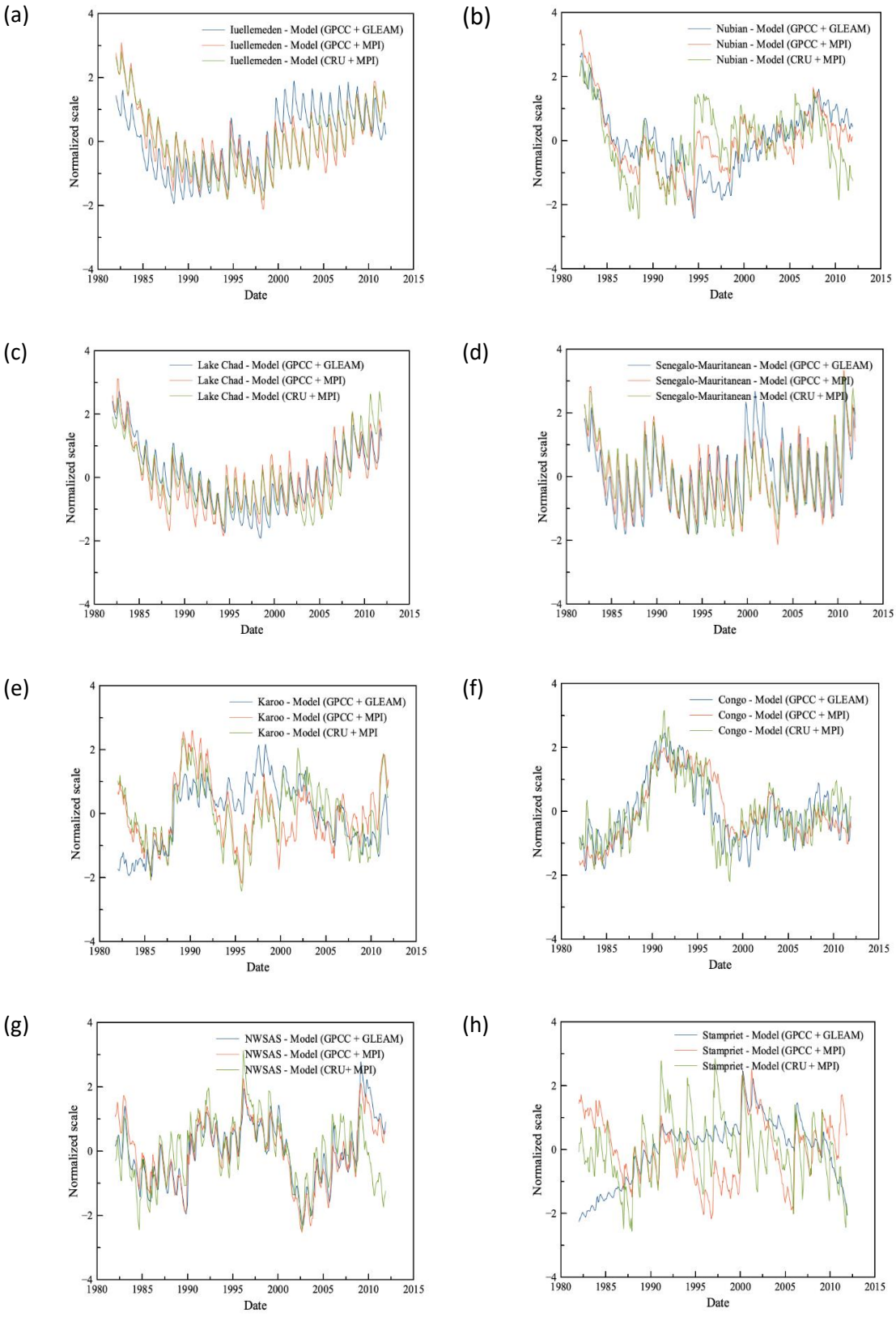

Figure 22: Model run with different data sets for Africa:

4.5 WAVELET ANALYSIS

This last section of this chapter will now look at the wavelet analyses of the differing climate variation index vs the modelled study areas. From this analysis the coherence can be identified to periodices and to specific time periods. To start off ENSO will be looked at first, followed by AMO and PDO. Not all the study areas and indexes will be discussed here as there are too many to be properly analysed. Some of the full set of the wavelet results can be found in Appendix 8-11. The ones selected will be those found to be most representative along with results that can tell us more about this approach.

HOW TO READ THE GRAPHS:

Although the steps laid out in the methodology for the wavelet coherence were taken out of necessity (CWT was preformed on the individual time series, XWT was done between pairs of time series and WCT on the XWT to identify statistically significant relationships between pairs), for the analyses, the focus will be on the wavelet coherence. This provides the most robust outcomes and are of the most interest to the reader (Jean et al, 2014). It identifies both frequency bands and time intervals at which groundwater and climate indexes time series are covarying (Holman et al, 2011). For the interest of the reader the full results of both CWT, XWT and WCT for som of the study area can be found in Appendix 8-11.

When going through the plots, there are a few methodological aspects to be aware of. Areas that ocupy the space inside the bold black lines are the times and periodicities of statistically significant wavelet coherences (at the 5% significance level) (Holman et al., 2011). The arrows indicate the phase relationship and the pale shaded area around the edge of the plot indicates the cone of influence (COI). The COI is where edge effects (caused by errors present at the beginning and end of the finite wavelet power spectrum) cannot be ignored (Holman et al., 2011).

SEEN IN ALL GRAPHS:

As would be expected there is little consistent wavelet coherence apparent for periodicities of less than one year in all the results, demonstrating that these large scale teleconnection indices are not the drivers of short-term (seasonal) variability in groundwater level dynamics, which are driven by local patterns of precipitation and evapotranspiration.

From wavelet analyses one can see whether there is a relationship or not, but it can't discern what the relationship is in terms of the increase or decrease in water availability. For this, the models' need to be checked in relation to the index on a graphed plot.

4.5.1 ENSO vs SWB Model

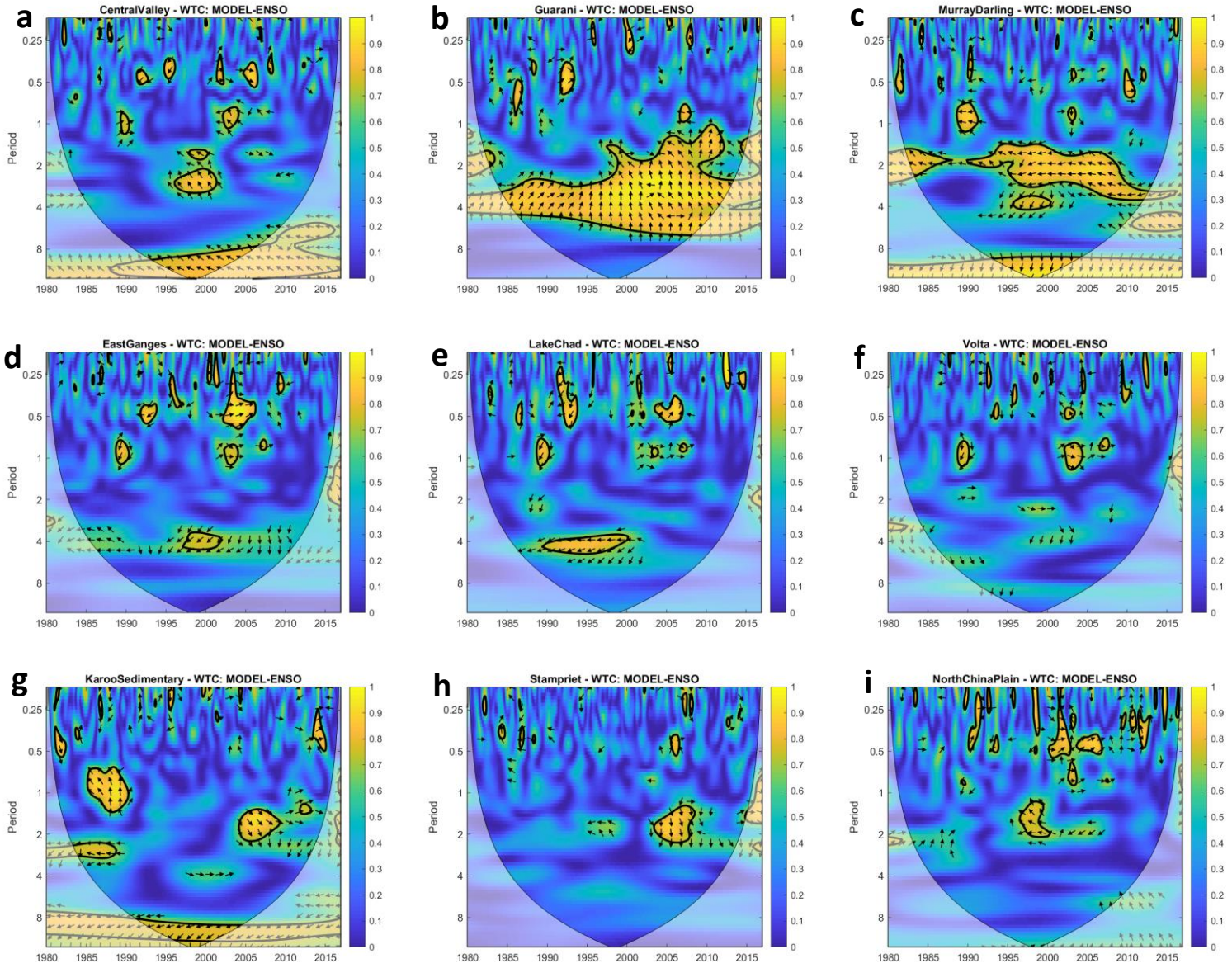

Figure 23: Wavelet coherence between ENSO and Model: a – i show examples from different locations from around the globe. Note that the spectral power to the right of the plot is dimensionless, the areas inside the black lines are at the 5% significance level, and the pale white edges show the COI. The vectors indicate the phase difference between the data; a horizontal arrow pointing from left to right signifies in phase and an arrow pointing vertically upward means the groundwater level series lags the teleconnection index by 90° (i.e., the phase angle is 270°)

NORTH AMERICA: In the Central Valley plot (Figure 23a), in areas above the 5 percent significance level you can see an anti-phase (in a top left direction, meaning a phase angle is between 90° and 180). This indicates that the model is lagging the index signal. However, it is important to know that when reading these graphs, you must be careful as a 90-degree lag of the model may also be interpreted as the index lagging the model by 290 degrees.

The areas of wavelet coherence are found in the two year period from 1995 to 2002 and a large continuous feature at the bottom of the graph between the 8 to 12 year period. This plot shows there is coherence with ENSO and Central Valley at the 3 to 12-year period range. The Central Valley also provided a good representation of both groundwater level and TWS change giving more confidence in

conclusions drawn from this plot. When checked against each other water storage apears to increase in El Niño years and decrease in La Niña years. This is backed up through other studies, and in particular research from Jean et al. (2014) and Gurdak et al. (2007).

SOUTH AMERICA: In the Guarani plot (Figure 23b) there is a large continuous area above five percent significance seen in the two to eight-year period. This area has a slow-moving phase lock, with near vertical arrows. This is indicating that the model is lagging the climate index and that there is coherence between Guarani and the ENSO index. When comparing the model with GRACE data there was a strong fit. The validation with GWL was too short of a timeframe to get a conclusive decision of how well it fits but it appeared to show similarities in the timing of the fluctuations. This and the fact the area of significance is particularly large and constant, its high coherence should be considered. This strong connection with ENSO sees strong El Niño years (circled in Figure 24) increase the water storage and vice versa with La Niña. The strong El Niño years (1982-83, 1997-98 and 2015-16) are being lagged by big spikes in water storage.

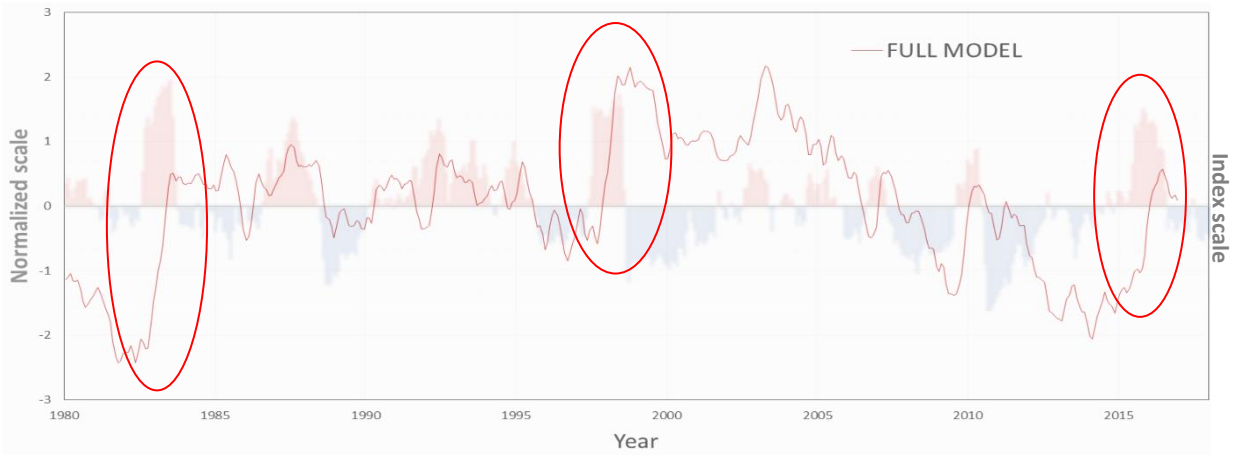

Figure 24: ENSO vs Guarani. Model is on the left axis, ENSO is on the right axis

ASIA: In the Murray Darling areas above the 5 percent significance level see an anti-phase (to the left, meaning an 180^{o} phase angle) indicating a relationship were by if the index is high, water level flux is low and when index is low, the water level flux is high. It also sees a slowly moving phase angle across the long continuous feature in the two year period, giving more support for there being a strong coherence. From checking the graphed SWB Model vs ENSO in Figure 25 that there is more groundwater available during La Niña then El Niño.

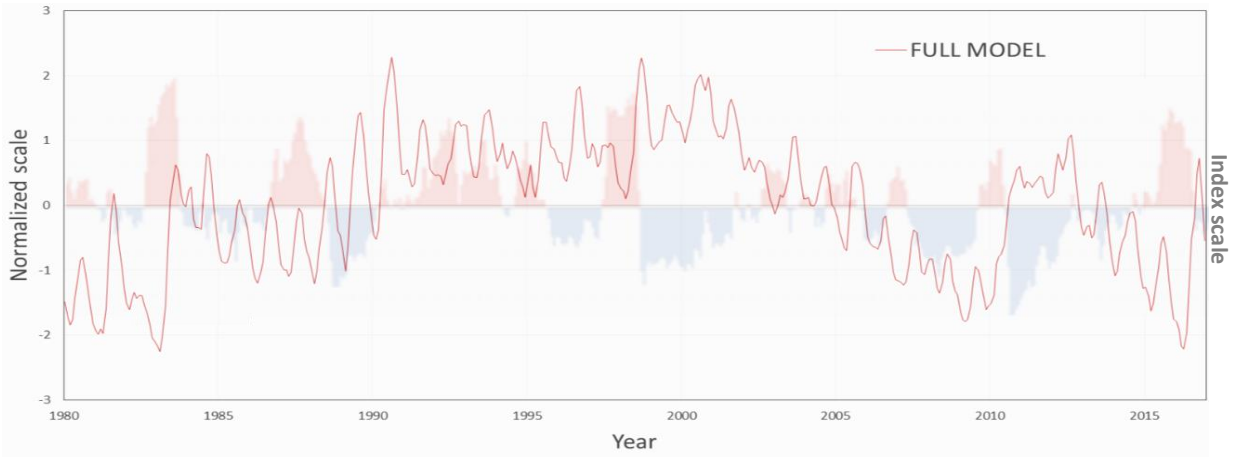

Figure 25: ENSO vs MDB. Model is on the left axis, ENSO is on the right axis

AFRICA: The remaining plots see far less evidence of coherence. In the African continent the Lack Chad and Volta study areas see virtually no indications of correlation. Where Karoo Sedimentary does, there is a continuous feature of significance seen in the eight-year period and three large zones in the 1-2 year period from 1985 to 1990 and from 2004 -2007. This matches the years of strong La Niña.

Stampriet on the other hand only sees one zone of significance, and that is the same 2004 to 2007 circle seen at the two-year period in Karoo sedimentary.

4.5.2 AMO vs SWB Model

AMO and the SWB model are looked at next. This is an important analysis as the AMO is one of the most influential climate variabilities operating at the global scale. The 6 plots in Figure 26 were picked from regions with similar results to show AMOs different influences on the globe. However, as this is a 30 -50 year scale it is very difficult to draw any strong conclusions from these plots as their time frames are too short to capture a full phase cycle.

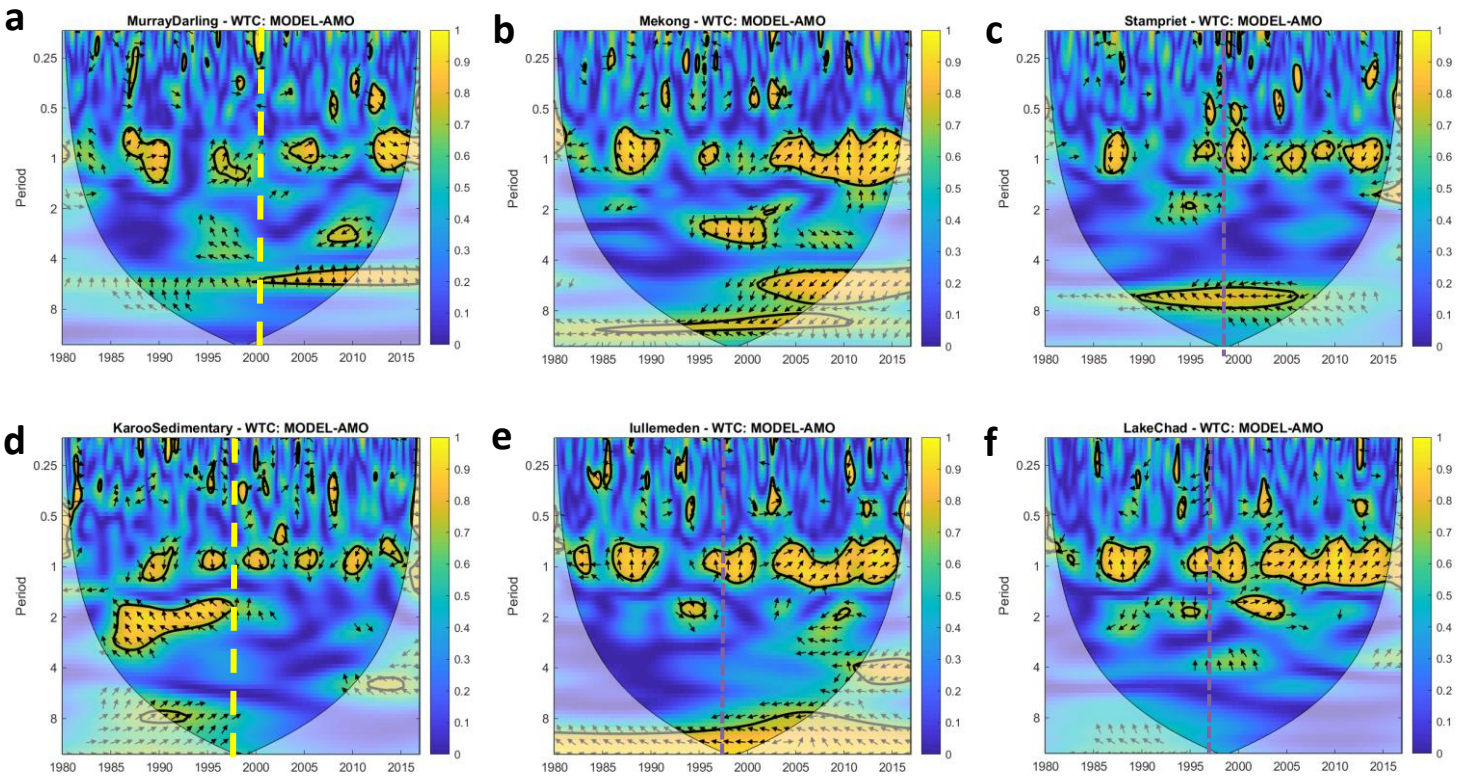

Figure 26: Wavelet coherence between AMO and Model: Note that the spectral power to the right of the plot is dimensionless, the areas inside the black lines are at the 5% significance level, and the pale white edges show the COI. The vectors indicate the phase difference between the data; a horizontal arrow pointing from left to right signifies in phase and an arrow pointing vertically upward means the groundwater level series lags the teleconnection index by 90° (i.e., the phase angle is 270°)

Around the year 1997 the AMO phase shifts from negative to positive. This appears to be indicated in a number of the plots. This is a large feature of significance that starts from around 1997 to 2001 and

continues through to the end of the study. This trend is seen in the Murray Darling Basin the Mekong, and the Karoo Sedimentary (shown by yellow dotted line).

When comparing the AMO index with the Australian Murray Darling Basin model (Figure 27) there is a clear increase of groundwater levels during the negative phase and a reversed decreasing trend after 2000 a decade after the phase flipped to positive.

Figure 26a gives evidence that negative phase doesn't have much effect on the GW level with the absence of zones of significance in the four to eight year period. There is a clear correlation between positive phases and GW decrease. When looking at the trends of the models for Asia this same general horseshoe trend around 1997 can be seen in the Ganges, the Tigris Euphrates, Indus, Saq Ram and Syr Darya models.

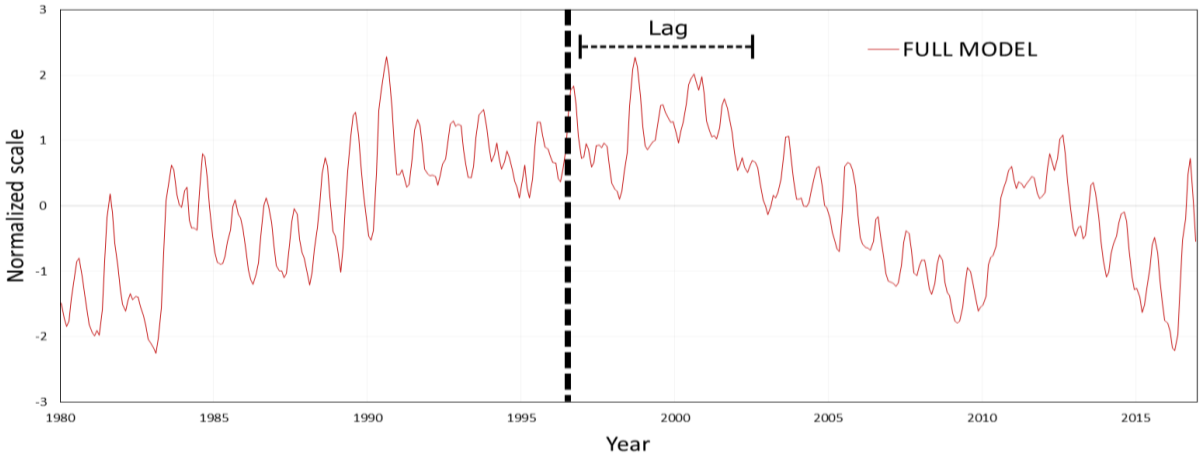

Figure 27: Model of MDB

The Mekong, like the Murray Darling Basin, seems to have a clear line in the plot (Figure 26b) showing a change from one side to the other, here it is around 2003. On the left of the line there are two smaller zones of significant and to the right of the line larger extended zones of significance can be seen. But unlike MDB the relationship with AMO is inversed, with the positive phase seeing an increasing GW level and the negative phase seeing a decreasing GW level.

Stampriet (Figure 26c) also shows a weaker change from pre- to post-AMO phase shift. Karoo Sedimentary (Figure 26d) shows a clear divide in the middle of the plot (like the MDB), but in this area the extended zone of significance is on the left side and in the two-year period.

WEST-AFRICAN study areas like Volta, Senegalo Mauritanean and North Western Sahara see very little correlation to the AMO in comparison to the rest of Africa.

SAHEL CENTRAL NORTH AFRICA: The Iullemeden and Lake Chad plots in Figure 26f and g show the areas representing the Sahel. Figure 28 below shows the modelled results for the Lake Chad study area which again shows the horseshoe trend. But here the trend is reversed so the negative phase before 1997 of AMO is associated with water declines and post-1997 the positive phase sees an increasing trend.

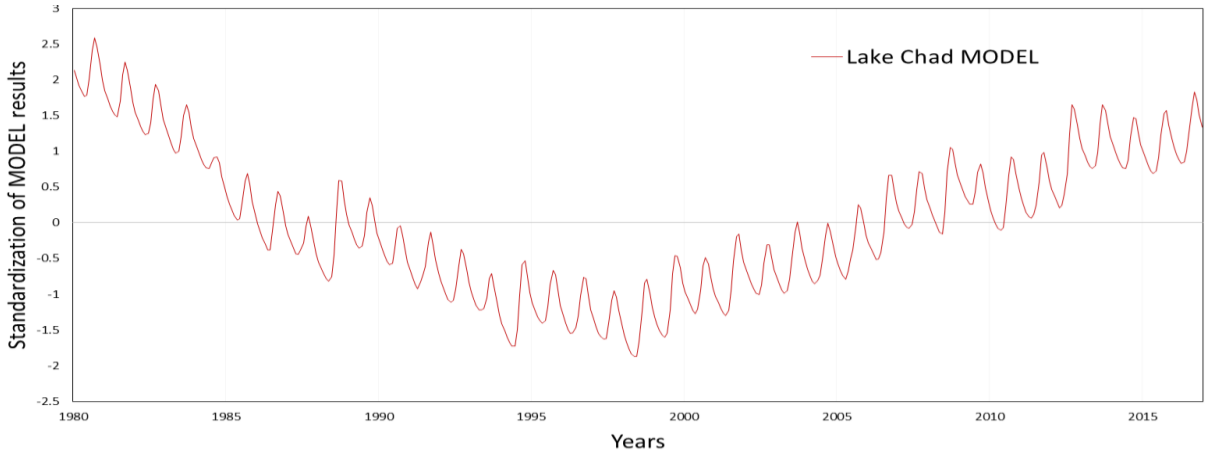

Figure 28: Lake Chad Model

4.5.3 PDO vs SWB Model

The PDO is another important climate oscillation. It is strongly linked with ENSO and can be seen effecting zones all over the world.

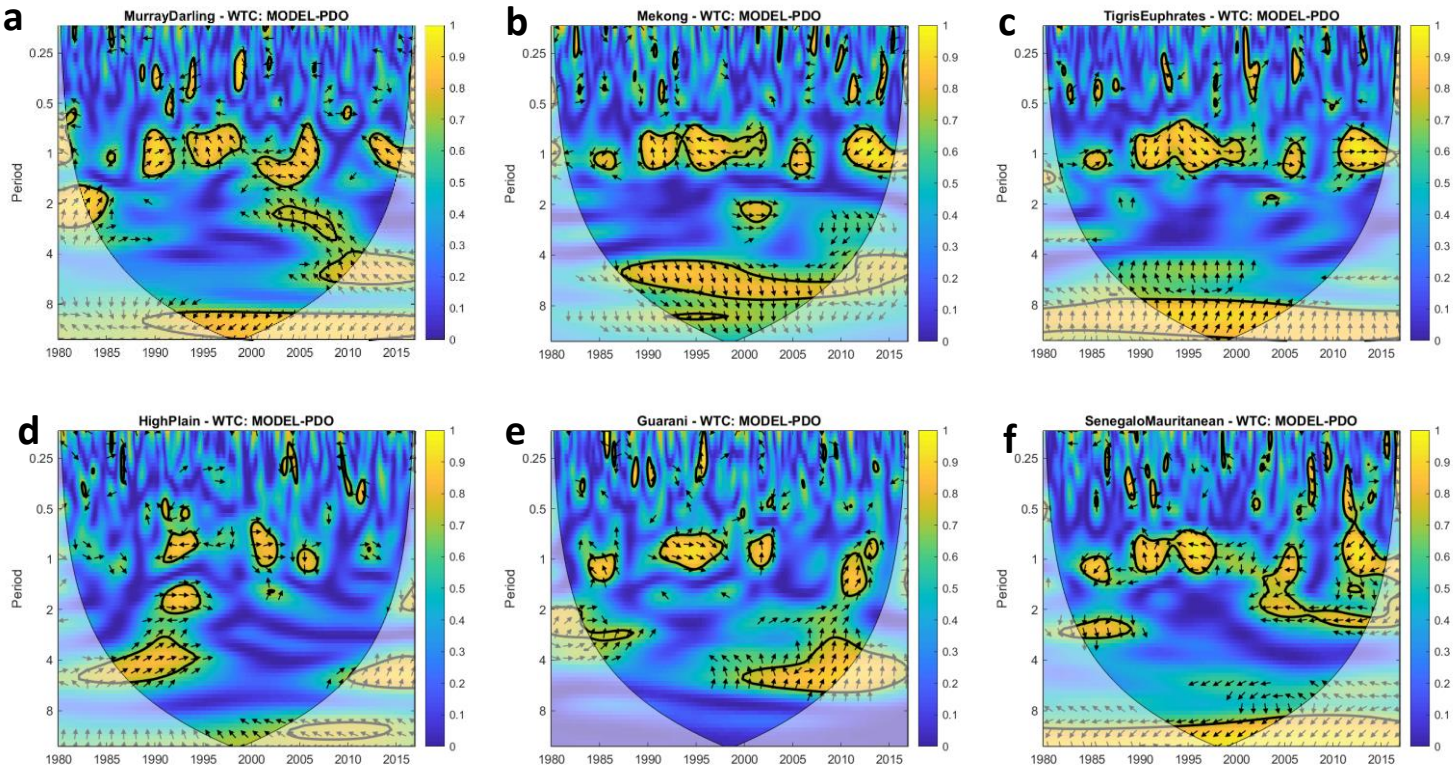

Figure 29: Wavelet coherence between PDO and Model: Note that the spectral power to the right of the plot is dimensionless, the areas inside the black lines are at the 5% significance level, and the pale white edges show the COI. The vectors indicate the phase difference between the data; a horizontal arrow pointing from left to right signifies in phase and an arrow pointing vertically upward means the groundwater level series lags the teleconnection index by 90° (i.e., the phase angle is 270°)

In almost all plots there can be found scattered zones of significant showing a strong coherence between groundwater storage change and PDO over the one to two year scale (Figure 29), However, this zone must be analysed carefully as not all are in phase lock (arrows all pointing in the same direction for a certain period (i.e Tigris Euphrates sees both in phase and a 90^{o} lag), providing an indication that the coherence may not be as strong as it looks.

Because PDO is dominated by inter-decadal oscillations, the model and PDO plots for Australia, Asia and northwest Africa see significant coherence at time scales of more than 6-15 years. Though many of the other regions have stronger wavelet power at the inter-annual time scale.

With PDO it is thought that its main influence on the global scale is its modulating the effect of ENSO. The literature has pointed out that this inter-annual relationship ENSO has with the climate is not stationary and that the inter-decadal oscillation of PDO can increase or decrease in relation to ENSO (Ouyang et al., 2014). This is illustrated in Figure 30 where the biggest peaks are associated with years where El Nina is matched with negative PDO.

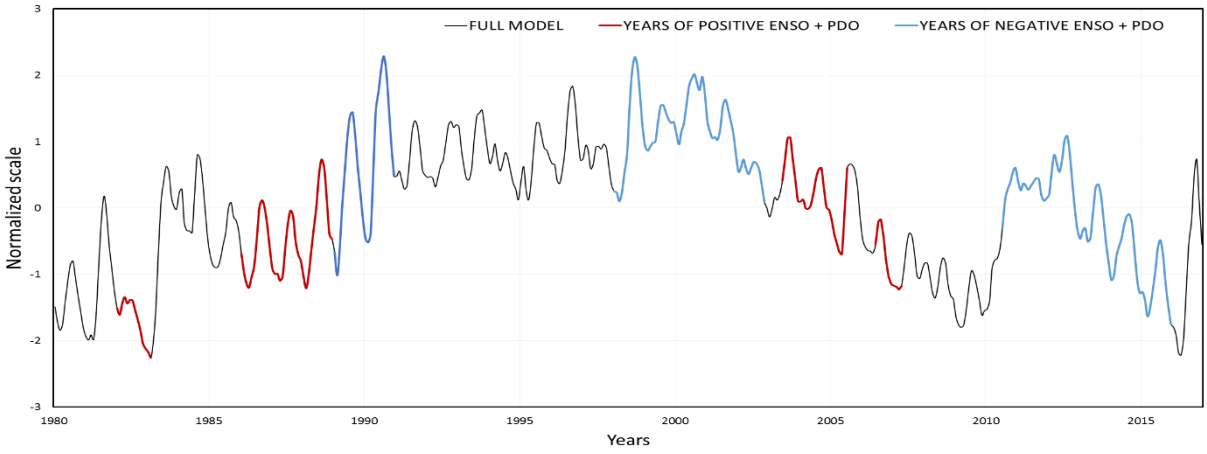

Figure 30: MDB Modelled results. With red indication years where ENSO and PDO are both positive and blue show negative.

The High Plains sees the worst fit because its P fluctuations are more erratic compared to the other sites. However, its fluctuations match that of GRACE in timing and size, its positioning appears to be being warped by the deviations from the linear trend.

Chapter 5 DISCUSSION

In this chapter the results and their characteristic features will be discussed. This will help provide an understanding of how the approach used in this thesis is working, and what this can tell us about climate variability, large aquifer systems and their mechanisms of water transport and storage. This chapter begins with an examination of the model. It looks at what the common features of the results indicate, and where the SWB Model works and where it does not. This will be followed by a discussion on the wavelet analyses results, and what this approach can tell us about climate variability versus pumping. Lastly the chapter will end with a general discussion going over the broader themes of this approach.

5.1 MODEL EVALUATION

5.1.1 Examining Key Features

This chapter begins with an examination of common features found throughout the GRACE data, SWB Model and GWL data. This will be done first to get a better idea about what the results tell us. It will also help to build an understanding of how the SWB Model is comparable to the GRACE and GWL data for further discussion in the following subsections.

NON-LINEAR TRENDS: When making the comparison and validation of the SWB model (with GRACE and GWL data) it is important to check the overall trends and tendency of the raw data (cumulative integral of P – ET) before it is detrended. Part of this approaches assumption is that detrending (linearly) will make the SWB model results valid for aquifer systems that see constant or negligible runoff. However, if the trend is not linear then the resulting fluctuations in the water flux can be very misleading. This can be seen in the Stampriet example (Figure 31) shown below. Here the original data (with trend) has an overall non-linear trend. This means that when the detrending removes the mean (red dashed line) the fluctuations around it are exaggerated (seen by red arrows) and areas where there are a lot of fluctuations but they are moving away from trend line (red circle), these are stretched thin or muted.

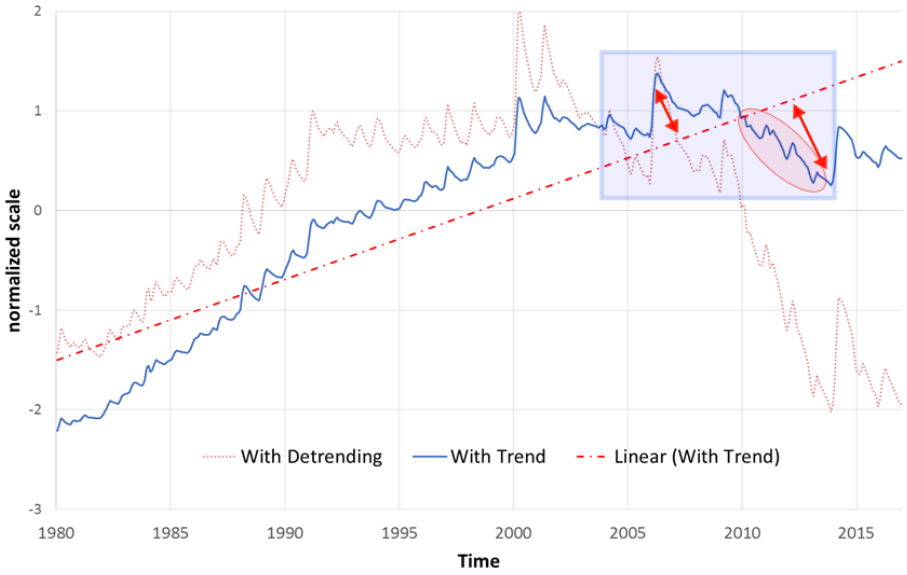

Figure 31: Stampriet Model results

However, by excluding areas that are not linear, conclusions can still be developed on parts of the data set. In Figure 32 the Volta data is seen before detrending and after.

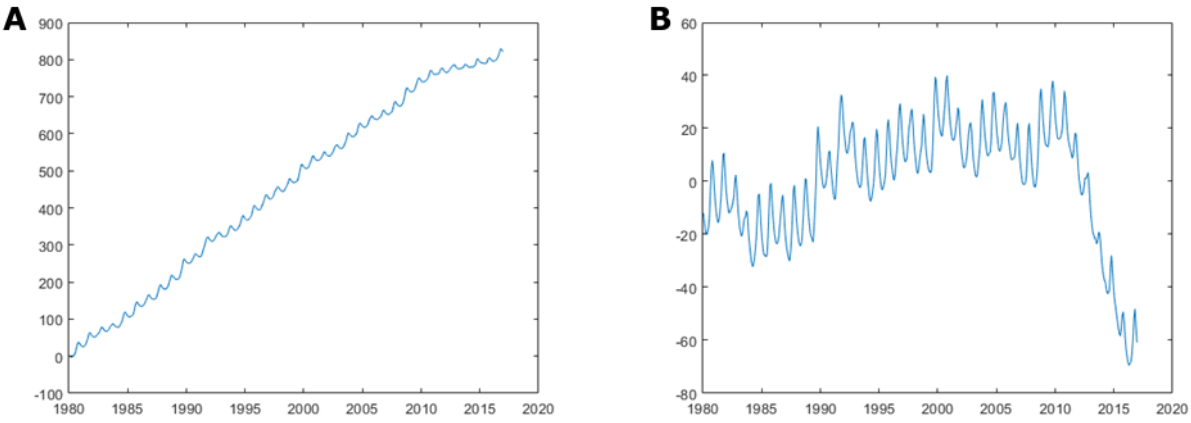

Figure 32: Volta data plotted A) Before detrending and B) after

It can be observed that Volta has a linear trend up until 2010 where it flattens off. In the detrended plot after 2010 there is a huge drop in the flux. As mentioned before this seems to be due to its exaggeration from the non-representative mean trend. However, looking at the SWB Model vs GWL in Figure 17a good fit can be seen. This is because the plot is only looking at the data from 1980 to 1995 (so is missing the deviation of the trend after 2010), meaning when the SWB Model is detruded (1980 to 1998), the trend being removed is linear. This must also be considered when running the wavelet analyses, it will be looking at the entire time frame, not just the linear parts. Nubia, Amu Darya and Saq Rum were other aquifer systems that showed non-linear trends.

Moreover, decreasing plots like the one seen in Volta can still be a result of temporary overexploitation (in addition to droughts), because the only thing removed was the long-term trend (linear). This highlights the need to check the raw data as depending on how non-linear the trend is the results can still produce useful insights as long as you know how to interpret the plot's features.

JAGGED VS SMOOTH: A very noticeable feature in some of the GRACE data is its often-jagged irregularities on its fluctuations, Saq Ram, MDB and Stampriet plots all show good examples of this. This could be caused by a number of influences.

When looking at the GRACE - SWB Model comparison it appears drier aquifer systems (with less water quantity passing through them) may be more responsive to any kind of precipitation event or groundwater abstraction than wetter systems. This shows in this irregular and jagged line, often having multiple peaks in each fluctuation. These drier systems include areas like Syr Darya, Murry Darling Basin, North China Plain and all the North American systems. This responsiveness to precipitation events is a function of the volume and regularity of water passing through the system. Where it is dry, and the precipitation is irregular, even small precipitation events will show-up as short-lived spikes. Whereas in areas with very wet seasons, such small precipitation events will not stand out in the data.

There are clear sharp negative spikes (seen in Saq Ram), this could also hint at the effects of groundwater exploitation in the dry season. In this context, large volumes of water are removed in dry spells, but these volumes are recovered during the wet season. The model would pick this up through its ET if the pumping was for irrigation.

Recently Cuthbert *et al*, (2019) showed how recharge in many arid environments is episodic, characterised by intense rainfall and dominated by focused recharge through losses from ephemeral overland flows. This could explain the irregular GRACE plots like the North Western Sahara Figure 13 and Saq Ram Figure 15, where the recharge is dominated by sporadic events rather than by 'regular' oscillating seasons.

IDENTIFIERS: Gaining an awareness of how some irregular jagged features are picked up by the model is also an indicator for identifying important influences in water storage change. For example, the Congo (Figure 13) has two wet seasons which are clearly evident in both the GRACE and SWB Model results as two small bumps on the peaks of each fluctuation. However, the Say Darya (Figure 15) also has multiple bumps on the fluctuation peaks, but these bumps are not reflected in the modelled results. This suggests the origin of the irregular GRACE results may not come directly from precipitation events (or from P –ET) and maybe are related to deeper aquifer flow, surface water or pumping.

This feature of the SWB Model picking up the irregular jagged parts of the fluctuations is a good sign the model will be a good fit with the GWS change. It is an indication that direct precipitation is the dominant determinate of TWS change. This is seen in Karoo Sedimentary, MDB, Indus and North China Plains.

SMOOTH: In areas that see marked wet and dry seasons, where large quantities of water can pass through the system, there are more rounded and regular undulations. This is seen in many of the plots, but the most notable are the monsoon aquifer systems – the Mekong and East Ganges (Figure 15 f and g), in the Sahel Zone (Figure 13 a, b, c and d) and in the Amazon (Figure 17a). All these areas have been classified in Figure 33 as places with large amplitude fluctuations in available water, where big available water changes are seen from season to season.

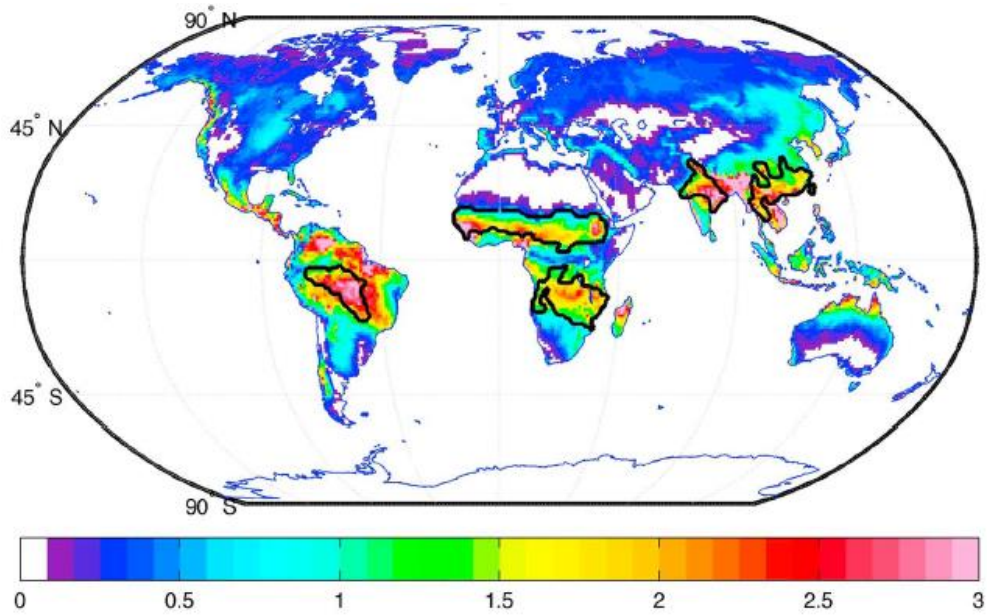

Figure 33: Amplitude of the complex spatial pattern of water availability, areas in black borders see the most difference between a dry and wet season in a year. the white regions mean no variability (can be always wet or always dry) (WMO-UNEP, 2008)(García-Garcí & Ummenhofer, 2015)

5.2 ENVIRONMENTAL FACTORS

When we look at the different environments in this global study and the studied aquifer systems' traits, we can see a number of patterns emerging. These patterns are related to certain aquifer boundary condition or size, and they manifest across a range of climate zones, geographic zones and economic zones. This section will briefly discuss these trends to identify traits that appear to improve the results seen through better fitting data sets.

BASINS: One of the strongest trends running through areas with good results was whether the shape file used (the area represented) was a basin or an aquifer. Basins provided a better fitting data sets and can be seen with the Murray Darling Basin, Mekong, Tigris-Euphrates and the Congo. In basins, their boundaries represented the whole catchment (unlike some of the aquifers). This means that in a basin, the model would be able to consider all the precipitation entering the area, and it also means that large inputs from surface water (that is formed away from the study area) will not interfere with the results. The Amu Darya and the East Ganges provide good example of aquifers which were characterised by having a lot of their surface water derived from large mountain ranges outside their boundaries. They see poor results when the SWB Model is compared to groundwater observations.

The basins tend to also be on a larger scale to a lot of the other sites. Generally, the larger the study area, the better the results. This approach is very coarse and neglects the intricate local interactions of the flow of water around the earth. So, the coarser the scale the less influence these local processes are seen to have.

DATA QUALITY: Another important factor is the quality of the climatic data. Areas of more robust and reliable climate data, of the likes seen in North American and Australia can be seen to have some of the best results with both GRACE and GWS change. In contrast, the African continent, was characterised by study areas with some of the poorest results – particularly in the north and south.

There are a number of issues that impact quality of data. These include poorer monitoring networks, short monitoring time frames (e.g as for the African GWL), and issues with the reliability of the climate data gathered. For example, the degree of variability in precipitation estimates in Africa have been shown to exhibit large differences in annual and seasonal precipitation estimates compared to other global data sets (Q. Sun et al., 2017). Africa is the region with least data which means it is the region where the model is likely to have highest uncertainty. The different global databases looked at in this report lead to quite similar results in Northern Africa, Sahara and Sahel, West and Central Africa, but quite different ones for East Africa (Nubian) and Southern Africa (Stampriet, Karoo). From Figure 22 it is also seen that the biggest deviations from the results of all the datasets is when GLEAM is used. However, for Stampriet good results are seen in GWL observation suggesting GLEAM might have a good data set for this area compared to the varying other ones.

BEST FIT: The GRACE compression saw the best results in areas that see large fluctuations and large amplitudes in their seasonality (areas of 1.5 and higher in Figure 33). These are climates that see monsoon type rains in the wet season and droughts in the dry season. The models fit with GWL also sees the closes similarities in amplitude and timing of the fluctuations. As the model is looking at fluxes or changes in storage, having these large quantities of water moving through them seems to smooth the results and give more weighting to the climatic factors (so giving P and ET more influence). This meant the climatic inputs ET and P where able to better represent the water flux of that area. These environments also showed good similarities with GWS change, especially in matching the amplitudes and frequencies of the fluctuations.

CONTINENTAL: Dry continental regions (both hot and cold) are another significant climatic zone. These areas have less climatic variability than those in the monsoon and Sahel zones, but they do have distinct wet and dry seasons (seeing an index value of 0.5 -1 in Figure 33). Areas in these regions include the North China Plains, The North Great Plains, Edward Trinity, the High Plains and Judith. In these study areas amplitudes, trends and positioning all match that of the TWS change data from GRACE quite well. These areas are also characterised by having models with irregular fluctuation patterns with more jagged oscillations, most of which are picked up by the SWB Model. This shows that for these areas have less influential surface water and groundwater characteristics in TWS change. The SWB Model is a good representation of the TWS change for these environments. For example, unlike the monsoon areas they are unlikely to periodically have large surface water inundation and large amounts of vegetation.

Another general trend seen in these aquifer systems is where their SWB Model fit seems to be strongly overestimating the ground water level change in the amplitude of the inter-annual fluctuations. This is the case for NCP, MDB, Volta and a lot of North America. This is interesting as they seem to fit with GRACE (in amplitude) perfectly. This has probably got something to do with the data sets standard deviation. In the GRACE and Model data the standard deviations can be seen to be quite different between them. However, they are proportioned to one another, the model appears to be a few magnitudes higher. So, when they are standardized the two data sets match. However, when compared to ground water observations there seems to be this overestimation in amplitude. This is most likely to do with the fact that groundwater is less responsive to climatic events (short event) due to the buffer zone in the soil and surface. This means the groundwater observation do not pick up on

these outlier events that will change the proportions of the residuals around the mean trends line and in so effecting the proportions of the amplitudes.

CONGO: The Congo provides a good example of an area you wouldn't expect to have good fitting data with GRACE (there was no GWL data). This study site illustrates how seasonal variation can be an important factor in the results of the model. In turn, this reminds us that as each aquifer system is defined by its geography and climate, knowing about the area allows you to draw better conclusions from the results. To take the Congo example further, the results of a good fitting GRACE TWS change was not an expected output from the analysis. This basin has a complex climate and fluvial environments, with a large drainage network where the annual discharge is around 40,000m^3/s (Becker et al., 2014). As the model only considers constant, steady or proportional discharge, one would think it would not model this system accurately. However the Congo Basin is uniquely located with respect to the Inter-Tropical Convergence Zone (ITCZ) such that precipitation peaks occur twice annually (Jung et al., 2010). This can be seen in both the GRACE data and the SWB Model with a double humped peak. This sees the northern parts of the area receiving their peak precipitation flow in October–November whereas the southern parts see it in March-April – creating a relatively subtle changes during rising and falling limbs of the seasonal hydrograph (Jung et al., 2010). The Congo wetlands are also known as swamp forests as they are located in broad topographic depressions of the central basin (Jung et al., 2010). Due to this the Congo system displayed less connectivity between the main channels and floodplain channels than did the Amazon system (Becker et al., 2014). With regular runoff being seen through the year, and with the de-trending of the model, runoff may play a small role in the terrestrial water storage flux leading to a good fit in both GRACE and GWL.

Surface Water – Groundwater: Where groundwater-level chronicles fit well with the SWB Model shows that groundwater and surface water storage changes are correlated. This is in agreement with Condon et al, (2019) where they argue that groundwater storage losses decrease overall surface water availability.

5.3 RELATION BETWEEN INDICES & MODELLED TWS

This section of the chapter will go through the wavelet analyses between the climate indices and the SWB Model. These results show the method produces initial evidence highlighting areas in time and frequency where there is significant coherence across environment types and regions of the globe. Here the discussion will only include ENSO, PDO and AMO as there was not enough time to go through all results (found in Appendix 8 - end).

ENSO

From these results the areas with the strongest correlation are monsoonal zones, along with Australia, South America and parts of the US.

A good case study for examining the reliability of the SWB Model and the quality of the wavelet analyses results in Southern Africa. From the results in Figure 23 it can be seen that Stampriet only has one small area of coherence, while Karoo sedimentary has many. In this region La Niña has been linked to strong precipitation. This coherence is clearly shown in the case of Karoo Sedimentary but not Stampriet.

These two aquifer systems from southern Africa would be expected to have similar results. The Karoo Sedimentary SWB Model is one of the best representations of the observed GWL data. This relationship between ENSO and increases and decreases of precipitation are suggested in the literature. Stampriet

SWB Model on the other hand does fit the data well, its overall intermittent trends are followed closely but the inter-annual and multiannual fluctuations are seen to go out of step from time to time (Figure 18). Suggesting that this could be why the coherence is missed. One zone of significant is picked up by both however and that is this 2004 to 2007 where the data jumps up from the decreasing intermittent trend or flattened off.

Central and north Africa see little effects from ENSO compared to the south and this also is seen in Lake Chad and Volta.

AMO

It is based upon the average anomalies of sea surface temperatures (SST) in the North Atlantic basin, typically over 0-80N. Its full cycle of around 50-70 years means that a full cycle is not captured within this 30 year study, however the switch from positive to negative is captured (around 1997). Nonetheless results are indicative only, and not definitive.

The AMO is an important climate variable with its influences being seen globally. This is most notable in the U shape seen in a lot of the modelled results around the year the AMO switch phases (1997). The orientation of the U shape highlights if the negative or positive phase of the AMO leads to increases or decreases in the TWS flux, this is seen to change depending where you are in the world.

The results for Australia fit with the general theory that a negative phase of the AMO dampens the effects of climate change while its positive phase exacerbates it. The positive phases see less rain and negative phases sees increased precipitation (Sun et al, 2015). This is what can be seen in Figure 27, after the positive phase switch in 1997, to the more inflammatory phase, the strong areas of significant coherence are seen. This suggests that during these positive phases the AMO there is more coherence to the climates around the world leading to more droughts and a decrease in the groundwater storage flux.

The effects of the switch however seem to be delayed; it sees a lag of about 6 years before the associated reduction in precipitation can be seen. However next door in the Mekong the positive phase of the AMO in summer brings higher rainfall while the negative phase brings less rainfall. This trend was also seen in García et al, (2015).

There is a strong correlation between AMO and TWS in the South African region. After looking at the model results of these study areas the U shape around 1997 is of the orientation of the MDB in Australia. In the negative phase, water levels rose and during the positive phase water levels have been decreasing. This fits with the literature which finds that the amount of rain that arrives there is dependent on the moisture being transported from both the Atlantic and Indian Oceans (García-Garcí & Ummenhofer, 2015). Down the Angolan and Namibian coast more rainfall is seen in times when the SST is warm in the tropical south-eastern Atlantic (this is also an effect of the positive phase).

The Sahel's climatic zone is also characterised by having its annual precipitation maximum in the summer. The positive AMO is associated with a northward shift of the Intertropical Convergence Zone (ITCZ), which produces this above-average rainfall in the Sahel (García-Garcí & Ummenhofer, 2015).

PDO

The PDO sees some of the strongest results with strong intermittent inter-annual zones of significance. There also seemed to be significant coherence in the eight to ten year period also. But unlike the intermittent inter-annual pattern, they appeared more constant.

5.4 CLIMATE-VARIABILITY VS GROUNDWATER ABSTRACTION

The results show that the climate oscillation patterns of ENSO, PDO, and AMO, NAO and IOD and associated hydroclimatic variability at least partly affect groundwater storage changes in the studied aquifers. Such changes are highly correlated with recharge from precipitation and might suggest that at these inter-annual to multi-decadal timescales, the GWS change variability might be in response to these long-term climate cycles and not only to seasonal or annual climate variations or human interferences such as pumping and irrigation (Gurdak et al., 2007; Taylor et al., 2012).

From the GRACE mission it has been identified that many of the largest global aquifers are being depleted (Thomas et al. 2019). With extractions often exceeding natural recharge rates in these key global freshwater bodies the depletion is commonly attributed to groundwater pumping (abstraction) for irrigation (Asoka *et al.* 2017). This often neglects the impacts of direct and indirect climate variability. Some studies suggest that the climatic oscillation patterns being looked at in this study are affecting aquifers recharge rates and groundwater level variability (Gurdak et al., 2007). Results here highlight this strong correlation between average total monthly groundwater change and climatic indices. It adds evidence to the idea that pumping is primarily a function of the meteorological conditions (Whittemore et a. 2015).

Irrigation is used to supplement the lack of precipitation in the summer season. Thus, precipitation (controlled by these climate indexes) determines when the water is pumped, and consequently is an indirect control on groundwater level. Precipitation also directly controls it through the recharge by infiltration. Abstraction is a secondary amplifier of climate variability. When precipitation and infiltration is low, abstraction is increased worsening the groundwater depletion. When there is a lot of rain and infiltration abstraction is decreased allowing for more groundwater level rise.

Another aspect to be aware of how deeper aquifers and their affects are seen in and related to the produced results**.** If abstraction is taking place in deeper aquifers (as is in the High plains aquifer) then this would not be observed shallow groundwater observations. This could help explain in part why the SWB Model fits with GRACE a lot better than the groundwater observations. Grace would account for the mass change made by extraction and the SWB Model would account for it through evapotranspiration (if used for agriculture).

The High Plains aquifer is one of the best examples of this as its heavy abstraction is well documented (McGuire, 2009). Pumping for irrigation (making up around 95% of the water being pumped) is considered to be the main driver of water depletion in the aquifer (Whittemore et al. 2015). When looking at the High Plains SWB Model vs the groundwater observations (Figure 20) the model's amplitudes are largely exaggerated, possibly being a result of the above mentioned deep abstraction process. As pumping is seasonal (largely due to irrigation) large fluctuations in inter-annual and seasonal cycles is expected and seen in the High Plain.

5.5 LIMITATIONS OF THE WORK

SHORT TIME PERIODS: One of the biggest restrictions on the analyses of the model with the groundwater observations is the often-short time periods being looked at. The two study areas in South America provide good examples of this. With their large amplitudes and short time length it is hard to draw strong conclusions on how well the groundwater observations fit with the SWB Model and to what degree does the model represent the groundwater. In most of the cases where there are short periods of groundwater observations more can be understood about the accuracy of the general trend then these inter-annual oscillations.

EVAPOTRANSPIRATION: Another area of where the model could improve on is in its correction of the systematic errors found in these global evapotranspiration databases. Producing no bias and corrected data could be a good improvement, comparing this to the body of work here would also help identify areas where this approach should be used with caution.

DE-TRENDING: There are no proven automatic techniques that can identify trends components in a time series data. This approach assumes these trend components to be monotonous in nature, based on the tendency of P - ET being this way and the simplicity of it. This analysis tries to be simple and reproducible with minimal statistical knowledge needed, it tries to be a “one size fits all” approach. However, if the trend is non-linear then the results can be misleading and distorted. Therefore, it is always important to check the data, so you know what section are having these effects.

Chapter 6 CONCLUSIONS AND RECOMMENDATIONS

This chapter provides a brief summary (section 6.1) that builds on the discussion chapter and acknowledges the main aim of this research set out in Chapter 1. It then presents the answers to the five research questions (Section 6.2) as presented in chapter 1. Furthermore, three sets of recommendations are given in Section 6.3. These provide ideas for: i) water managers and policy makers; ii) future research; and iii) modelling practitioners.

6.1 CLOSING DISCUSSION

The GRACE satellite mission is an extremely powerful tool that is capable of shedding light on the movement of water in large aquifers when it is complemented by higher spatial-resolution GWS changes from ground-based monitoring and modelling analyses. GRACE data does not, however, allow you to draw any exhaustive conclusion about the impact of climatic oscillations cycles on groundwater resources because of its limited timescale of about 15 years.

From the results of the wavelet analyses the most influential and important climate variabilities can be identified for an area, the results harmonise with the supporting literature on the effects of the climate variability used in this body of work. In addition to this, the approach goes a step further by comparing the magnitude and strength of each indices' impact on ground water, and also indicating at what periods and years they have had the most influence. The approach is an effective way to assess the impact of climate variability on groundwater in large aquifers as a preliminary analysis.

The SWB Model has shown it can recreate groundwater levels effectively, allowing for the timeframe of the study to go back far enough to capture these multi decadal climate variabilities. It has demonstrated its potential as an effective tool to assess groundwater storage change due to climate variability. It has also demonstrated that it can use "cost-effective" open-access global datasets which facilitate the replication of the model. These datasets include global climatic data bases, user-friendly Level-3 GRACE data grids of monthly surface mass changes, and groundwater observations found on national data bases and in literature). The specialty knowledge, resources and time required is also lower than that of other approaches that require the interpretation of less user-friendly satellite data, and/or heavy statistical analyses. Collectively, these advantages make the use of the SWB Model a very cost-effective approach for developing a more robust understanding of groundwater storage changes. The loss of accuracy in its "one size fits all" approach is balanced by its gains in its usability and flexibility as an initial examination of large aquifers. Significantly, its usefulness is most notably evident in areas of the globe that are remote, poorly monitored and where there are limited resources for these kinds of analyses. In these settings – often characterised by minimal real-world observations – the approach can be employed to help build more nuanced understanding of water storage dynamics in these important large aquifers. It is also an approach that can be helpful for supporting decision-making in large transboundary aquifers where data acquisition can be slow and tedious (but where approaches that build understanding of the underlying environmental dynamics can help drive multi-country cooperation and coordination).

6.2 ANSWERS TO RESEARCH QUESTIONS

6.2.1 Research Question 1:

Evaluate the SWB model as a tool for global scale groundwater evaluations against climate variability (atmospheric and ocean climate indices) under the framework of the UNESCO Groundwater and Climate Change (GRAPHIC) program.

When looking at groundwater over large areas it is very rare to have comprehensive and reliable data from any kind of comprehensive monitoring network. The expense and effort needed for this kind of monitoring is often beyond the resources of the groups and organisations involved. However, with the future projected climate scenarios there is a growing need to learn about how climate and groundwater systems work, and how they relate to one another. With this context of limited data and climate uncertainty there is a need to develop innovative approaches and methods to build water management and water resource planning into evidence-based decision making. This SWB model is a usable and dynamic tool that addresses this issue. It can be used to provide a useful preliminary analysis that helps in understanding the relationship between natural climate indices and ground water storage flux. It also can help in discerning the most prominent water storage processes and mechanisms within an aquifer system.

Overall, as a tool for global scale groundwater evaluations the SWB Model performed well. Most of the plots comparing groundwater observations and the SWB Model saw matching multi-decadal patterns. When it came to inter-annual fluctuations the results become less clear with no obvious regain or climate having a monopoly on good results.

it is important to note that the SWB Model results only look at groundwater storage flux. The effects of climate change and long-term abstraction have been removed through detrending the data and cannot be discussed through the results of this study.

One of the model's main strengths lies in the benefits it can provide for regions with limited resources and capabilities. The simplicity of the model and the automation and refined methodology of the data processing developed in this body of work provides a powerful tool that could be easily replicated and applied in regions with expertise, knowledge and capacity gaps. Accordingly, it fits well within the framework of the UNESCO Groundwater and Climate Change (GRAPHIC). It has been developed with a focus on developing regions (in particular Africa), it uses open source data, and it aims to provide easily reproducible analyses.

6.2.2 Research Question 2

Refine and automate data processing to increase accuracies and usability of the methodology.

One of the main challenges with looking at global data sets is that it is hard to isolate and extract the exact data required for any particular analyses. This problem is exacerbated when there are daily global datasets for a 37 year period that need to be processed. This study demonstrated – through the use of MATLAB – that scripts are able to be made that can quickly produce a list of monthly total averages for a specified boundary, and of P and ET from the 0.25° by 0.25° gridded daily global data sets for a 37 year period. This was also able to be done to a high degree of accuracy for the resolution of this study.

6.2.3 Research Question 3

Identify the circumstances and characteristic that see the SWB Model at its most appropriate for the representation of GRACE and groundwater storage change.

From the evaluation of the SWB Model, it is clear the overall results compared to GRACE were really good, showing that as an extension tool for GRACE derived TWS change, it is a strong and effective tool that can be used in sites in most parts of the world.

Not surprisingly, when using it to represent groundwater storage change, the good results are less globally ubiquitous. Though the overall outputs were strong there are several main factors that dictate where the model will be most accurate. For one, having the Model's assumption met – like having a linear trend – largely improves the fits with GRACE and GWS change. However, depending on how non-linear the trend is, the model could to an extent still be used (with caution) and still show useful results in the wavelet analyses. Aquifer systems that did not see outlier precipitation events and that showed regular (in quantity and timing) precipitation, found the strongest fits in fluctuation amplitudes. One of the strongest dynamics was whether or not the aquifer systems' primary factor in TWS change was direct precipitation. Sites with matching groundwater and surface water catchments also saw the model showing better results between GRACE, and to an extent ground water observations. Lastly aquifer systems of the larger order consistently saw the best results.

6.2.4 Research Question 4

Identify how global climatic oscillations cycles (like ENSO, PDO, and AMO) affect groundwater storage in large aquifers (area > 100 000 km²) around the world.

The wavelet method shows that groundwater-level dynamics in spatially distinct and hydro-geologically separate aquifers are strongly linked by environmental coherence, driven by climatic patterns over large parts of the Earth's surface.

The results highlighted in this study provide some idea about the level of coherence each climate index has with the aquifer system. These results suggest PDO has a strong coherence with its multi-decadal oscillation with most aquifer systems. This is made more evident by the continuous nature of the zones showing high significance in the 8 to 12 year periods. This also fits with PDO 20 year cycle. The next two most important indices appear to be AMO and ENSO. The AMO effects could be seen in a lot of the modeled results intermittent trend, where a distinct U shape would be orientated around the 1997 phase shift from negative to positive. Depending where in the world the site dictated the orientation of this,

Looking at the wavelet analyses of AMO it is important to note that the phase charges for this climate oscillation are longer than this study (shift accrued in 1997), however looking at the output of the SWB Model (plotted) the effects of the AMO dominated a lot of them. The wavelet analyses can identify times and periods where groundwater was influenced by climate. This research provides a starting point for further analyses to be undertaken at local and regional levels where effective water management and planning takes place.

6.2.5 Research Question 5

Assess if variability in groundwater storage changes on inter-annual to multi-decadal timescales are more correlated to climatic factors or to temporal trends in groundwater pumping.

Although the effects of climate change and long-term abstraction have been removed through detrending the data we can still see influenced by irrigation pumping through evapotranspiration. Increases in evapotranspiration (from pumping) can see the data's intermittent trends decrease or increase. More notably and more problematic is the effect on inter-annual variation. Agricultural pumping usually is seasonal seeing more done in dryer months. This leads to exaggerated amplitudes. Untangling these effects is an important step and provide a good starting point from which to improve this approach further.

6.3 RECOMMENDATIONS

6.3.1 Improving ground water management

The results obtained here provide a tool to support groundwater management and policy decision-making. Both the SWB model and GRACE have a low spatial resolution that is too coarse to supply groundwater level data that is suitable for water managers to use directly. However, this level of resolution is useful for highlighting the need for better management, and with its broad scale it can help in setting regional to national management-level strategies. Water managers and policy makers can begin to use the information presented here in several different ways to improve and strengthen decision making and decision-making processes. These include:

- Strengthening links between agencies and government departments (e.g. between Department of Water Affairs and Meteorological Agencies) at national and regional levels. This could be a precurser to examining whether groundwater level variability in some areas might be more correlated to precipitation variability than currently thought.
- Helping to identify locations and optimal time periods for water storage and managed artificial recharge (MAR) operations in accordance to ENSO, PDO, and AMO phases.
- Giving consideration to updating groundwater abstraction permits so they are in accordance to with ENSO, PDO, and AMO phases and their likely effects.

6.3.2 Future research

All though a lot can be learnt about the relationship between climate variability and groundwater and the role of dominant TWS processes, there are a number of areas where improvements could be made. This reality arises largely from the number of different aspects that impact on groundwater storage, and from the large scale of the approach. Areas of future research that could build on this study could include:

- Finding more complete and representative groundwater observations would be a good way to improve confidence in resulting conclusions. This could be done through increasing

observation numbers in the study area, reducing the chance outliers may affect results. It would also reduce the chance of observations representing local scale groundwater storage change and not regional. Increasing the time frame of the observations would also give more weighting in the validation of the model.

- Adding non-agricultural abstractions and runoff data to the model, though in a way that does not add to much complexity. This would increase its accuracy and allow you to enable the development of more conclusive conclusions about the results and groundwater storage. A study could be done on comparing results found here to a model that include runoff, another one that includes pumping and one that includes both. This could then help identify to what extent and range do they interfere.
- If the effects of observational errors found throughout the climate data and errors associated with assumptions could be reduced, then that would mean study areas could be developed on smaller scales.

However, as part of the SWB Model's aim is to have a degree of simplicity it is important to keep an eye on the actual outcomes sought. The accuracy of the process could certainly be improved in many sections, but researchers need to focus on the difference this could make to management and policy decision makers when the scale of the areas involved – often from national to regional levels – are so large.

6.4 A CONCLUDING COMMENT

Finally, this study has involved a number of people and organisations through both the collection and analysis of data from sites all around the world. This involvement (albeit small) still contributes to build an awareness of assessing the linked influence of precipitation, groundwater recharge and anthropogenic pumping as related to changes in groundwater storage. The study contributes to provide understanding of the need to recognize the impact of coupled human-natural systems under climate variability to aid in addressing key water resources challenges and sustainability assessments of groundwater resources.

References

Alley, W. M., & Konikow, L. F. (2015). Bringing GRACE Down to Earth. *Groundwater*, *53*(6), 826–829. https://doi.org/10.1111/gwat.12379

Asoka, A., Gleeson, T., Wada, Y., & Mishra, V. (2017). Relative contribution of monsoon precipitation and pumping to changes in groundwater storage in India. *Nature Geosci*, *10*(2), 109–117. https://doi.org/10.1038/NGEO2869

Beck, H. E., Zimmermann, N. E., McVicar, T. R., Vergopolan, N., Berg, A., & Wood, E. F. (2018). Present and future Köppen-Geiger climate classification maps at 1-km resolution. Scientific Data. 5: 180214. .

Becker, M., da Silva, J. S., Calmant, S., Robinet, V., Linguet, L., & Seyler, F. (2014). Water level fluctuations in the Congo Basin derived from ENVISAT satellite altimetry. *Remote Sensing*, *6*(10), 9340–9358. https://doi.org/10.3390/rs6109340

Brekke, L. D., Kiang, J. E., Olsen, J. R., Pulwarty, R. S., Raff, D. A., Turnipseed, D. P., … White, K. D. (2009). Climate change and water resources management: A federal perspective. *US Geological Survey Circular*, (1331), 1–76.

Coarvalho Resende, T. (2015). Levaluation de L imact de la variabilite climatique sur les ressources en eau souterraine dans les grands aquiferes. Université de Rennes, 1-48

Carvalho Resende, T., Longuevergne, L., Gurdak, J. J., Leblanc, M., Favreau, G., Ansems, N., … Aureli, A. (2018). Assessment of the impacts of climate variability on total water storage across Africa: implications for groundwater resources management. *Hydrogeology Journal*. https://doi.org/10.1007/s10040-018-1864-5

Condon, L. E., & Maxwell, R. M. (2019). *Simulating the sensitivity of evapotranspiration and streamflow to large-scale groundwater depletion*. *Sci. Adv* (Vol. 5). https://doi.org/10.1126/sciadv.aav4574

Cuthbert, M. O., Taylor, R. G., Favreau, G., Todd, M. C., Shamsudduha, M., Villholth, K. G., … Vouillamoz, J. (2019). Observed controls on resilience of groundwater to climate variability in sub-Saharan Africa. *Nature*, *572*(7768), 230–234. https://doi.org/10.1038/s41586-019-1441-7

Eckstein, G., & Sindico, F. (2014). The law of transboundary aquifers: Many ways of going forward, but only one way of standing still. *Review of European, Comparative and International Environmental Law*, *23*(1), 32–42. https://doi.org/10.1111/reel.12067

FAO. (2015). Food and Agriculture Organization of the United Nations. *FAO Publications*, 83. Retrieved from www.fao.org/publications

García-Garcí, D., & Ummenhofer, C. C. (2015). Multidecadal variability of the continental precipitation annual amplitude driven by AMO and ENSO. *Geophysical Research Letters*, *42*(2), 526–535. https://doi.org/10.1002/2014GL062451

Gemitzi, A., & Lakshmi, V. (2018). Estimating groundwater abstractions at the aquifer scale using GRACE observations. *Geosciences (Switzerland)*, *8*(11), 1–14. https://doi.org/10.3390/geosciences8110419

Global Risks 2015 10th Edition. (2015). *World Economic Forum*, *10th Editi*, 138. Retrieved from https://https//www.issuelab.org/resource/global-risks-2015-10th-edition.html

Gorelick, S. M., & Zheng, C. (2015). Global change and the groundwater management challenge. *Water*

Resources Research, *51*(5), 1–25. https://doi.org/10.1111/1462-2920.12735

Grinsted, A., Moore, J. C., & Jevrejeva, S. (2004). Application of the cross wavelet transform and wavelet coherence to geophysical time series. *Nonlinear Processes in Geophysics*, *11*(5/6), 561–566. https://doi.org/10.5194/npg-11-561-2004

Gurdak, J. J., Hanson, R. T., Mcmahon, P. B., Bruce, B. W., Mccray, J. E., Thyne, G. D., & Reedy, R. C. (2007). Climate Variability Controls on Unsaturated Water. https://doi.org/10.2136/vzj2006.0087

Hill, T. &. (2007). STATISTICS: Methods and Applications. StatSoft Tulsa, OK. http://library.aceondo.net/ebooks/Economics/Statistics_Methods_and_Applications.pdf.

Holman, I. P., Rivas-Casado, M., Bloomfield, J. P., & Gurdak, J. J. (2011). Identifying non-stationary groundwater level response to North Atlantic ocean-atmosphere teleconnection patterns using wavelet coherence. *Hydrogeology Journal*, *19*(6), 1269–1278. https://doi.org/10.1007/s10040-011-0755-9

Hossain, A. (2014). Groundwater Depletion in the Mississippi Delta as Observed by the Gravity Recovery and Climate Experiment (GRACE) Satellite System, (April).

Jalota, S. K., Vashisht, B. B., Sharma, S., & Kaur, S. (2018). Climate Change and Groundwater. In *Understanding Climate Change Impacts on Crop Productivity and Water Balance* (pp. 149–181). Elsevier. https://doi.org/10.1016/B978-0-12-809520-1.00004-5

Jean Kuss, A. M., & Gurdak, J. J. (2014). Groundwater level response in U.S. principal aquifers to ENSO, NAO, PDO, and AMO. *JOURNAL OF HYDROLOGY*, *519*, 1939–1952. https://doi.org/10.1016/j.jhydrol.2014.09.069

Jung, H. C., Hamski, J., Durand, M., Alsdorf, D., Hossain, F., Lee, H., … Zeaul Hoque, A. K. M. (2010). Characterization of complex fluvial systems using remote sensing of spatial and temporal water level variations in the Amazon, Congo, and Brahmaputra rivers. *Earth Surface Processes and Landforms*, *35*(3), 294–304. https://doi.org/10.1002/esp.1914

Knudsen, M. F., Seidenkrantz, M. S., Jacobsen, B. H., & Kuijpers, A. (2011). Tracking the Atlantic Multidecadal Oscillation through the last 8,000 years. *Nature Communications*, *2*(1), 178. https://doi.org/10.1038/ncomms1186

Kusche, J., Schmidt, R., Petrovic, S., & Rietbroek, R. (2009). Decorrelated GRACE time-variable gravity solutions by GFZ, and their validation using a hydrological model. *Journal of Geodesy*, *83*(10), 903–913. https://doi.org/10.1007/s00190-009-0308-3

Liesch, T., & Ohmer, M. (2016). Comparison of GRACE data and groundwater levels for the assessment of groundwater depletion in Jordan. https://doi.org/10.1007/s10040-016-1416-9

Margat, J., & Jac van der, G. (2013). *Groundwater around the World*. CRC Press.

Mccullough, C. (2013). Global Trends in Equivalent Water Height with GRACE and GLDAS.

McGuire, V. (2009). Water-level changes in the High Plains aquifer, predevelopment to 2007, 2005-06, and 2006-07. *Publications of the US Geological Survey*, 18. Retrieved from http://digitalcommons.unl.edu/cgi/viewcontent.cgi?article=1015&context=usgspubs

Neeling, J. . D. (1994). DYNAMICS OF COUPLED OCEAN - ATMOSPHERE MODELS : The Tropical Problem.

Nezlin, N. P., Kostianoy, A. G., & Lebedev, S. A. (2004). Interannual variations of the discharge of Amu Darya and Syr Darya estimated from global atmospheric precipitation. *Journal of Marine Systems*, *47*(1–4), 67–75. https://doi.org/10.1016/j.jmarsys.2003.12.009

Ouyang, R., Liu, W., Fu, G., Liu, C., Hu, L., & Wang, H. (2014). Linkages between ENSO / PDO signals and precipitation , streamflow in China during the last 100 years, 3651–3661. https://doi.org/10.5194/hess-18-3651-2014

Sakumura, C., Bettadpur, S., & Bruinsma, S. (2014). Ensemble prediction and intercomparison analysis of GRACE time-variable gravity field models, 1389–1397. https://doi.org/10.1002/2013GL058632.1.

Siebert, S., Burke, J., Faures, J. M., Frenken, K., Hoogeveen, J., Döll, P., & Portmann, F. T. (2010). Groundwater use for irrigation - A global inventory. *Hydrology and Earth System Sciences*, *14*(10), 1863–1880. https://doi.org/10.5194/hess-14-1863-2010

Springer, A., Kusche, J., Hartung, K., Ohlwein, C., & Longuevergne, L. (2014). New Estimates of Variations in Water Flux and Storage over Europe Based on Regional (Re)Analyses and Multisensor Observations. *Journal of Hydrometeorology*, *15*(6), 2397–2417. https://doi.org/10.1175/jhm-d-14-0050.1

Sun, C., Li, J., Feng, J., & Xie, F. (2015). A decadal-scale teleconnection between the North Atlantic Oscillation and subtropical eastern Australian rainfall. *Journal of Climate*, *28*(3), 1074–1092. https://doi.org/10.1175/JCLI-D-14-00372.1

Sun, Q., Miao, C., Duan, Q., Ashouri, H., Sorooshian, S., & Hsu, K.-L. (2017). A Review of Global Precipitation Data Sets: Data Sources, Estimation, and Intercomparisons. *Reviews of Geophysics*, *56*(1), 79–107. https://doi.org/10.1002/2017RG000574

Thomas, B. F., & Famiglietti, J. S. (2019a). Identifying Climate-Induced Groundwater Depletion in GRACE observations. *Scientific Reports*. https://doi.org/10.1038/s41598-019-40155-y

Thomas, B. F., & Famiglietti, J. S. (2019b). Identifying Climate-Induced Groundwater Depletion in GRACE Observations. *Scientific Reports*, 1–9. https://doi.org/10.1038/s41598-019-40155-y

Velpuri, N. M., Senay, G. B., Driscoll, J. M., Saxe, S., Hay, L., Farmer, W., & Kiang, J. (2019). Gravity Recovery and Climate Experiment (GRACE) Storage Change Characteristics (2003–2016) over Major Surface Basins and Principal Aquifers in the Conterminous United States. *Remote Sensing*, *11*(8), 936. https://doi.org/10.3390/rs11080936

Wang, H., Gao, J. E., Zhang, M. jie, Li, X. hua, Zhang, S. long, & Jia, L. zhi. (2015). Effects of rainfall intensity on groundwater recharge based on simulated rainfall experiments and a groundwater flow model. *Catena*, *127*, 80–91. https://doi.org/10.1016/j.catena.2014.12.014

Wang, S. Y. S., Lin, Y. H., Gillies, R. R., & Hakala, K. (2016). Indications for protracted groundwater depletion after drought over the Central Valley of California. *Journal of Hydrometeorology*, *17*(3), 947–955. https://doi.org/10.1175/JHM-D-15-0105.1

Whittemore, D. O., Butler, J. J., & Wilson, B. B. (2015). Assessing the major drivers of water-level declines: new insights into the future of heavily stressed aquifers. *Hydrological Sciences Journal*, *61*(1), 134–145. https://doi.org/10.1080/02626667.2014.959958

WMO-UNEP. (2008). *Climate Change and water - IPCC Technical Paper VI. Climate change and water*. https://doi.org/10.1016/j.jmb.2010.08.039

Appendices:

Appendix 1: Simple Water Balance Model

SIMPLE WATER BALANCE MODEL

LOCATE DATA

```
% Move to the location where your P and ET files are kept
cd (File location where your P and E are keeps)
```

SWB MODEL

```
% PUT IN YOUR P FILE
P=load('P_.txt')

X_P=P(:,1)
Y_P=P(:,2)
P_Model=cumtrapz(X_P,Y_P)
plot (X_P,P_Model)

% PUT IN YOUR E FILE
E=load('E_.txt')

X_E=E(:,1)
Y_E=E(:,2)
E_Model=cumtrapz(X_E,Y_E)
DTWS=(P_Model-E_Model)
DTWS_det=detrend(P_Model-E_Model)

% HERE YOU WILL FIND ALL PLOTS
t=X_P
plot(t,Y_P)
plot(t,Y_E)
E = (Y_P - Y_E)
plot(t,E)
plot(t,P_Model)
plot(t,E_Model)
plot(t,DTWS)
plot(t,DTWS_det)
```

SAVE AS

```
dlmwrite('SAVE NAME AS.txt',DTWS,'-append','newline','pc')
```

MOVE IT

```
movefile('SAVEED NAME AS.txt','C:\NEW LOCATION')
```

Appendix 2: Global Evapotranspiration data set

Global Evaporation data set

Open file

```
cd 'C:\Users\mal007\Desktop\MSc_IHE\Climate_Model\P and E\Shapefiles'\Aquifers\Africa\Stampriet\
```

Importing Lat-Long data

```
% Inporting Lat and Long data
 opts = spreadsheetImportOptions("NumVariables", 3);
% Specify sheet and range
 opts.Sheet = "Sheet1";
 opts.DataRange = "B2:D3";
 % Specify column names and types
 opts.VariableNames = ["first", "second", "Numberofcells"];
 opts.SelectedVariableNames = ["first", "second", "Numberofcells"];
 opts.VariableTypes = ["double", "double", "double"];
  % Import the data
 LatLongCells = readtable("LatLongCells.xlsx", opts, "UseExcel", false);
```

Load Mask

```
% Load mask
load('Mask.mat')

%MaskTransposed= Mask.'
                              LatLongCells = table2array(LatLongCells)
                              clear opts
                              a= LatLongCells(1,1)
                              b= LatLongCells(2,1)
                              c= LatLongCells(1,3)
                              d= LatLongCells(2,3)
                              b = b+1
cd 'C:\Users\mal007\Desktop\MSc_IHE\Climate_Model'\'P and E'\P&E_Full\E\DATA\
% Extract data
files = dir('*.nc')
for i = 1:numel(files)
```

JAN

```
Jan_daly_Evap = ncread((files(i).name),'E',[a b 1],[c d 31],[1 1 1]);
% times by mask
Jan_daly_Evap_With_Mask = Jan_daly_Evap.*Mask;

% rimove - values
Jan_daly_Evap_With_Mask(Jan_daly_Evap_With_Mask <0 ) = 0;

% this is for feb - now you need to average it all and save it
x = Jan_daly_Evap_With_Mask;
Y = cat(3,x);
Jan_cells_Sum = sum(Y,3);
```

FEB

```
Feb_daly_Evap = ncread((files(i).name),'E',[a b 32],[c d 28],[1 1 1]);

% times by mask
Feb_daly_Evap_With_Mask = Feb_daly_Evap.*Mask;
% rimove - values
Feb_daly_Evap_With_Mask(Feb_daly_Evap_With_Mask <0) = 0;

% this is for feb - now you need to average it all and save it
x = Feb_daly_Evap_With_Mask;
Y = cat(3,x);
Feb_cells_Sum = sum(Y,3);
```

Mar

```
Mar_daly_Evap = ncread((files(i).name),'E',[a b 60],[c d 31],[1 1 1]);
% times by mask
Mar_daly_Evap_With_Mask = Mar_daly_Evap.*Mask;

% rimove - values
Mar_daly_Evap_With_Mask(Mar_daly_Evap_With_Mask <0 ) = 0;

% this is for feb - now you need to average it all and save it
x = Mar_daly_Evap_With_Mask;
Y = cat(3,x);
Mar_cells_Sum = sum(Y,3);
```

Apr

```
Apr_daly_Evap = ncread((files(i).name),'E',[a b 91],[c d 30],[1 1 1]);
```

```
% times by mask
Apr_daly_Evap_With_Mask = Apr_daly_Evap.*Mask;

 % rimove - values
Apr_daly_Evap_With_Mask(Apr_daly_Evap_With_Mask <0 ) = 0;
999
% this is for feb - now you need to average it all and save it
x = Apr_daly_Evap_With_Mask;
Y = cat(3,x);
Apr_cells_Sum = sum(Y,3);
```

May

```
% For May
May_daly_Evap = ncread((files(i).name),'E',[a b 121],[c d 31],[1 1 1]);
% times by mask
May_daly_Evap_With_Mask = May_daly_Evap.*Mask;
% rimove - values
May_daly_Evap_With_Mask(May_daly_Evap_With_Mask <0 ) = 0;
% this is for feb - now you need to average it all and save it
x = May_daly_Evap_With_Mask;
Y = cat(3,x);
May_cells_Sum = sum(Y,3);
mean_May = nanmean(May_cells_Sum,"all");

dlmwrite('E-_daily-EACH_MONTH.txt',mean_May,'-append','newline','pc');
```

Jun

```
Jun_daly_Evap = ncread((files(i).name),'E',[a b 152],[c d 2],[1 1 1]);
% times by mask
Jun_daly_Evap_With_Mask = Jun_daly_Evap.*Mask;
% rimove - values
Jun_daly_Evap_With_Mask(Jun_daly_Evap_With_Mask <0 ) = 0;
% this is for feb - now you need to average it all and save it
x = Jun_daly_Evap_With_Mask;
Y = cat(3,x);
Jun_cells_Sum = sum(Y,3);
mean_Jun = nanmean(Jun_cells_Sum,"all");
dlmwrite('E-_daily-EACH_MONTH.txt',mean_Jun,'-append','newline','pc');
```

July

```
July_daly_Evap = ncread((files(i).name),'E',[a b 182],[c d 31],[1 1 1]);
% times by mask
July_daly_Evap_With_Mask = July_daly_Evap.*Mask;
% rimove - values
July_daly_Evap_With_Mask(July_daly_Evap_With_Mask <0 ) = 0;
% this is for feb - now you need to average it all and save it
x = July_daly_Evap_With_Mask;
Y = cat(3,x);
July_cells_Sum = sum(Y,3);
mean_July = nanmean(July_cells_Sum,"all");
dlmwrite('E-_daily-EACH_MONTH.txt',mean_July,'-append','newline','pc');
```

Aug

```
Aug_daly_Evap = ncread((files(i).name),'E',[a b 213],[c d 31],[1 1 1]);
% times by mask
Aug_daly_Evap_With_Mask = Aug_daly_Evap.*Mask;
% rimove - values
Aug_daly_Evap_With_Mask(Aug_daly_Evap_With_Mask <0 ) = 0;
x = Aug_daly_Evap_With_Mask;
Y = cat(3,x);
Aug_cells_Sum = sum(Y,3);
mean_Aug = nanmean(Aug_cells_Sum,"all");
dlmwrite('E-_daily-EACH_MONTH.txt',mean_Aug,'-append','newline','pc');
```

Sep

```
Sep_daly_Evap = ncread((files(i).name),'E',[a b 244],[c d 30],[1 1 1]);
% times by mask
Sep_daly_Evap_With_Mask = Sep_daly_Evap.*Mask;
% rimove - values
Sep_daly_Evap_With_Mask(Sep_daly_Evap_With_Mask <0 ) = 0;
x = Sep_daly_Evap_With_Mask;
Y = cat(3,x);
Sep_cells_Sum = sum(Y,3);
mean_Sep = nanmean(Sep_cells_Sum,"all");
dlmwrite('E-_daily-EACH_MONTH.txt',mean_Sep,'-append','newline','pc');
```

Oct

```
Oct_daly_Evap = ncread((files(i).name),'E',[a b 274],[c d 30],[1 1 1]);
% times by mask
Oct_daly_Evap_With_Mask = Oct_daly_Evap.*Mask;
% rimove - values
Oct_daly_Evap_With_Mask(Oct_daly_Evap_With_Mask <0 ) = 0;
x = Oct_daly_Evap_With_Mask;
```

```
Y = cat(3,x);
Oct_cells_Sum = sum(Y,3);
mean_Oct = nanmean(Oct_cells_Sum,"all");
dlmwrite('E-_daily-EACH_MONTH.txt',mean_Oct,'-append','newline','pc');
```

Nov

```
Nov_daly_Evap = ncread((files(i).name),'E',[a b 305],[c d 30],[1 1 1]);
% times by mask
Nov_daly_Evap_With_Mask = Nov_daly_Evap.*Mask;
% rimove - values
Nov_daly_Evap_With_Mask(Nov_daly_Evap_With_Mask <0 ) = 0;
x = Nov_daly_Evap_With_Mask;
Y = cat(3,x);
Nov_cells_Sum = sum(Y,3);
mean_Nov = nanmean(Nov_cells_Sum,"all");
dlmwrite('E-_daily-EACH_MONTH.txt',mean_Nov,'-append','newline','pc');
```

Dec

```
Dec_daly_Evap = ncread((files(i).name),'E',[a b 335],[c d Inf],[1 1 1]);
% times by mask
Dec_daly_Evap_With_Mask = Dec_daly_Evap.*Mask;
% rimove - values
Dec_daly_Evap_With_Mask(Dec_daly_Evap_With_Mask <0 ) = 0;
x = Dec_daly_Evap_With_Mask;
Y = cat(3,x);
Dec_cells_Sum = sum(Y,3);
mean_Dec = nanmean(Dec_cells_Sum,"all");
dlmwrite('E-_daily-EACH_MONTH.txt',mean_Dec,'-append','newline','pc');
end
```

RE-NAME

```
% Get all text files in the current folder
files = dir('*.txt');
% Loop through each file
for id = 1:length(files)
    % Get the file name
    [~, f,ext] = fileparts(files(id).name);
    rename = strcat('KarooSedimentary_E_Test',ext) ;
    movefile(files(id).name, rename);
end
```

MOVE TO

```
movefile('KarooSedimentary_E_Test.txt','C:\Users\mal007\Desktop\MSc_IHE\Climate_Model\P and E\P&E_Full\Aquifer\Africa\')
```

Appendix 3: Global Precipitation Data Scrip

GLOBAL PRECIPITATION DATA SCRIP

```
cd 'C:\Users\mal007\Desktop\MSc_IHE\Climate_Model\P and
E\Shapefiles\Aquifers'\Africa\Stampriet\
                            % Inporting Lat and Long data
                            opts = spreadsheetImportOptions("NumVariables", 3);
                            % Specify sheet and range
                            opts.Sheet = "Sheet1";
                            opts.DataRange = "B2:D3";
                            % Specify column names and types
                            opts.VariableNames = ["first", "second", "Numberofcells"];
                            opts.SelectedVariableNames = ["first",
"second","Numberofcells"];
                            opts.VariableTypes = ["double", "double", "double"];
                        % Import the data
                        LatLongCells = readtable("LatLongCells.xlsx", opts, "UseExcel",
false);
 % Load mask
 load('Mask.mat')
 MaskTransposed= Mask.'
 save('base workspace',"MaskTransposed")

                                    LatLongCells = table2array(LatLongCells)
                                    clear opts
                                    Row1 = LatLongCells(1,1) % Row 1
                                    Col1 = LatLongCells(2,1) %colum 1
                                    Down= LatLongCells(1,3) % # of cells down
                                    Across = LatLongCells(2,3) % # of cells across
                                    Col1 = Col1+1
                                    Rol1 = Row1+1
 cd 'C:\Users\mal007\Desktop\MSc_IHE\Climate_Model\P and E'\P&E_Full\P\
 files = dir('*.nc')
 for i = 1:numel(files)
 Full_Monthly_Target_Grid = ncread((files(i).name),'precip',[Col1 Row1 1069],[Across Down
12],[1 1 1]);
 % times by mask
 Full_Monthly_Target_Grid_Mask = Full_Monthly_Target_Grid.*MaskTransposed;
  % rimove - values
```

```
  Full_Monthly_Target_Grid_Mask(Full_Monthly_Target_Grid_Mask <0 ) = 0;
  end
  mean = nanmean(Full_Monthly_Target_Grid_Mask, 1:2);
  dlmwrite('STAMPRIET_P_Full.txt',mean,'-append','newline','pc')
```

```
movefile('STAMPRIET_P_Full.txt','C:\Users\mal007\Desktop\MSc_IHE\Climate_Model\P and E\P&E_Full\Aquifer\Africa\')
```

Appendix 4: SWB Model results for Africa

Senegalo Mauritanean

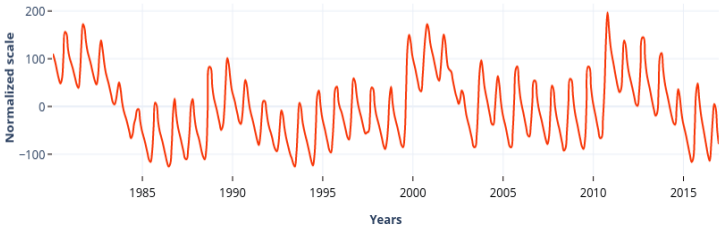

Lake Chad

Iullemeden

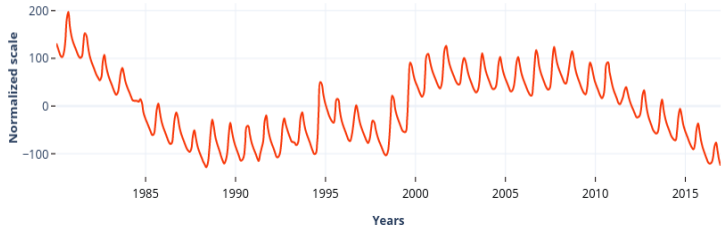

Volta

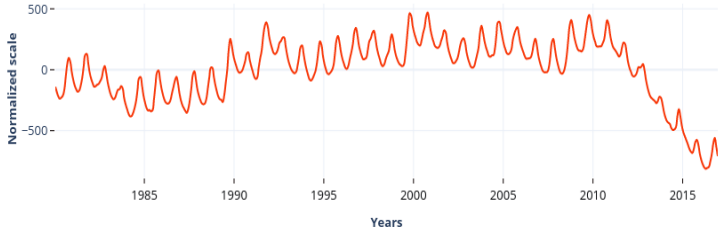

Nubian

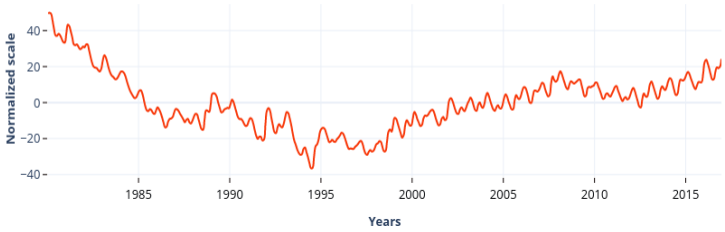

North Western Sahara

Congo

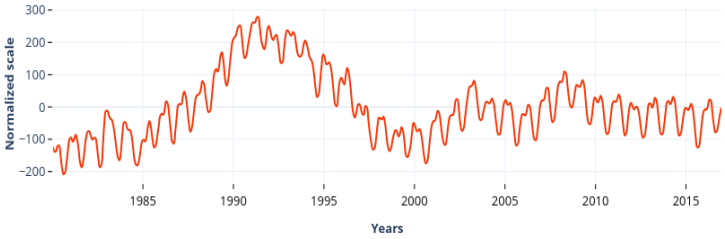

Karoo Sedimentary

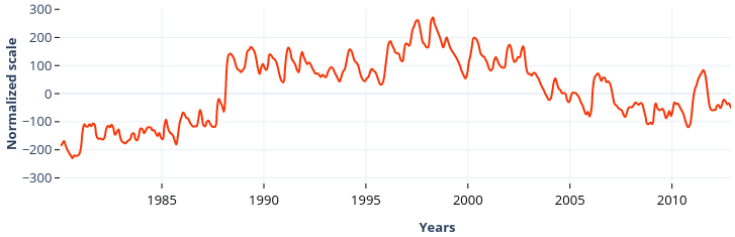

Stampriet

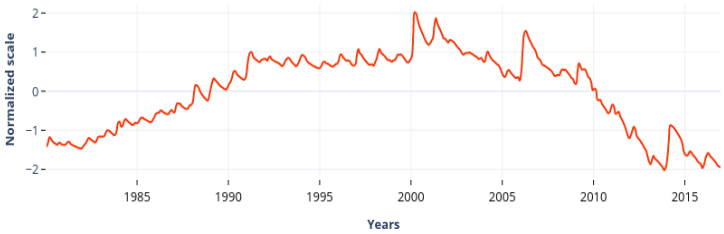

Appendix 5: SWB Model results for Asia

Amu Daray

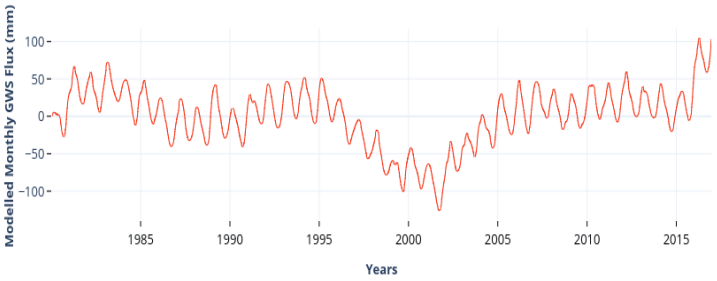

Syr Daray

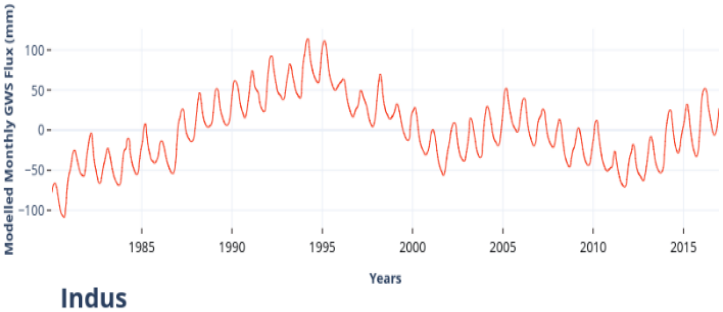

Saq Ram

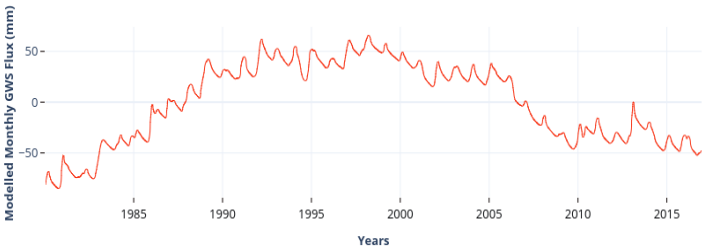

Indus

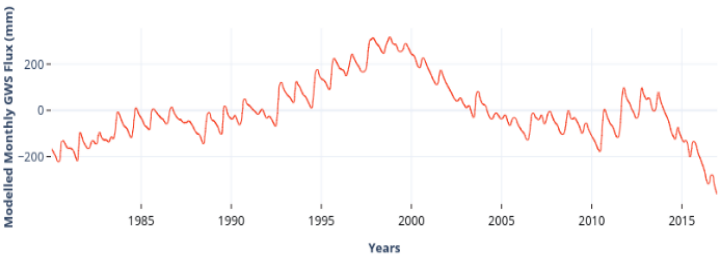

Tigris Euphrates

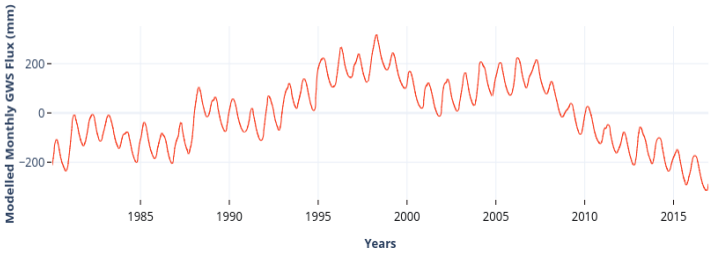

East Ganges

Mekong

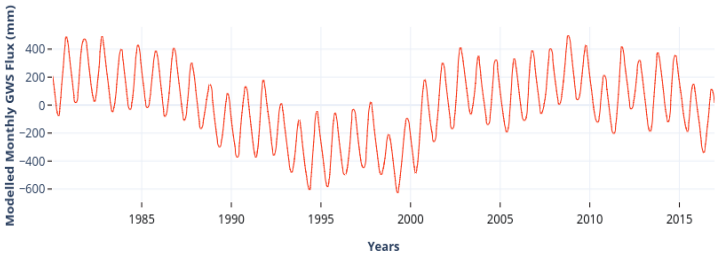

Murry Darling

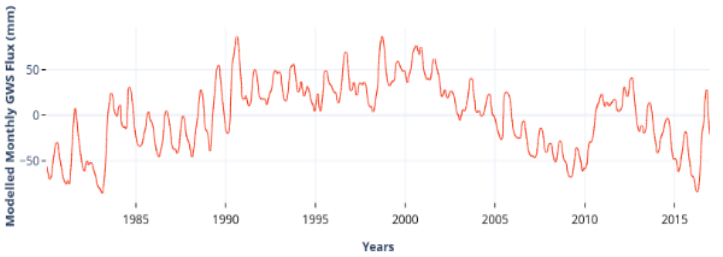

North China Plain

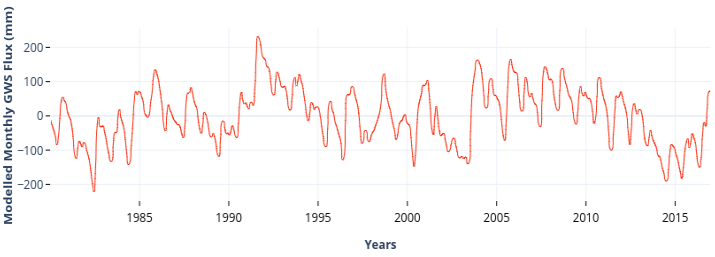

Ganges

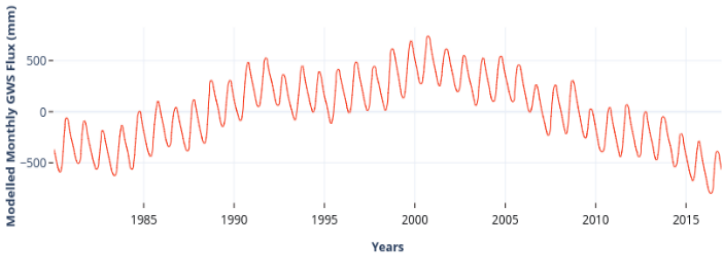

Appendix 6: SWB Model results for North America

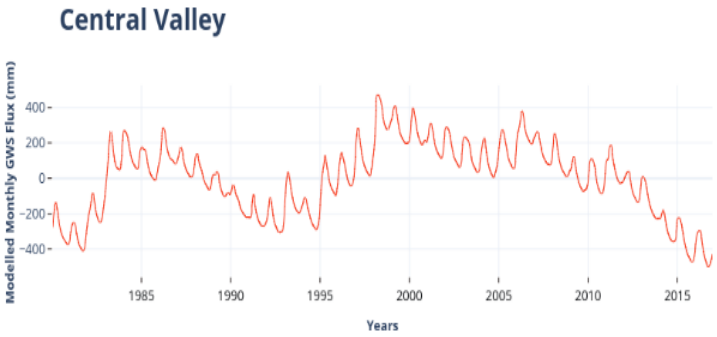

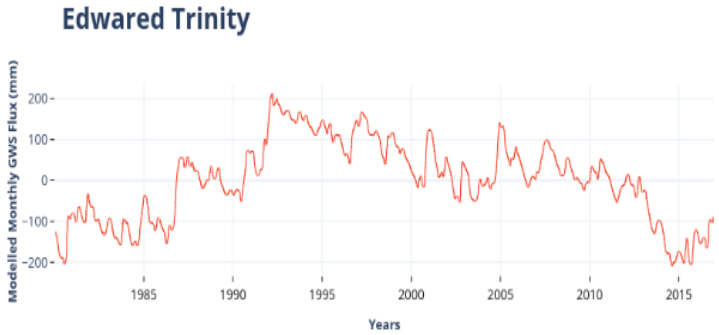

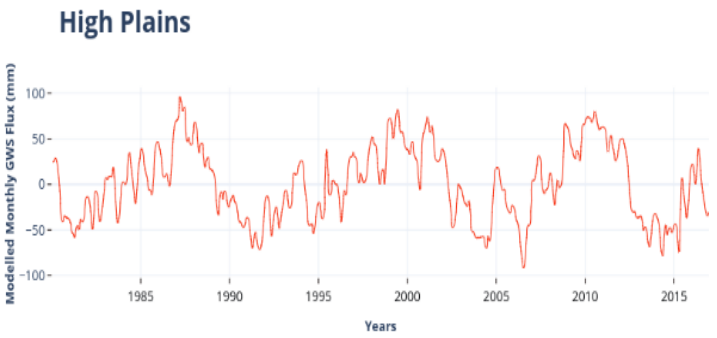

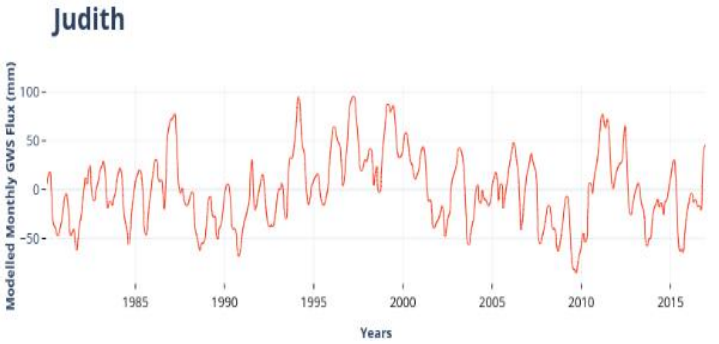

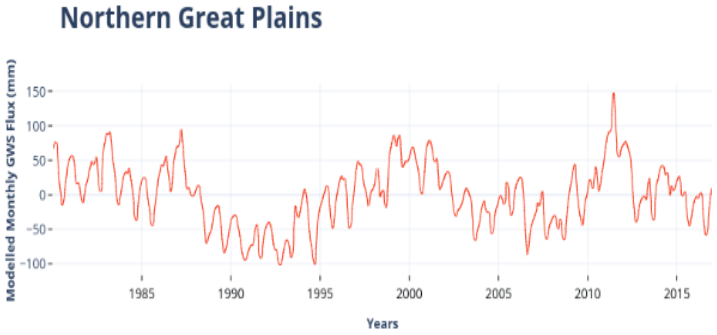

Appendix 7: SWB Model results for South America

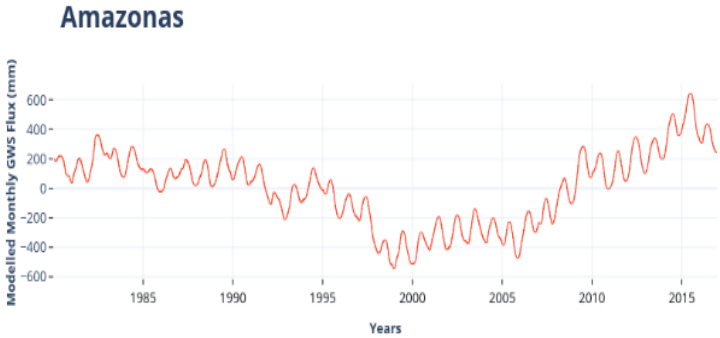

Appendix 8: Wavelet Analysis - Mekong

Mekong

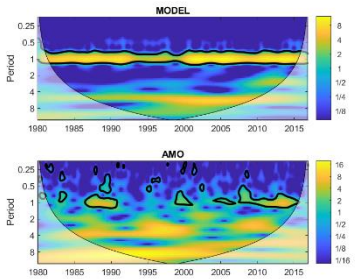

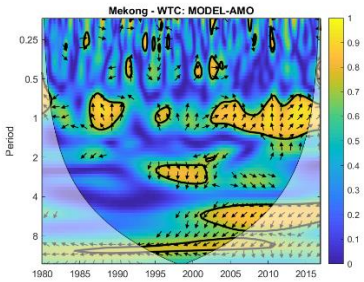

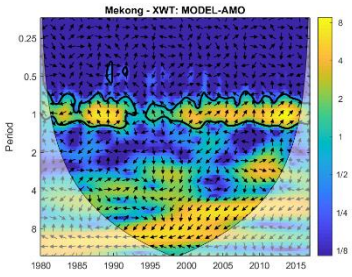

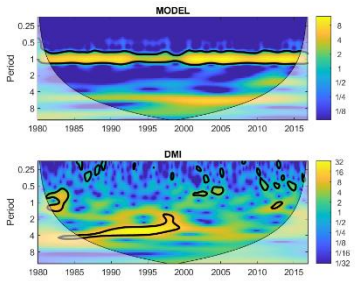

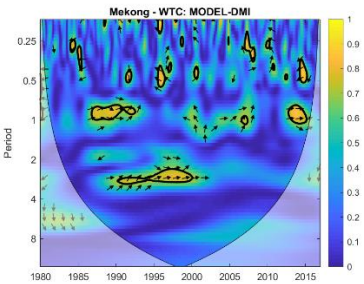

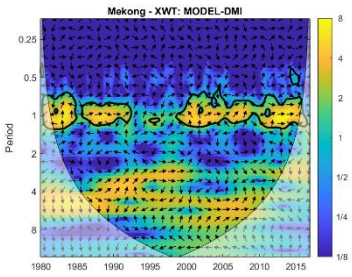

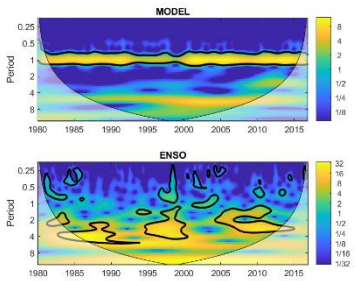

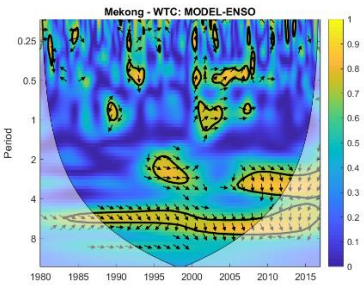

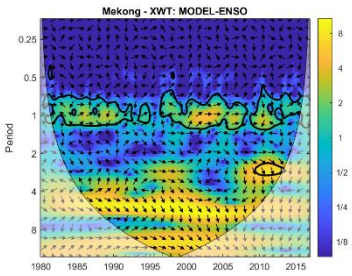

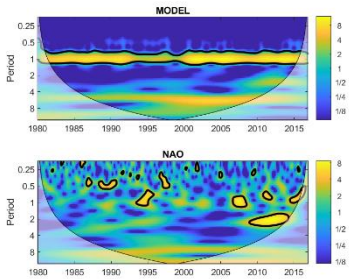

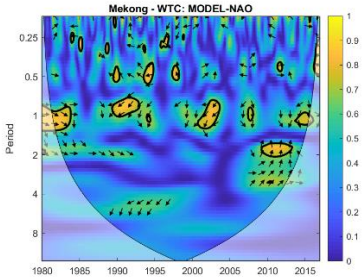

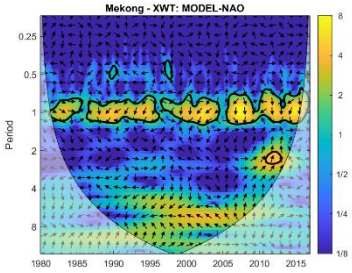

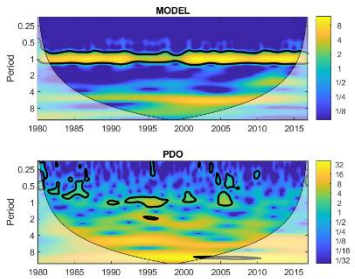

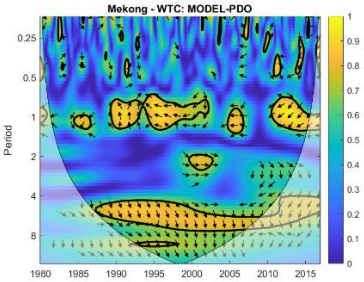

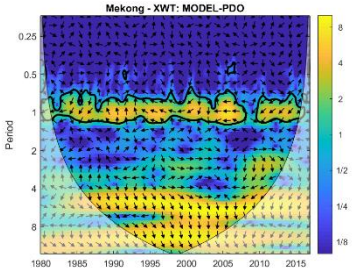

Appendix 9: Wavelet Analysis – Murray Darling Basin

MDB

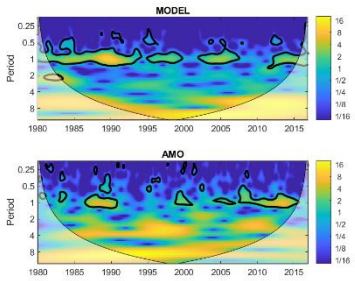

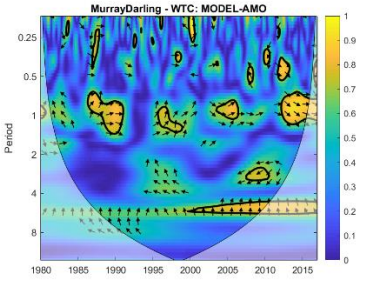

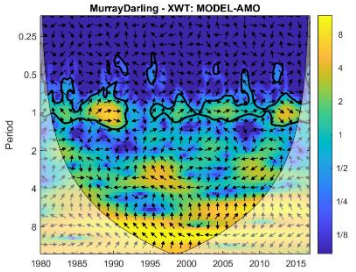

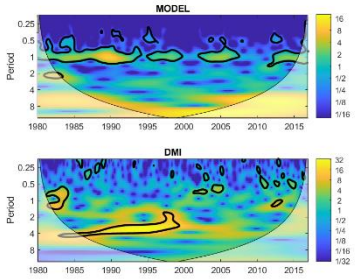

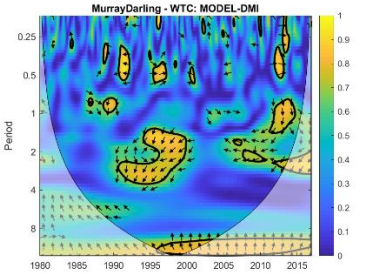

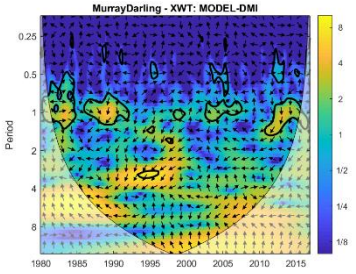

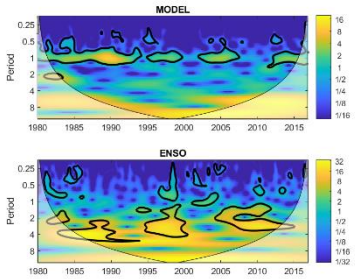

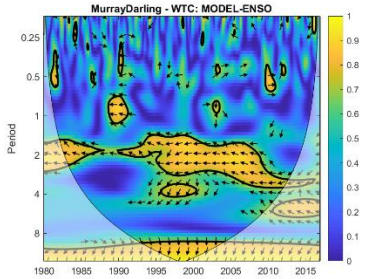

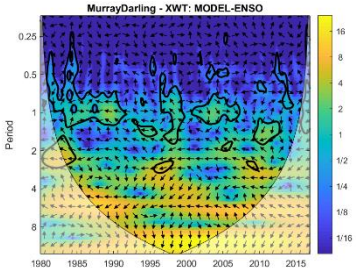

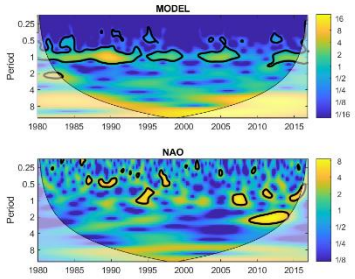

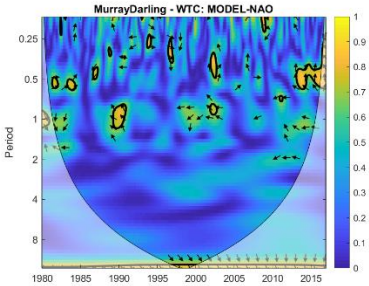

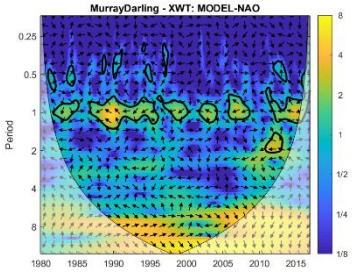

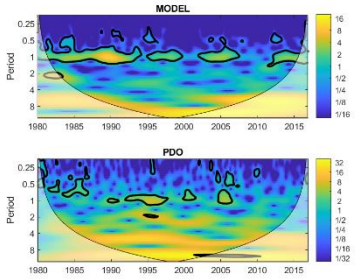

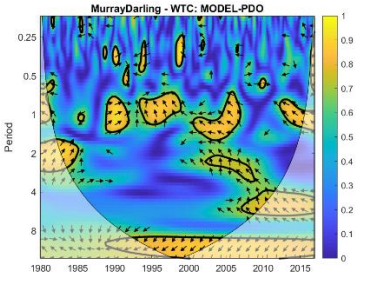

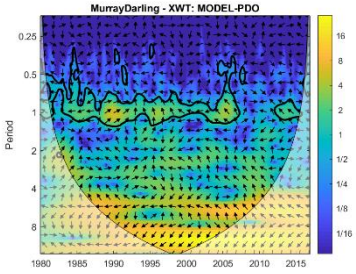

Appendix 10: Wavelet Analysis – High Plains

High Plains

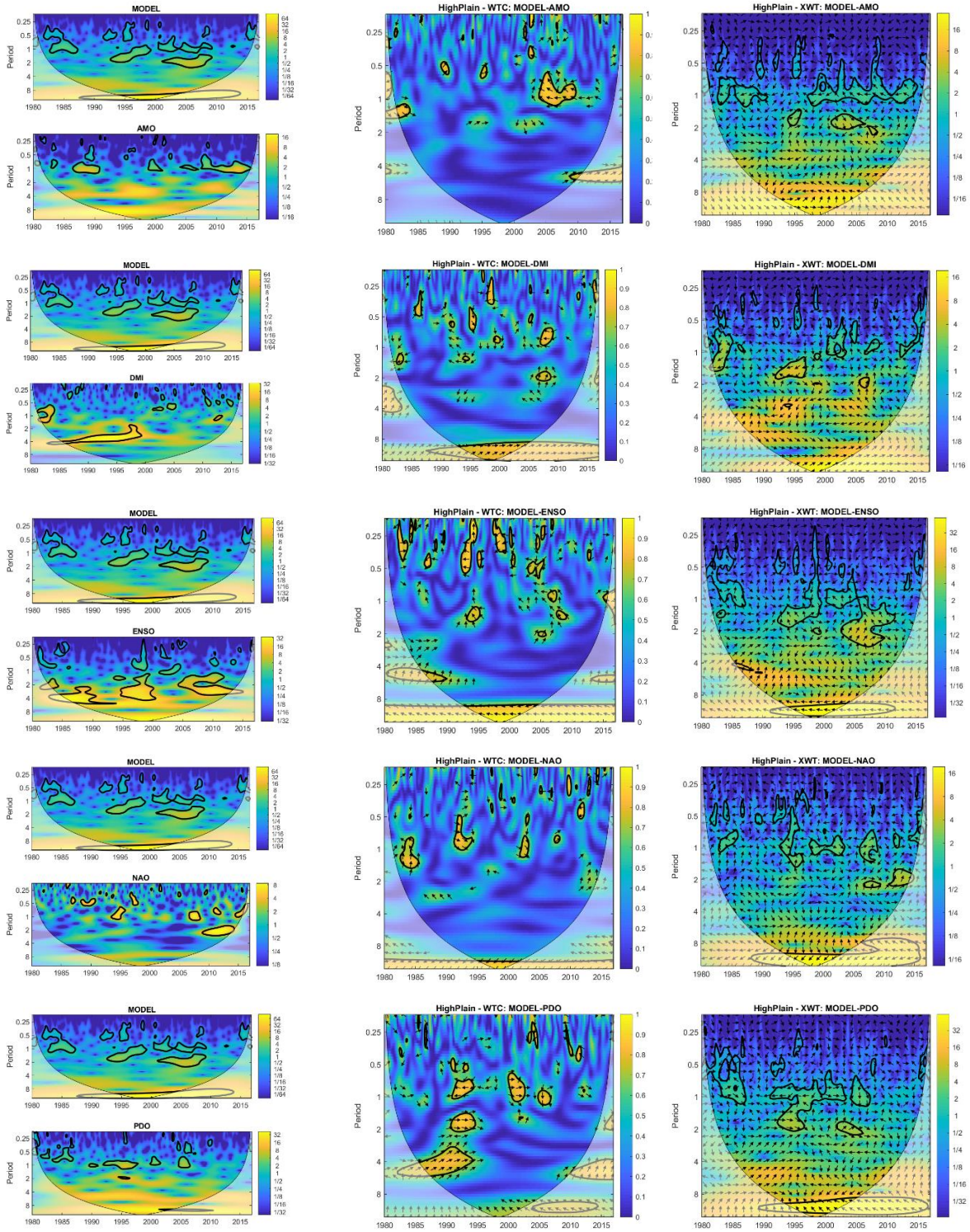

Appendix 11: Wavelet Analysis – Amu Darya

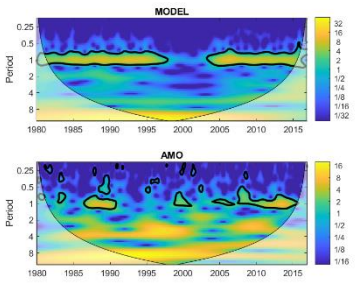

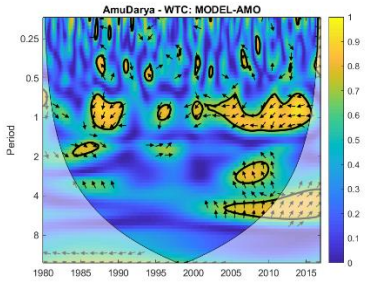

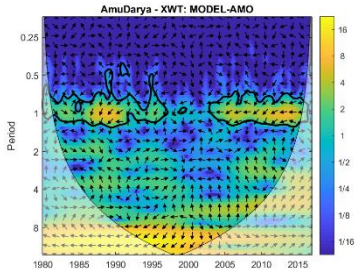

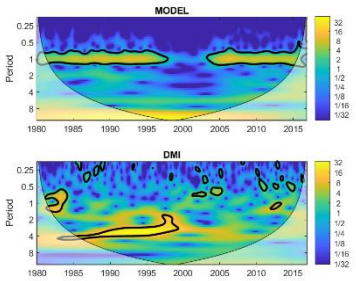

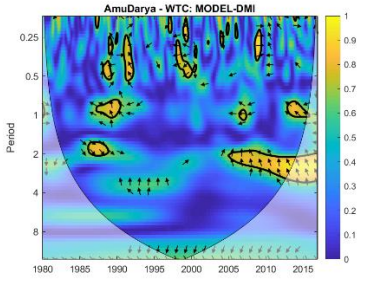

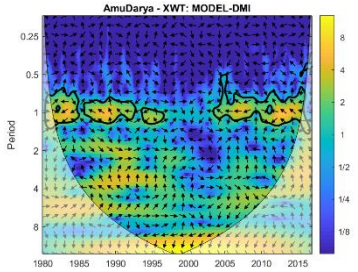

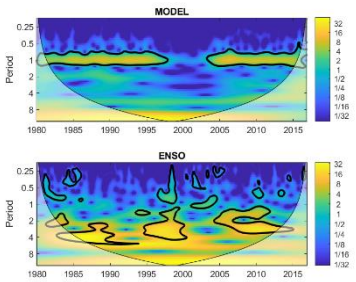

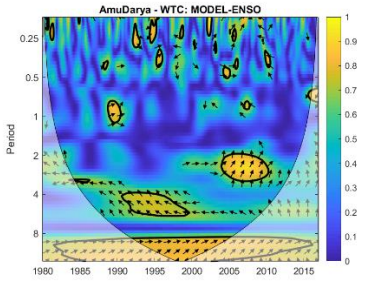

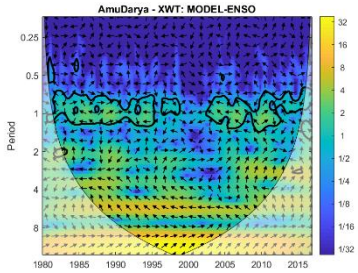

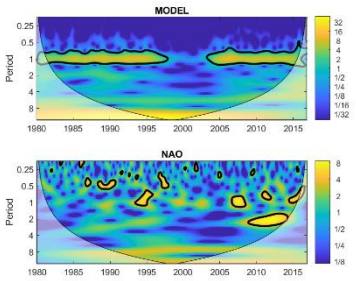

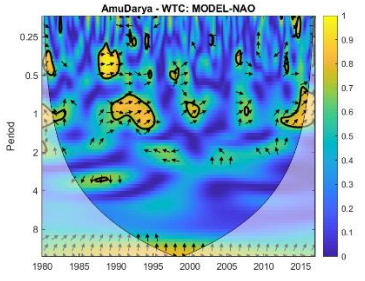

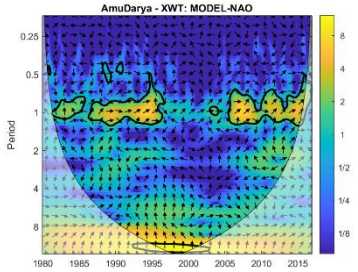

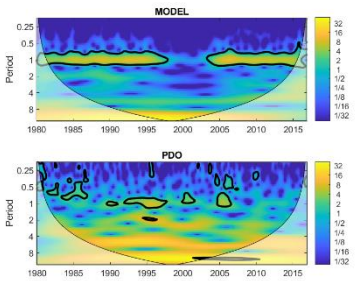

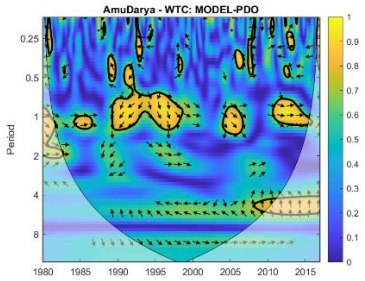

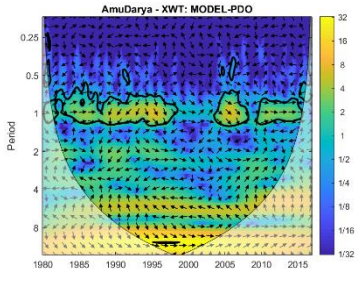

Appendix 12: Wavelet Analysis - Karoo Sedimentary

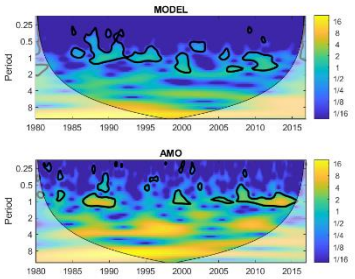

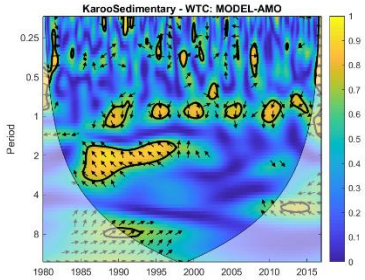

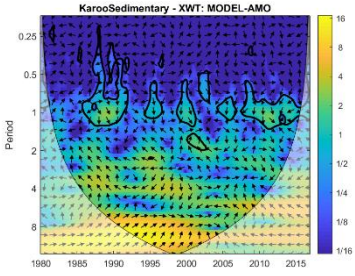

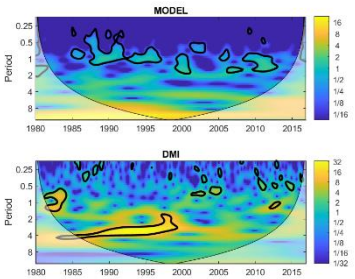

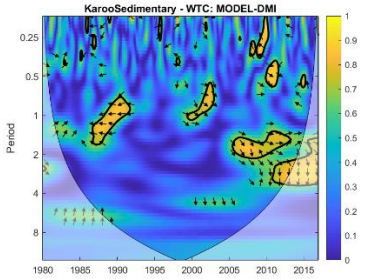

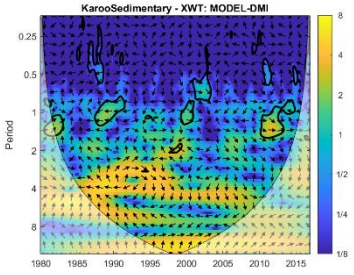

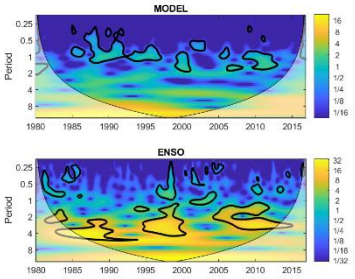

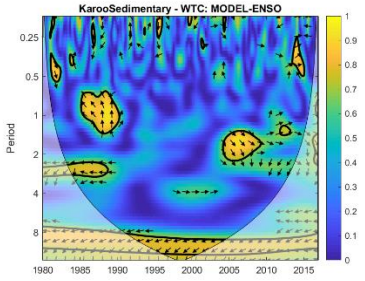

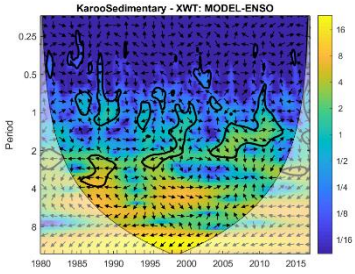

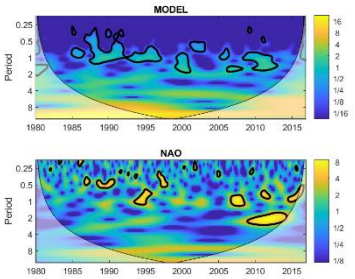

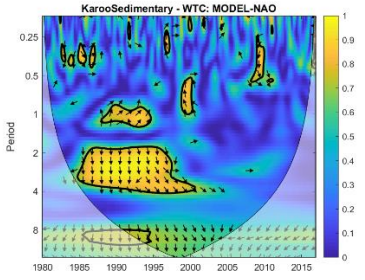

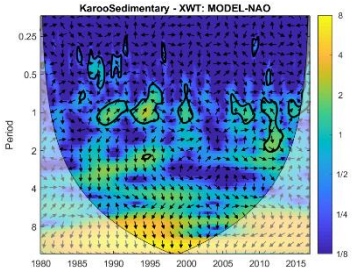

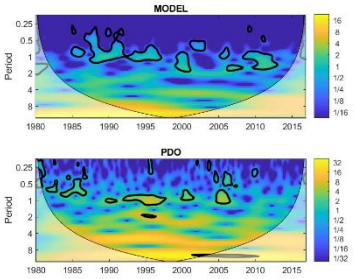

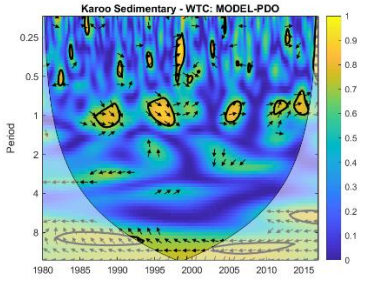

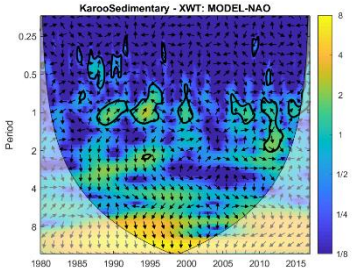

Appendix 13: Wavelet Analysis – Stampriet

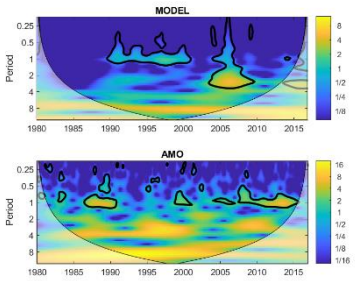

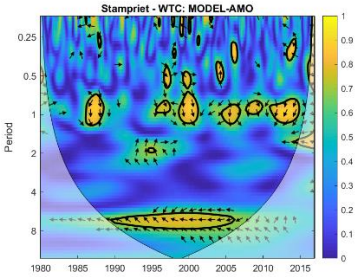

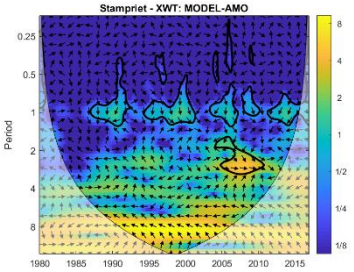

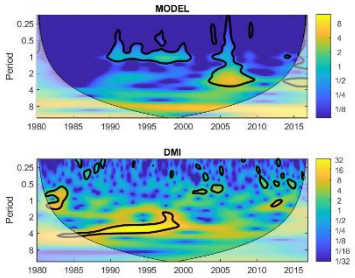

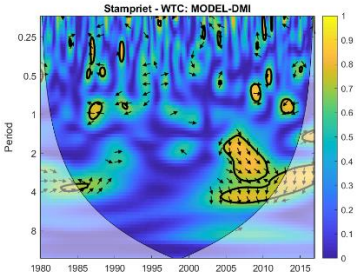

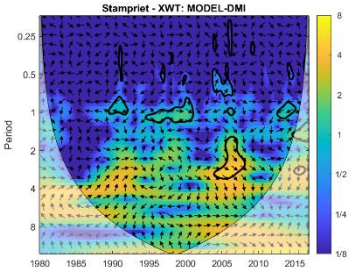

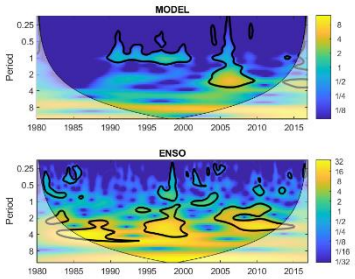

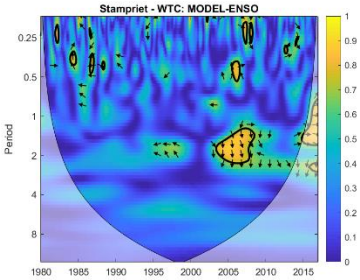

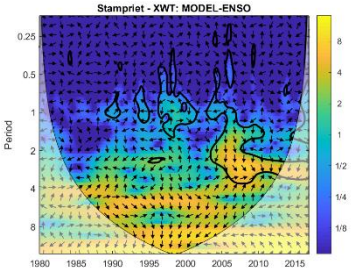

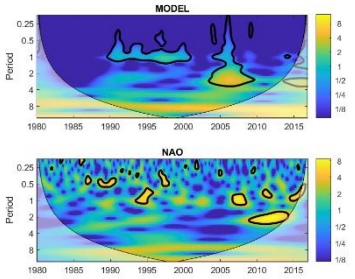

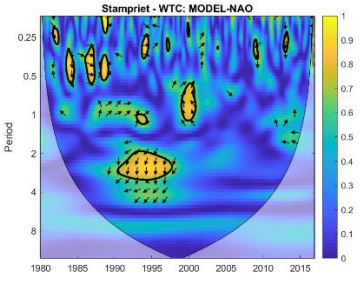

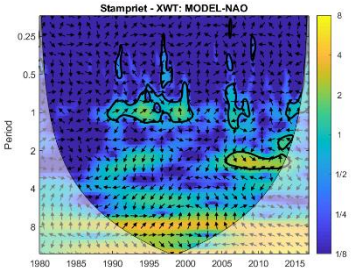

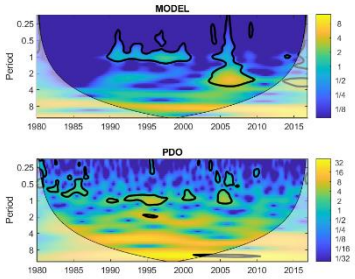

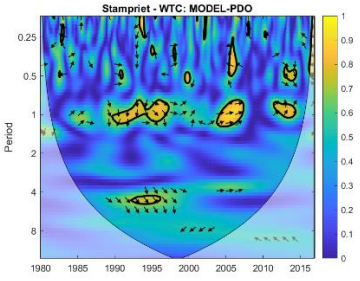

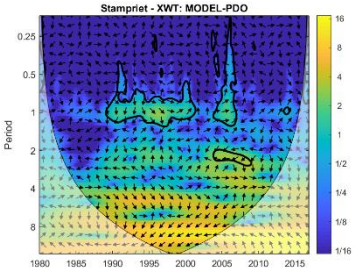

Appendix 14 Wavelet Analysis –Senegalo Mauritanean

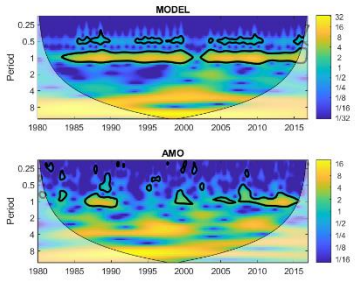

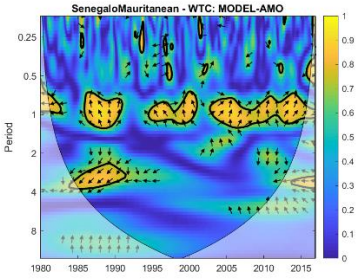

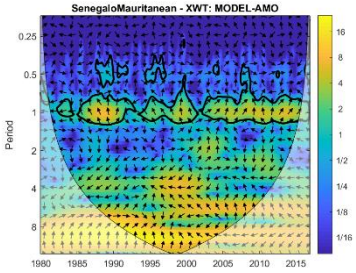

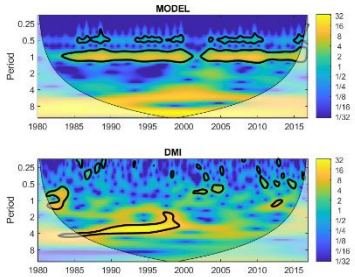

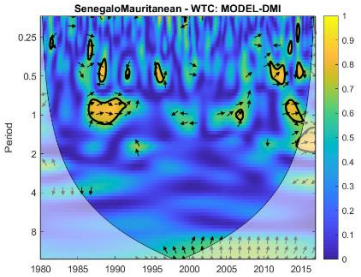

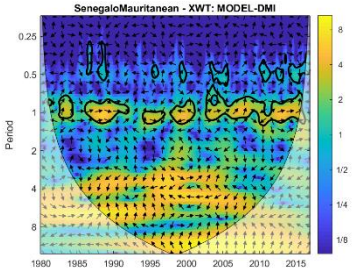

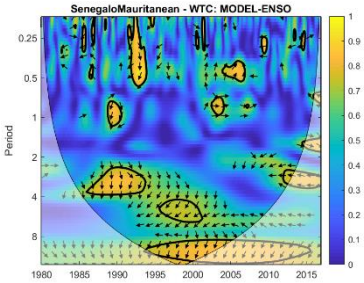

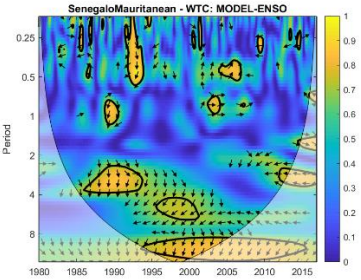

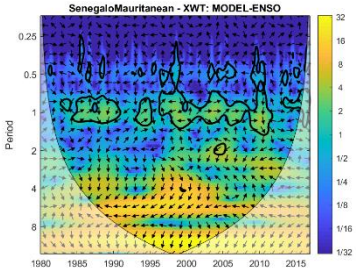

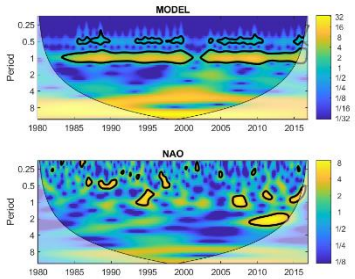

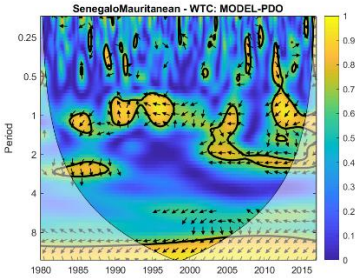

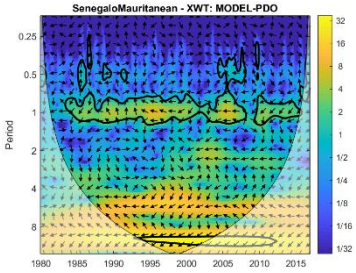

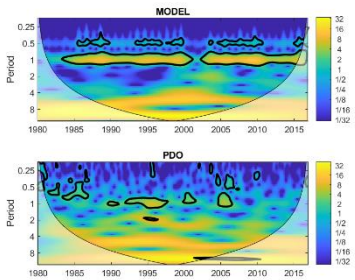

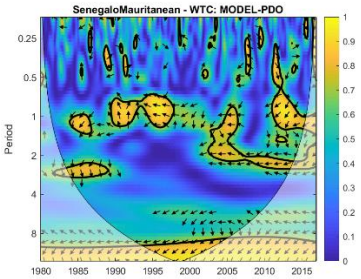

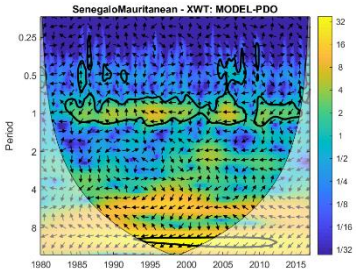

Appendix 15 Wavelet Analysis – East Ganges

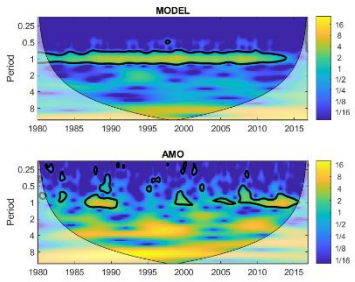

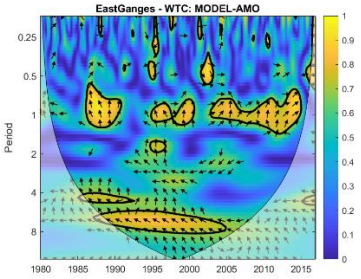

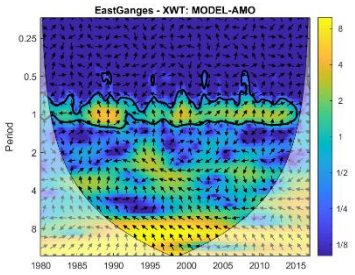

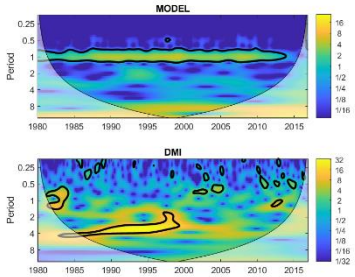

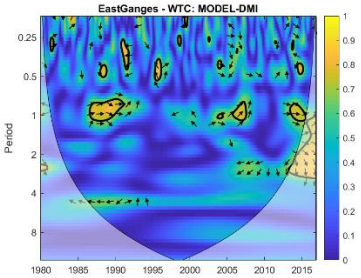

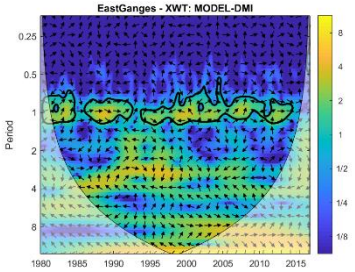

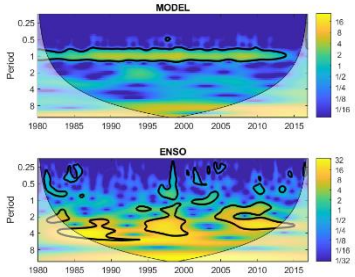

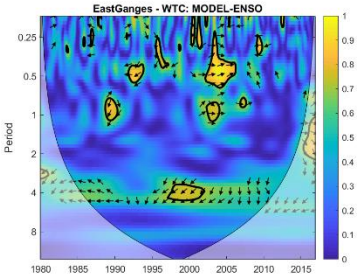

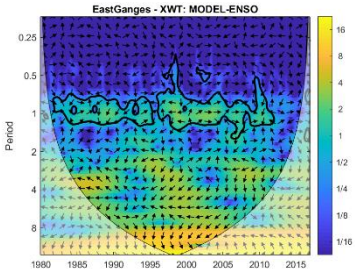

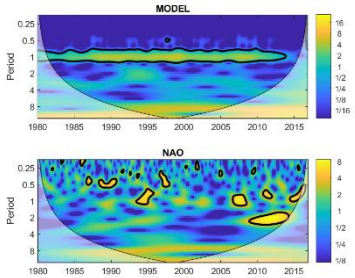

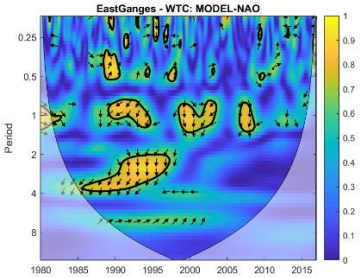

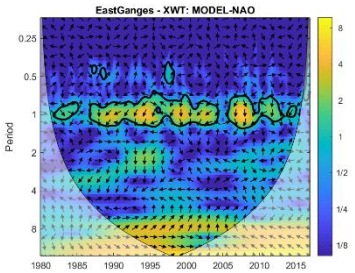

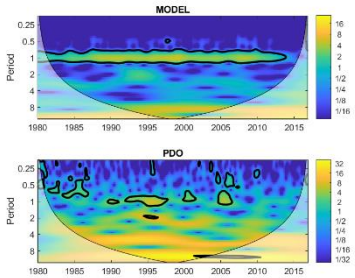

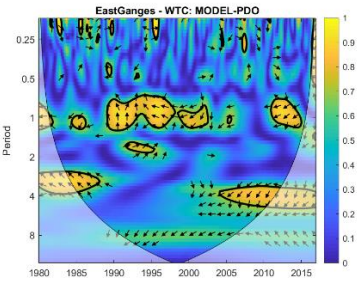

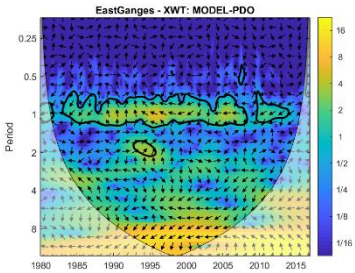

Appendix 16 Wavelet Analysis – Indus

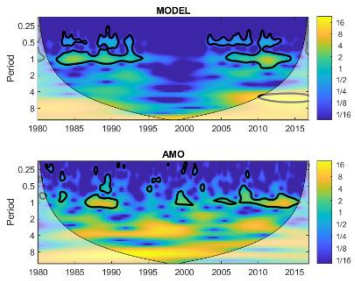

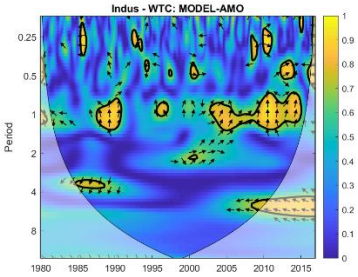

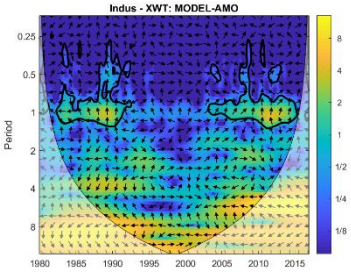

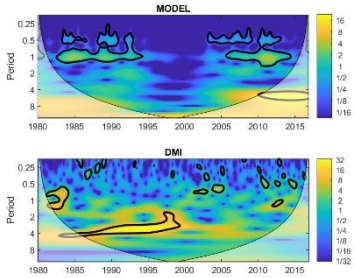

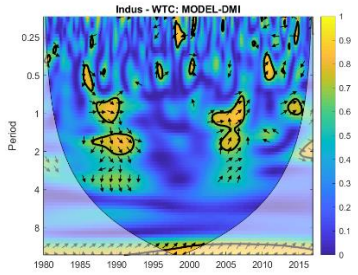

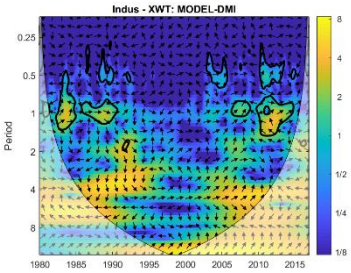

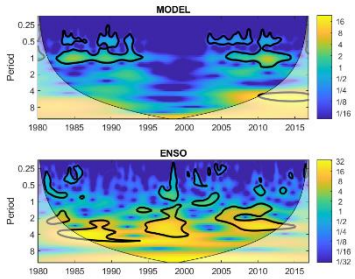

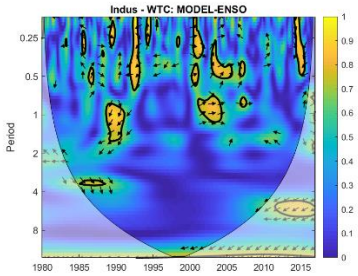

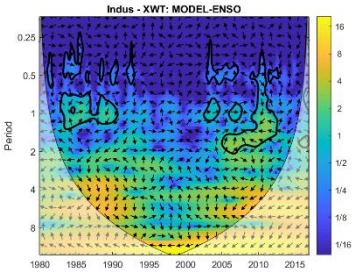

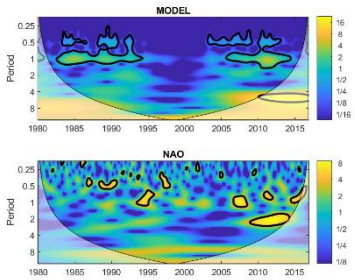

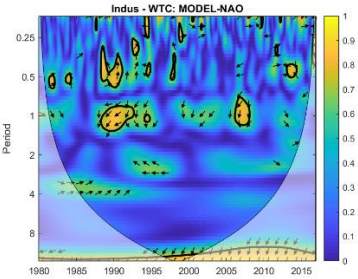

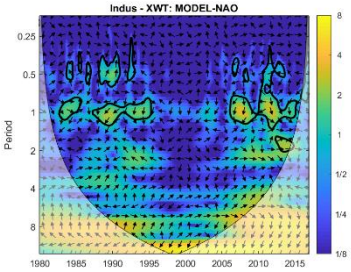

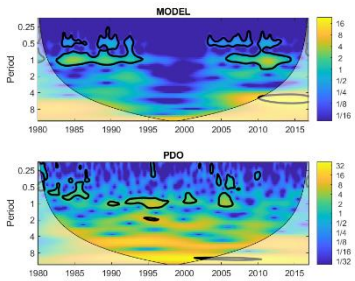

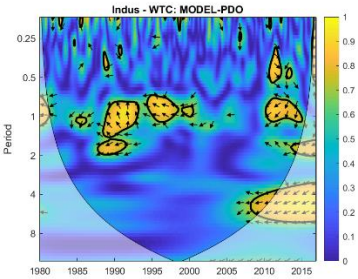

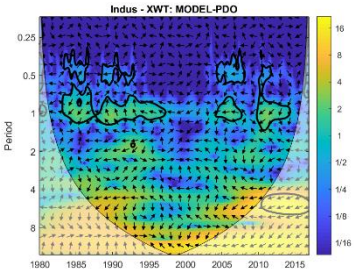

Appendix 17 Wavelet Analysis – Amazonas